

# UC Merced

## UC Merced Electronic Theses and Dissertations

### Title

CD8 T cell function and contributions in autoimmune disease

### Permalink

<https://escholarship.org/uc/item/6bd666s4>

### Author

Mullins, Genevieve Nicole

### Publication Date

2021

### Copyright Information

This work is made available under the terms of a Creative Commons Attribution-NonCommercial-NoDerivatives License, available at <https://creativecommons.org/licenses/by-nc-nd/4.0/>

Peer reviewed|Thesis/dissertation

UNIVERSITY OF CALIFORNIA, MERCED

CD8 T cell function and contributions in autoimmune disease.

A dissertation submitted in partial satisfaction of the requirements for the degree  
Doctor of Philosophy

In

Quantitative and Systems Biology

by

Genevieve Nicole Mullins

Committee in charge:

Professor Jennifer O. Manilay, Chair

Professor Katrina K. Hoyer

Professor Kirk D.C. Jensen

Professor Anna E. Beaudin

2021

© Copyright

Chapter 2 © 2020 *Scientific Reports*

All other chapters © 2021 Genevieve Nicole Mullins

All rights reserved

The dissertation of Genevieve Nicole Mullins is approved, and it is acceptable in quality and form for publication on microfilm and electronically:

*Katrina Hoyer*

---

Katrina K. Hoyer

*Jennifer O. Manilay*

---

Jennifer O. Manilay, Chair

*Kirk Jensen*

---

Kirk D.C. Jensen

*Anna Beaudin*

---

Anna E. Beaudin

## DEDICATION

This dissertation, the first one written in my family, is dedicated to the family and friends who have supported me the last several years, without them I would not have managed this. Specifically, I want to dedicate this to Ethan Low, who has been my partner for a decade and has been there for every stressful, exhausting night. Thank you, my love, for being there to keep me motivated and being there to ensure I take breaks to stay sane. Beyond that, I want to thank you for giving me more family, and so I want to thank my mother-in-law, Claire Zeno, for being a second mom to me for the last decade. I really appreciate everything you've done for me and hope that, in time, I can repay you for all of it. Additionally, I want to dedicate this to my sister, Kaitlan Mullins, who is one of my best friends and is always there to complain to. We have been through a lot together, and while there were times that *really* sucked, I am glad we had each other to get through it and will continue to be there for each other, even if we are far apart. Finally, to my mother, Amanda Lee Wise, who passed during the last few months of this journey, and so never got to see me get to the end. I miss you and I am sure you would be proud of me for finishing my formal education and being the first in the family to receive a PhD. I know you always believed in me, and I know you will be with me in spirit and memory as I transition into the next phase of my life.

## TABLE OF CONTENTS

	Page
List of Abbreviations	vi
List of Symbols	ix
List of Figures	x
Acknowledgements	xi
Curriculum Vita	xiii
Dissertation Abstract	xvi
Chapter 1	1
References	10
Figures	18
Chapter 2	20
Chapter 3	41
References	51
Figures	55
Chapter 4	64
References	70
Figures	73

## LIST OF ABBREVIATIONS

Ab, antibody  
AID, activation induced cytidine deaminase  
AIHA, autoimmune hemolytic anemia  
APC, antigen-presenting cell  
Bcl6, B cell lymphoma 6 protein  
BFA, brefeldin A  
BM, bone marrow  
BMF, bone marrow failure  
CBC, complete blood counts  
CCR7, C-C motif chemokine receptor 7  
CD, cluster of differentiation  
CD8 T<sub>fc</sub>, CXCR5+PD-1+ CD8 effector T (CD8 T follicular)  
CFA, complete Freund's adjuvant  
CIA, collagen-induced arthritis  
CLP, common lymphocyte progenitor  
CMP, common myeloid progenitor  
CTL, cytotoxic T lymphocyte  
CTLA-4, cytotoxic T lymphocyte antigen 4  
CXCR4, C-X-C motif chemokine receptor 4  
CXCR5, C-X-C motif chemokine receptor 5  
dKO, double knockout  
EAE, Experimental autoimmune encephalomyelitis  
ELISA, enzyme linked immunosorbent assay  
FACS, fluorescent activated cell sorting  
Fas<sup>lpr</sup>, MRL/MpJ-Fas<sup>lpr</sup>/J  
FBS, fetal bovine serum

FDR, false discovery rate  
Foxp3, forkhead box p3  
GC, germinal center  
GMP, granulocyte-monocyte progenitor  
HCT, hematocrit  
ICOS, inducible T-cell co-stimulator  
IFA, incomplete Freund's adjuvant  
IFN $\gamma$ , interferon gamma  
IL, interleukin  
IL-21R, B6N.129-II21rtm1Kopf/J  
IL-2-KO, IL-2 deficient  
IL-2R $\alpha$ -KO, IL-2R $\alpha$  deficient  
KLH, keyhole limpet hemocyanin  
KO, knockout  
LCMV, lymphocytic choriomeningitis virus  
LSK, Lineage-negative, Sca-1-positive, c-Kit-positive progenitors  
LN, lymph node  
MEP, megakaryocyte-erythrocyte progenitor  
MFI, mean fluorescence intensity  
NOD, non-obese diabetic  
non-Tfc, CD8 CXCR5-PD-1 $^{lo/-}$   
non-Tfh, CD4 CXCR5-PD-1 $^{lo/-}$   
OCT, optimal cutting temperature  
PBS, phosphate buffered saline  
PCA, principal component analysis  
PD-1, programmed cell death 1  
PE, predicted early

PL, predicted late  
PMA, phorbol 12-myristate 13-acetate  
PNA, peanut agglutinin  
pS6, phosphorylated ribosomal protein S6  
pSTAT5, phosphorylated Signal transducer and activator of transcription 5  
RBC, red blood cell  
rh, recombinant human  
rm, recombinant mouse  
RNAseq, RNA sequencing  
RT, room temperature  
S6, ribosomal protein S6  
SA, streptavidin  
scurfy aIL-2, scurfy mice treated with anti-IL-2 antibody  
scurfy, BALB/c hemizygous male *Foxp3sf/Y*  
scurfy-HET, heterozygous female *Foxp3sf/+*  
SLE, systemic lupus erythematosus  
SPL, spleen  
STAT5, Signal transducer and activator of transcription 5  
 $T_{CM}$ , central memory T cell  
TCR, T cell receptor  
 $T_{EM}$ , effector memory T cell  
Tfh, CD4 T follicular helper  
Tfreg, T follicular regulatory cells  
Treg, regulatory T cell  
UC, University of California  
WBC, white blood cell  
WT, wildtype

## LIST OF SYMBOLS

$\alpha$ , alpha; antibody against

$\beta$ , beta

$^{\circ}$ , degree

$\epsilon$ , epsilon

$\gamma$ , gamma

$\mu$ , micro

n, nano

+, positive expression

-, negative expression

## LIST OF FIGURES

	Page
Figure 1-1	4
Figure 1-2	5
Figure 3-1	42
Figure 3-2	42
Figure 3-3	43
Figure 3-4	43
Figure 3-5	44
Figure 3-6	45
Figure 3-7	45
Figure 3-8	46
Figure 3-9	46
Figure 3-10	47
Figure 4-1	67
Figure 4-2	68

## ACKNOWLEDGEMENTS

Here I would like to acknowledge all the individuals who have contributed to the work presented here.

First, I want to express my deepest gratitude to my mentor, Dr. Katrina K. Hoyer, for guiding and training me as a scientist for the last six years. I appreciate that you were willing to let me join your lab as a final-year undergraduate and that you believed in my ability enough to let me have an individual project. These gave me a solid foundation to build on as I transitioned into being a graduate student in your lab. Even when it was hard to take, you have given me the advice and chastising I needed as I developed my skills in your lab. I've learned so much from you over the last six years; techniques, experiment planning, writing, and presenting. The lessons I have learned and the growth and progress I have made under your mentorship will stay with me as I continue in my career. Thank you so much for the guidance you have provided.

Next, I would like to thank my thesis committee members, for continued guidance and support. Dr. Jennifer O. Manilay for being a fantastic, cooperative, and supportive chair. Dr. Kirk D.C. Jensen for the advice, not only to move my research forward, but also on proceeding into my future. Dr. Anna E. Beaudin for providing great perspective and advice to my project. I also want to thank all three of you for showing me how much fun we can have as scientists, both in enjoying our work, but also outside of the lab no matter where we are in our careers.

I would also like to thank the expertise and technical guidance of the UC Merced core facilities. At UC Merced's Stem Cell Instrumentation Foundry: Dr. David M. Gravano for the use of the flow cytometry instruments, experimental guidance and advice, and training. At UC Merced's Department of Animal Research Services: Mr. Roy Hognlund and Mrs. Emily Slocum for animal facility support, maintenance, and expertise. At UC Merced's Imaging and Microscopy Facility: Dr. Anand Subramaniam and Dr. Kennedy Nguyen for the use of the LSM 880 confocal microscope, and technical expertise, guidance, and training.

Lastly, I would like to acknowledge my lab mates and friends that have supported me through graduate school and have made it such an enjoyable experience and helping me practice my presentations and edit my papers. Dr. Kristen Valentine for training me while I was an undergraduate and early graduate student in the lab, and then for being a supportive colleague. Ms. Anh Diep and Ms. Nadia Miranda for not just being my colleagues in the lab, but also my friends. Mr. Oscar Davalos and Mr. Jonathan Anzules for teaching me more about computation and coding. Mrs. Christi Waer-Turner and Ms. Susana Tejeda-Garibay for being excellent additions to our lab and being supportive as I

leave the lab, but also for being such enjoyable people to be around. Finally, to the undergraduates in the lab that helped with keeping things in the lab moving smoothly, especially Kayla Williams and Lek Wei (Anson) Seow for being such wonderful mentees. Thanks to all of you, and I will miss working with you, but I hope I will be able to stay in contact with you all once I leave.

Chapter 2: T cell signaling and Treg dysfunction correlate to disease kinetics in IL-2R $\alpha$ -KO autoimmune mice.

The text of this thesis/dissertation is a reprint of the material as it appears in the *Scientific Reports*. Originally published in *Scientific Reports*. Genevieve N. Mullins, Kristen M. Valentine, Mufadhal Al-Kuhlani, Dan Davini, Kirk D.C. Jensen, and Katrina K. Hoyer. T cell signaling and Treg dysfunction correlate to disease kinetics in IL-2R $\alpha$ -KO autoimmune mice. *Sci Rep* 10, 21994 (2020). Copyright © 2020 Springer Nature Limited, Inc.

This work was supported by the National Institutes of Health Grants R00HL090706 and R15HL146779 to K.K.H., and an Aplastic Anemia and MDS International Foundation Grant to K.M.V.

Chapter 3: CD8 follicular T cells localize throughout the follicle during germinal center reactions and maintain cytolytic and helper properties.

Genevieve N. Mullins, Kristen M. Valentine, Oscar Davalos, Lek Wei Seow, Katrina K. Hoyer

The authors thank Roy Hoglund and the staff members of the UC Merced Department of Animal Research Services for animal husbandry care, the UC Merced Stem Cell Instrumentation Foundry (SCIF) for their assistance in cell sorting, Anand Subramaniam and the UC Merced Imaging and Microscopy Facility for assistance and use of microscopy equipment, Anh Diep for experimental assistance and technical support, and undergraduate research assistant Nicole Quiroz-Lumbe.

This work was supported by the National Institutes of Health Grant R00HL090706 and R15HL146779 to K.K.H., the 2019 University of California Presidential Dissertation Year Fellowship to K.M.V., and the University of California. The Zeiss LSM 880 microscope used for imaging was purchased by NSF grant DMR-1625733.

## CURRICULUM VITA

### EDUCATION AND RESEARCH

2011-2016	Bachelor of Science, Biology University of California, Merced School of Natural Sciences
2011-2016	Bachelor of Arts, Psychology University of California, Merced School of Social Sciences, Humanities, and Arts
2012-2015	University of California, Merced School of Natural Sciences Biology Instructional Labs (Dr. Jim Whalen)
2015-2016	University of California, Merced School of Natural Sciences Laboratory of Dr. Katrina Hoyer
2015-2016	University of California, Merced School of Natural Sciences Stem Cell Instrumentation Foundry (Dr. David Gravano)
2016-2021	Doctor of Philosophy, Quantitative and Systems Biology University of California, Merced School of Natural Sciences Laboratory of Dr. Katrina Hoyer

### GRANTS, FELLOWSHIPS, AND AWARDS

2011-2015	UC Regents' Scholarship University of California, Merced
2011-2016	Chancellor's Honors List University of California, Merced
2016	Outstanding Undergraduate Award University of California, Merced School of Natural Sciences
2017	NSF GRFP Honorable Mention
2018	ASUCM FURS grant for undergraduate mentee University of California, Merced
2020	Rotary District 5220 2020-21 Scholarship, Finalist
2016-2021	Teaching Assistant University of California, Merced School of Natural Sciences

## **PUBLICATIONS AND PRESENTATIONS**

GN Mullins, DM Gravano. Flow cytometry course. 2-day lecture presented to UC Merced graduate students through UC Merced SCIF (2016). Merced, CA.

GN Mullins, KM Valentine, D Davini, KK Hoyer. Comparison of Disease Presentation in CD25 and IL-2 Deficient Mouse Models. Abstract presented as a poster at the UC Merced Research Week (2016). Merced, CA.

GN Mullins, KM Valentine, D Davini, KK Hoyer. Evaluation of Disease Presentation in IL-2R $\alpha$  Deficient Mouse Model. Abstract presented as a poster at UC Merced GROW (2017). Merced, CA.

GN Mullins, KM Valentine, D Davini, M Al-Kuhlani, KK Hoyer. Signaling Responsiveness Driving Autoimmune Disease Pathology and Kinetics. Abstract presented as a poster at Midwinter Conference of Immunologists (2018). Asilomar, CA.

GN Mullins, KM Valentine, D Davini, M Al-Kuhlani, KDC Jensen, KK Hoyer. Defining T cell Parameters Driving Autoimmune Disease Pathology and Kinetics. Abstract presented as a poster at UCSF/UCB/UCM Immunology Retreat (2018). Santa Cruz, CA.

GN Mullins, KM Valentine, TJ Lawrence, KK Hoyer. CD8 T follicular cell phenotype and function in autoimmune disease. Abstract presented as an oral presentation at UCSF/UCB/UCM Immunology Retreat (2018). Santa Cruz, CA.

KM Valentine, D Davini, TJ Lawrence, GN Mullins, M Manansala, M Al-Kuhlani, JM Pinney, JK Davis, AE Beaudin, SS Sindi, DM Gravano, KK Hoyer. CD8 Follicular T Cells Promote B Cell Antibody Class Switch in Autoimmune Disease. *J. Immunol.*, July 2018. doi: 10.4049/jimmunol.1701079. PMID: 29743314.

GN Mullins, KM Valentine, TJ Lawrence, KK Hoyer. CD8 T follicular cell signaling in autoimmune disease. Abstract presented as a poster at Keystone Symposia on Molecular and Cellular Biology, B cell-T cell Interactions (2019). Keystone, CO.

GN Mullins, KM Valentine, TJ Lawrence, KK Hoyer. CD8 T follicular cell signaling in autoimmune disease. Abstract presented as a poster at the UC Merced Research Week (2019). Merced, CA.

GN Mullins, KM Valentine, O Davalos, KK Hoyer. CD8 T follicular cell phenotype and function in autoimmune disease. Abstract presented as an oral presentation at UC Merced QSB Annual Retreat (2019). Yosemite, CA.

GN Mullins, KM Valentine, D Davini, M Al-Kuhlani, KDC Jensen, KK Hoyer. Defining T cell Parameters Driving Autoimmune Disease Pathology and Kinetics. Abstract presented as a poster at Midwinter Conference of Immunologists (2020). Asilomar, CA.

GN Mullins, KK Hoyer. Molecular Immunology guest lecture on flow cytometry. Presented to UC Merced Molecular Immunology course (2020). Merced, CA.

GN Mullins, KM Valentine, D Davini, M Al-Kuhlani, KDC Jensen, KK Hoyer. Defining T cell Parameters Driving Autoimmune Disease Pathology and Kinetics. Abstract presented as a poster at the UC Merced Research Week (2020). Merced, CA.

GN Mullins, KM Valentine, O Davalos, LK Seow, Hoyer KK. CD8 T follicular cell phenotype and function in autoimmune disease. Dissertation work presented orally at University of North Carolina, Chapel Hill, remotely (2020).

GN Mullins, KM Valentine, D Davini, M Al-Kuhlani, KDC Jensen, KK Hoyer. T cell signaling and Treg dysfunction correlate to disease kinetics in IL-2R $\alpha$ -KO autoimmune mice. *Sci Reports*, December 2020. doi: 10.1038/s41598-020-78975-y. PMID: 33319815.

GN Mullins, KM Valentine, O Davalos, LK Seow, Hoyer KK. CD8 follicular T cells localize throughout the follicle during germinal center reactions and maintain cytolytic and helper properties. Submitted April 2021.

CD8 T cell function and contributions in autoimmune disease.

by

Genevieve Nicole Mullins

Doctor of Philosophy in Quantitative and Systems Biology

University of California, Merced, 2021

Professor Katrina K. Hoyer

Autoimmune diseases comprise more than 80 well characterized disorders that affect 7% of Americans. Cellular and molecular studies of autoimmune disease are extensive, yet few viable long-term treatments exist. Thus, basic research into the cellular and molecular mechanisms underlying autoimmune disease is needed to improve and develop novel treatments. My work seeks to understand the contribution of CD8 T cells and novel CXCR5+ CD8 T cells to autoimmune disease by exploring the mechanisms by which CD8 T cells promote disease. Using a model of systemic autoimmune disease (IL-2R $\alpha$ -KO), I show that a culmination of factors, including regulatory T cell dysfunction, changes in T cell activation, and differences in cytokine signaling combine to drive disease progression and kinetics. Further, I show that CXCR5+ CD8 T cells localize to the germinal center and B cell follicle, produce cytokines indicative of CD4 T follicular helper (Tfh) cells throughout the B cell follicle, and that CD8-derived IL-4, but not IL-21 impacts B cell function. This work demonstrates that CXCR5+ CD8 T cells share many features with CD4 Tfh cells but may contribute to B cell function through a different combination of mechanisms than CD4 Tfh cells. Future work should assess the contribution of other cytokines and cell surface proteins to CXCR5+ CD8 T cell function, as well as the factors that control the differentiation of this novel subset, particularly in the context of autoimmune disease.

## **CHAPTER 1**

### **Background and historical context**

## CHAPTER 1: BACKGROUND AND HISTORICAL CONTEXT

### Autoimmunity and IL-2 signaling

#### *Autoimmune disease*

Autoimmune disease comprises more than 80 well characterized disorders that affect 7% of Americans (1). Autoimmune disease is immunological destruction of self-tissue due to breakdown of immunological tolerance. There are two stages of immunological tolerance, central and peripheral. Central tolerance refers to tolerance established during immune cell development, whereas peripheral tolerance refers to tolerance mechanisms that control self-reactive responses during immune cell interaction with antigen. Regulatory T cells (Treg) are generated as one major mechanism of both central and peripheral tolerance. Cellular and molecular studies of autoimmune disease are extensive, yet few viable long-term treatments exist. Thus, basic research into the cellular and molecular mechanisms underlying autoimmune disease is needed to improve and develop novel treatments.

We focus on identifying underlying mechanisms of autoimmunity across multiple diseases. To achieve this, we utilize models of disease manifestations of autoimmune hemolytic anemia (AIHA), bone marrow failure (BMF), diabetes, and lupus. AIHA is characterized by autoantibodies against red blood cells (RBC). This leads to RBC destruction through Fc-mediated phagocytosis and complement-mediated lysis (2). BMF is a set of disorders in which bone marrow stem cells fail to properly generate cellular components of blood, including RBC, and can be autoimmune in nature. Treg and IL-2 signaling-deficient or impaired mice provide models for spontaneous, systemic autoimmunity, including AIHA and BMF (IL-2-KO, IL-2R, surfy). Type 1 diabetes results from the autoimmune destruction of insulin-producing beta-cells in the pancreatic islets, causing in defects in insulin production. The most utilized model for studying immune mediated diabetes is non-obese diabetic (NOD) mice that develop hyperglycemia and immune infiltration of the pancreatic islets leading to decreases in insulin production (3). Lupus is a systemic autoimmune disease affecting multiple organs, and is best characterized by a butterfly rash, and antibodies against nuclear proteins and double-stranded DNA. MRL/MpJ-*Fas*<sup>lpr</sup>/J (MRL-lpr) mice have a mutation in the *Fas* gene that leads to massive lymphoproliferation. These mice spontaneously develop multiple auto-antibodies and develop dermatitis, glomerulonephritis, severe thymic atrophy, and renal disease (4, 5). Mouse models allow for the evaluation of underlying mechanisms driving human autoimmune disease initiation and progression.

### *Tregs in tolerance and autoimmunity*

To maintain tolerance, Tregs function to suppress T cell activation, proliferation, and effector function by acting directly on self-reactive T cells and directing antigen-presenting cell (APC) function. Tregs can arise in the thymus in response to self-antigens (tTregs) or in the periphery primarily in response to foreign antigen (pTregs) and differentiate further in response to environmental stimuli (6). Suppressive functions are mediated in three major ways: through the action of soluble factors, the binding of inhibitory receptors, and through the competition of growth factors (7-9). The key proteins that mediate these functions include, but are not limited to IL-10, CTLA-4, Tim3, Lag3, TGF- $\beta$ , adenosine, Nrp1, and IL-2R $\alpha$  (7, 10-14). Specifically, soluble factors like IL-10 and TGF $\beta$  decrease antigen presentation and APC activation, reduce intracellular signaling downstream of T cell co-stimulatory receptor CD28, and induce the generation of additional Tregs (15). CTLA-4 competes with CD28 on naïve T cells for its binding partner CD80/CD86, thus preventing T cell co-stimulation and inducing an inhibitory signal (16). Extracellular ATP is proinflammatory and upregulates CD86 on APCs (17). Expression of CD39 and CD73 allow Tregs to convert extracellular ATP into adenosine, reducing inflammation (18). Finally, Tregs compete with activated T cells for local IL-2 through the use of high-affinity IL-2R to block T cell proliferation (19, 20). Tregs constitutively express IL-2R $\alpha$  providing an advantage over naïve T cells that must upregulate IL-2R $\alpha$  upon activation to respond to IL-2 with high affinity (21-23).

Tregs have also been studied for their therapeutic potential in transplantation and autoimmune disease, with the assumption that re-establishing tolerance through boosting Treg numbers or function will alleviate the aberrant immune activation in these settings. Treg therapies include adoptive cell transfer of Tregs after in vitro expansion and enhancing Treg survival and function through administration of IL-2 (24-26). Hundreds of clinical trials focused on enhancing Tregs in a variety of settings are in progress or completed (27). Early success from trials in type 1 diabetes and systemic lupus erythematosus show promise for the use of adoptive Treg transfer for autoimmune disease (28). Ongoing work looks to further enhance Treg function in vitro prior to transfer, including through genetic manipulation, and to develop “off the shelf” Tregs with conserved MHCs so individual patient Tregs do not need to be isolated and manipulated for therapy (27, 28).

### *IL-2 signaling*

IL-2 is a growth factor for and produced by activated T cells and plays a role in the differentiation of effector and memory T cells. Signaling response to IL-2 differs among T cell populations. IL-2 signaling overtime is more sustained in CD8 T cells, lasting several hours, contrasting CD4 T cells due to intracellular

pools of IL-2R $\beta$  that don't exist in CD4 T cells (29). IL-2 signaling in CD8 T cells also reduces the T cell receptor signaling threshold required for proliferation but does not do this in CD4 T cells (30). IL-2 also drives the differentiation of Th1 and Th2 and inhibits the generation of Th17 and Tfh cells (31, 32). In activated CD8 T cells IL-2 induces expression of IFN $\gamma$ , TNF $\alpha$ , granzyme, and perforin, molecules required for their function as cytolytic cells (31). Low IL-2 signaling drives CD8 T cells to become memory cells by allowing the expression of Bcl6 and IL-7R $\alpha$  through reduced Blimp-1, whereas high IL-2 signaling leads to effector differentiation through upregulation of Blimp-1 and T-bet (31). IL-2 is also a cytokine required for the survival, development, and function of Tregs (33). The receptor for IL-2 is comprised of three receptor chains – IL-2R $\alpha$  (CD25), IL-2R $\beta$  (CD122), and the common gamma chain or  $\gamma$ c (CD132) (33, 34). Upon IL-2 receptor activation three signaling pathways, MAPK, PI3K, and JAK1/3-STAT5 pathways, are triggered (Figure 1-1) (34-36). These pathways promote cell survival and proliferation, induction of glycolytic metabolism, and STAT5-mediated gene expression. This activates a gene expression profile that includes Foxp3, IL-2R $\alpha$ , and mitogenic and survival genes like c-myc, bcl-2, and bcl-x (34, 37, 38). Mice deficient in IL-2 or any part of its receptor develop spontaneous, multi-organ autoimmune disease driven by the reduction in functional Tregs, as decreased IL-2 signaling leads to reduced survival and suppressive function of Tregs (39-45).

Mice lacking IL-2R $\alpha$  (IL-2R $\alpha$ -KO) are a useful model of human autoimmune disease as they develop many disease phenotypes seen in human autoimmune disease, such as AIHA, BMF, inflammatory bowel disease, and dacryoadenitis (39-42, 44). These mice and mice lacking other components of the IL-2 signaling pathway have reduced Treg numbers and function, a major contributor to the spontaneous autoimmune disease that develops (46, 47). Defects in IL-2 responsiveness is also present in several human manifestations of autoimmune disease, including type I diabetes, multiple sclerosis, and systemic lupus erythematosus (48-51). IL-2R $\alpha$ -KO mice develop excessive lymphocyte proliferation, lymphocyte activation, and auto-antibodies against RBCs due to reduced Treg suppressive function. On the C57BL/6 background these mice develop normally but autoimmune disease arises in early adulthood. Two disease kinetics emerge in these mice, with those succumbing at 8-12 weeks due to anemia and a combination of irritable bowel disease and anemia at 16 weeks and older (41). In contrast, BALB/c mice begin to develop signs of autoimmunity as neonates (<21 days old), with approximately 25% succumbing to anemia by 21 days and the remainder succumbing out as far as 40+ days old. The kinetics of the development of these phenotypes is documented, but the underlying mechanism driving these differences are largely unknown and will be discussed in Chapter 2.

## **Germinal Center Reactions**

Autoimmune diseases can be antibody-mediated or cell-mediated and localize to only a few tissues or create systemic damage. Antibody-mediated autoimmune diseases are characterized by the presence of high-affinity auto-antibodies targeted against self-tissues. To generate high-affinity antibodies, activated B cells must undergo a process of affinity maturation in the germinal center (GC). This process involves repeated rounds of proliferation, somatic hypermutation, and selection which is driven primarily through signals provided by specialized helper T cells (CD4 T follicular helper cells; Tfh) that reside within the germinal center (52-55) (Figure 1-2). During autoimmune disease CD4 Tfh cells and activated GC B cells expand leading to disease-causing high-affinity autoantibodies.

Autoantibodies can be targeted against a large variety of cells or tissues to cause damage and disease. These autoantibodies are produced in large quantities, up to 2000 per second, by auto-reactive B cells that have differentiated into plasma cells (56). Antibodies can then cause damage through multiple mechanisms, common to normal antibody function. In general, antibodies function through several mechanisms, including activating complement, mediating FcR-dependent phagocytosis and cell lysis, and neutralization of extracellular pathogens and toxins that is defined by the heavy constant region of the antibody (57). In AIHA, autoantibodies are generated against RBCs, which bind to RBCs and target them for Fc-mediated phagocytosis and complement-mediated lysis. RBCs are thus destroyed, leading to anemia. Anti-DNA and anti-nuclear antibodies are generated in lupus, thus targeting almost any tissue or cell type in the body. Tissue damage and inflammation, particularly in the kidneys, are caused by the deposition of autoantibodies and antigen complexes that lead to complement activation and Fc-mediated activation of immune cells (58).

CD4 Tfh cells are phenotypically defined by expression of CXCR5 and PD-1 and downregulation of CCR7 allowing entry into the B cell follicle and exit from the T cell zone (59). Functionally, these cells are defined by the ability to induce GC B cell proliferation, somatic hypermutation, class-switch recombination, and the differentiation of long-lived plasma cells and memory B cells (52, 55, 60). The most important signals CD4 Tfh cells provide to GC B cells are those derived from CD40 and IL-21 (52, 61, 62). Ligation of CD40 induces activation of several downstream pathways, including the PI3K/Akt/mTOR, NFκB, and MAPK/Erk pathways that induce cell growth, survival, and proliferation, and more recently have been implicated in timing the number of GC B cell divisions (63, 64). Binding of IL-21 to its receptor on B cells activates the PI3K/Akt/mTOR

and JAK/STAT pathways promoting proliferation and gene expression (62, 63, 65-67). Together these signals induce the transcription of Bcl6, Blimp-1, and activation induced cytidine deaminase (AID), proteins important in somatic hypermutation, isotype switching, and differentiation into memory B cells or plasma cells (62). Antibody isotype switching and somatic mutation is performed by AID and is guided by cytokine signals from the environment, primarily from Tfh cells; different combinations of cytokines determine the Ig heavy constant region that is rearranged, providing antibodies with different effector functionality dependent on the environmental cues (68, 69).

CD4 Tfh cells are an interesting T cell population, as they arise under multiple immune settings and differentiate alongside other CD4 T cell effectors. CD4 Tfh cells require strong antigen stimulation, IL-6 signals, low IL-2 signals, and ICOS co-stimulation in order to gain Bcl6 and CXCR5 expression (60, 70-78). The gain of CXCR5 expression allows CD4 Tfh cells to migrate to the T-B border. Once there, CD4 Tfh cells interact with B cells to re-enforce key migratory protein expression (high CXCR5 and low CCR7), which will continue as CD4 Tfh cells move first into the follicle and then the germinal center (55). Once in the germinal center, CD4 Tfh cells influence B cell differentiation, antibody class switch, and memory, as described above (60).

### **CXCR5+ CD8 T cells**

Recently, a population of CD8 T cells expressing CXCR5 has been identified in autoimmune disease, cancer, and chronic viral infection (79-85). These cells are proposed to acquire a variety of functions dependent on the setting in which they arise, including cytotoxic cells, progenitor memory cells, and CD4 Tfh-like cells. CXCR5+ CD8 T cells have become a subset of interest due to their ability to remain cytotoxic in chronic viral infections and cancer, as well as the novel capacity for helper functions traditionally associated with CD4 T cells.

CXCR5+ CD8 T cells are phenotypically and functionally similar to CD4 Tfh cells with retained cytolytic function and progenitor potential. CD8 T cells arise in multiple autoimmune models that express CXCR5 and PD-1 and localize to the germinal center where they promote antibody class-switching and plasma cell differentiation (52, 60, 79). Further, these cells express other markers indicative of CD4 Tfh cell function, including CD40L, ICOS, IL-21, and Bcl6 (79). CXCR5+ CD8 T cells expressing these follicular helper markers and participating in B cell responses have also been identified in colorectal cancer, hepatocellular carcinoma, Hodgkin lymphoma, chronic hepatitis B infection, and chronic LCMV infection (82, 85-88). Overall, these results indicate that a CXCR5+ CD8 T cell

subset acquires a follicular helper phenotype and functions in autoimmune disease, chronic viral infection, and cancer to promote B cell antibody responses.

Given the similarity in phenotype and function between CD4 Tfh and CXCR5+ CD8 T cells, it is possible that CXCR5+ CD8 T cells migrate into the B cell follicle and GC in a similar manner to CD4 Tfh cells. As described above, this involves gaining CXCR5 expression and losing CCR7 expression in order to migrate away from the T cell zone and toward the B cell zone, where interactions with B cells increase this expression pattern to allow for full migration into the B cell follicle. CD8 T cells have been found within the germinal center in autoimmune disease, but whether these cells express the combination of chemokine receptors that traditionally aid CD4 Tfh cell entry into the GC center has not been fully studied (79). Further, CXCR4 determines CD4 Tfh helper localization for extrafollicular reactions, but also regulates localization within the germinal center (89-91). CXCR5+ CD8 T cells have not yet been assessed for their localization in this respect, and whether these cells, as with CD4 Tfh helper cells, localize primarily to certain regions of the germinal center.

Traditional CD8 T cells activate and differentiate into cytolytic effectors responsible for killing virally infected and cancerous cells. Cytotoxic CD8 T cells (cytotoxic T lymphocytes; CTL) are defined by the ability to induce antigen-specific target cell apoptosis. This cytotoxicity is mediated by the secretion of granzymes and perforin and the surface expression of FasL (92). Within autoimmune disease, the cytolytic function of CD8 T cells can be both harmful, by directly destroying self-tissue, or beneficial, by limiting self-antigen and inflammation (93). In chronic viral infections and cancer CXCR5+ CD8 T cells retain cytotoxic functional capacity when CXCR5- CD8 T cells become exhausted and non-functional in these settings (83, 94). In bladder cancer, pancreatic tumors, colorectal cancer, hepatocellular carcinoma, and chronic LCMV infection CXCR5+ CD8 T cells express cytolytic molecules, including IFN $\gamma$ , TNF, granzymes, and perforin, and exhibit antigen-specific lysis of target cells (80, 81, 83, 94, 95). Thus CXCR5+ CD8 T cells fit the standard definition of cytotoxic CD8 T cells within the context of chronic viral infection and cancer.

CXCR5+ CD8 T cells, given their unique ability to enter the germinal center to mediate either help or cell killing, are being studied for their therapeutic potential. As such, the regulation and differentiation of this population is being investigated. CXCR5+ CD8 T cells express the transcription factor Bcl6, important for the expression of their key chemokine receptor, CXCR5 (74, 96, 97). Expression is thought to be driven and maintained by E2A and TCF-1, since these transcription factors have been found to regulate Bcl6 in CD4 T cells (85, 94, 98-102). It is assumed that IL-2 and its signaling pathway inhibit CXCR5+ CD8 T cell generation, likely through IL-2 upregulation of the Bcl6 antagonist,

Blimp-1 as occurs in CD4 Tfh regulation (97, 98, 103). Extracellular signals that promote the differentiation of this subset still require investigation, although IL-6 is at least one candidate, given it has been shown to induce IL-21-producing CD8 T cells and influence CD4 Tfh cell differentiation (73, 104). Further study is required to fully understand the signals and pathways that drive the differentiation and function of these novel CXCR5+ CD8 T cells.

CXCR5+ CD8 T cells are also described as memory precursor effector cells (MPECs) during chronic viral infection and following PD-1 blockade (100, 105, 106). MPECs are defined by the expression of CD127, TCF-1, and T-bet, lack of KLRG1, and low cytokine production (107, 108). These cells persist when transferred and can generate memory and terminally exhausted cell populations (107, 108). A population of CXCR5+ CD8 T cells have been identified that are TCF-1+ PD-1+ Tim3 low and lack effector molecules (105, 106). These cells have limited proliferation but are capable of producing cytokine following stimulation (105, 106). Further, since these cells have self-renewal potential and respond to PD-1 blockade therapy, these cells are of interest as targets for cancer therapeutics (100, 109).

CXCR5+ CD8 T cells have a variety of phenotypes and proposed functions. They have been described as cytotoxic, follicular helper-like, and precursors to either exhausted or memory cells (98, 99, 105, 109-112). These functions are distributed across different immunological settings. As these cells continue to be studied, whether these CXCR5+ CD8 T cells are the same population or are in fact different subsets, and how the differing phenotypes and functions are generated and regulated will need to be assessed.

## **Summary**

In this dissertation, we seek to understand the contribution of CD8 T cells and CXCR5+ CD8 Tfc cells to autoimmune disease by exploring the mechanisms by which CD8 T cells promote disease. The mechanisms underlying the development and progression of autoimmune disease has yet to be fully established. Using a model of systemic autoimmune disease (IL-2R $\alpha$ -KO), we show that a culmination of factors, including Treg dysfunction, changes in T cell activation, and differences in cytokine signaling combine to drive disease progression and kinetics (Chapter 2). The function of CXCR5+ CD8 T cells and their localization, particularly how this relates to their role within the germinal center reaction, remains to be assessed. Here we show that CXCR5+ CD8 T cells localize to the germinal center and B cell follicle, produce cytokines indicative of CD4 Tfh cells throughout the B cell follicle, and that CD8-produced IL-21 does not impact B cell function as CD4 Tfh-produced IL-21 does (Chapter

3). This work demonstrates that CXCR5+ CD8 T cells share many features with CD4 Tfh cells but may contribute to B cell function through a different combination of mechanisms than CD4 Tfh cells.

## REFERENCES

1. 2012. Autoimmune diseases. Office on Women's Health, Womenshealth.gov.
2. Barcellini, W. 2015. New Insights in the Pathogenesis of Autoimmune Hemolytic Anemia. *Transfus Med Hemother* 42: 287-293.
3. Chen, Y. G., C. E. Mathews, and J. P. Driver. 2018. The Role of NOD Mice in Type 1 Diabetes Research: Lessons from the Past and Recommendations for the Future. *Front Endocrinol (Lausanne)* 9: 51.
4. Liu, J., G. Karypis, K. L. Hippen, A. L. Vegoe, P. Ruiz, G. S. Gilkeson, and T. W. Behrens. 2006. Genomic view of systemic autoimmunity in MRLlpr mice. *Genes Immun* 7: 156-168.
5. Andrews, B. S., R. A. Eisenberg, A. N. Theofilopoulos, S. Izui, C. B. Wilson, P. J. McConahey, E. D. Murphy, J. B. Roths, and F. J. Dixon. 1978. Spontaneous murine lupus-like syndromes. Clinical and immunopathological manifestations in several strains. *J Exp Med* 148: 1198-1215.
6. Sakaguchi, S., T. Yamaguchi, T. Nomura, and M. Ono. 2008. Regulatory T cells and immune tolerance. *Cell* 133: 775-787.
7. Bayati, F., M. Mohammadi, M. Valadi, S. Jamshidi, A. M. Foma, and E. Sharif-Paghaleh. 2020. The Therapeutic Potential of Regulatory T Cells: Challenges and Opportunities. *Front Immunol* 11: 585819.
8. Sakaguchi, S., N. Mikami, J. B. Wing, A. Tanaka, K. Ichiyama, and N. Ohkura. 2020. Regulatory T Cells and Human Disease. *Annu Rev Immunol* 38: 541-566.
9. Wing, J. B., A. Tanaka, and S. Sakaguchi. 2019. Human FOXP3+ regulatory T cell heterogeneity and function in autoimmunity and cancer. *Immunity* 50: 302-316.
10. Couper, K. N., D. G. Blount, and E. M. Riley. 2008. IL-10: the master regulator of immunity to infection. *J Immunol* 180: 5771-5777.
11. Wan, Y. Y., and R. A. Flavell. 2007. 'Yin-Yang' functions of transforming growth factor-beta and T regulatory cells in immune regulation. *Immunol Rev* 220: 199-213.
12. Liu, H., I. Shalev, J. Manuel, W. He, E. Leung, J. Crookshank, M. F. Liu, J. Diao, M. Catral, D. A. Clark, D. E. Isenman, R. M. Gorczynski, D. R. Grant, L. Zhang, M. J. Phillips, M. I. Cybulsky, and G. A. Levy. 2008. The FGL2-FcgammaRIIB pathway: a novel mechanism leading to immunosuppression. *Eur J Immunol* 38: 3114-3126.
13. Grossman, W. J., J. W. Verbsky, B. L. Tollefsen, C. Kemper, J. P. Atkinson, and T. J. Ley. 2004. Differential expression of granzymes A and B in human cytotoxic lymphocyte subsets and T regulatory cells. *Blood* 104: 2840-2848.
14. Yadav, M., C. Louvet, D. Davini, J. M. Gardner, M. Martinez-Llordella, S. Bailey-Bucktrout, B. A. Anthony, F. M. Sverdrup, R. Head, D. J. Kuster, P. Ruminski, D. Weiss, D. Von Schack, and J. A. Bluestone. 2012. Neuropilin-1 distinguishes natural and inducible regulatory T cells among regulatory T cell subsets in vivo. *J Exp Med* 209: 1713-1722, S1711-1719.
15. Arce-Sillas, A., D. D. Álvarez-Luquín, B. Tamaya-Domínguez, S. Gomez-Fuentes, A. Trejo-García, M. Melo-Salas, G. Cárdenas, J. Rodríguez-Ramírez, and L. Adalid-Peralta. 2016. Regulatory T Cells: Molecular Actions on Effector Cells in Immune Regulation. *J Immunol Res* 2016: 1720827.
16. Ha, D., A. Tanaka, T. Kibayashi, A. Tanemura, D. Sugiyama, J. B. Wing, E. L. Lim, K. W. W. Teng, D. Adeegbe, E. W. Newell, I. Katayama, H. Nishikawa, and S. Sakaguchi. 2019. Differential control of human Treg and effector T cells in tumor immunity by Fc-engineered anti-CTLA-4 antibody. *Proc Natl Acad Sci U S A* 116: 609-618.

17. Vitiello, L., S. Gorini, G. Rosano, and A. la Sala. 2012. Immunoregulation through extracellular nucleotides. *Blood* 120: 511-518.
18. Deaglio, S., K. M. Dwyer, W. Gao, D. Friedman, A. Usheva, A. Erat, J. F. Chen, K. Enyoloji, J. Linden, M. Oukka, V. K. Kuchroo, T. B. Strom, and S. C. Robson. 2007. Adenosine generation catalyzed by CD39 and CD73 expressed on regulatory T cells mediates immune suppression. *J Exp Med* 204: 1257-1265.
19. Kondělková, K., D. Vokurková, J. Krejsek, L. Borská, Z. Fiala, and A. Ctirad. 2010. Regulatory T cells (TREG) and their roles in immune system with respect to immunopathological disorders. *Acta Medica (Hradec Kralove)* 53: 73-77.
20. Romano, M., G. Fanelli, C. J. Albany, G. Giganti, and G. Lombardi. 2019. Past, Present, and Future of Regulatory T Cell Therapy in Transplantation and Autoimmunity. *Front Immunol* 10: 43.
21. Sakaguchi, S., N. Sakaguchi, M. Asano, M. Itoh, and M. Toda. 1995. Immunologic self-tolerance maintained by activated T cells expressing IL-2 receptor alpha-chains (CD25). Breakdown of a single mechanism of self-tolerance causes various autoimmune diseases. *J Immunol* 155: 1151-1164.
22. Feinerman, O., G. Jentsch, K. E. Tkach, J. W. Coward, M. M. Hathorn, M. W. Sneddon, T. Emonet, K. A. Smith, and G. Altan-Bonnet. 2010. Single-cell quantification of IL-2 response by effector and regulatory T cells reveals critical plasticity in immune response. *Mol Syst Biol* 6: 437.
23. O'Gorman, W. E., H. Dooms, S. H. Thorne, W. F. Kuswanto, E. F. Simonds, P. O. Krutzik, G. P. Nolan, and A. K. Abbas. 2009. The initial phase of an immune response functions to activate regulatory T cells. *J Immunol* 183: 332-339.
24. Dall'Era, M., M. L. Pauli, K. Remedios, K. Taravati, P. M. Sandoval, A. L. Putnam, A. Lares, A. Haemel, Q. Tang, M. Hellerstein, M. Fitch, J. McNamara, B. Welch, J. A. Bluestone, D. Wofsy, M. D. Rosenblum, and A. C. o. Excellence. 2019. Adoptive Treg Cell Therapy in a Patient With Systemic Lupus Erythematosus. *Arthritis Rheumatol* 71: 431-440.
25. Bluestone, J. A., J. H. Buckner, M. Fitch, S. E. Gitelman, S. Gupta, M. K. Hellerstein, K. C. Herold, A. Lares, M. R. Lee, K. Li, W. Liu, S. A. Long, L. M. Masiello, V. Nguyen, A. L. Putnam, M. Rieck, P. H. Sayre, and Q. Tang. 2015. Type 1 diabetes immunotherapy using polyclonal regulatory T cells. *Sci Transl Med* 7: 315ra189.
26. Trotta, E., P. H. Bessette, S. L. Silveria, L. K. Ely, K. M. Jude, D. T. Le, C. R. Holst, A. Coyle, M. Potempa, L. L. Lanier, K. C. Garcia, N. K. Crellin, I. J. Rondon, and J. A. Bluestone. 2018. A human anti-IL-2 antibody that potentiates regulatory T cells by a structure-based mechanism. *Nat Med* 24: 1005-1014.
27. Esensten, J. H., Y. D. Muller, J. A. Bluestone, and Q. Tang. 2018. Regulatory T-cell therapy for autoimmune and autoinflammatory diseases: The next frontier. *J Allergy Clin Immunol* 142: 1710-1718.
28. Raffin, C., L. T. Vo, and J. A. Bluestone. 2020. Treg cell-based therapies: challenges and perspectives. *Nat Rev Immunol* 20: 158-172.
29. Smith, G. A., J. Taunton, and A. Weiss. 2017. IL-2R $\beta$  abundance differentially tunes IL-2 signaling dynamics in CD4. *Sci Signal* 10.
30. Au-Yeung, B. B., G. A. Smith, J. L. Mueller, C. S. Heyn, R. G. Jaszczak, A. Weiss, and J. Zikherman. 2017. IL-2 Modulates the TCR Signaling Threshold for CD8 but Not CD4 T Cell Proliferation on a Single-Cell Level. *J Immunol* 198: 2445-2456.

31. Ross, S. H., and D. A. Cantrell. 2018. Signaling and Function of Interleukin-2 in T Lymphocytes. *Annu Rev Immunol* 36: 411-433.
32. Spolski, R., P. Li, and W. J. Leonard. 2018. Biology and regulation of IL-2: from molecular mechanisms to human therapy. *Nat Rev Immunol* 18: 648-659.
33. Malek, T. R., and I. Castro. 2010. Interleukin-2 receptor signaling: at the interface between tolerance and immunity. *Immunity* 33: 153-165.
34. Lan, R. Y., C. Selmi, and M. E. Gershwin. 2008. The regulatory, inflammatory, and T cell programming roles of interleukin-2 (IL-2). *J Autoimmun* 31: 7-12.
35. Schmandt, R., M. Fung, N. Arima, N. Zhang, B. Leung, C. May, S. Gibson, M. Hill, W. Green, and G. B. Mills. 1992. T-lymphocyte proliferation: tyrosine kinases in interleukin 2 signal transduction. *Baillieres Clin Haematol* 5: 551-573.
36. Liao, W., J. X. Lin, and W. J. Leonard. 2011. IL-2 family cytokines: new insights into the complex roles of IL-2 as a broad regulator of T helper cell differentiation. *Curr Opin Immunol* 23: 598-604.
37. Hoyer, K. K., H. Dooks, L. Barron, and A. K. Abbas. 2008. Interleukin-2 in the development and control of inflammatory disease. *Immunol Rev* 226: 19-28.
38. Lord, J. D., B. C. McIntosh, P. D. Greenberg, and B. H. Nelson. 2000. The IL-2 receptor promotes lymphocyte proliferation and induction of the c-myc, bcl-2, and bcl-x genes through the trans-activation domain of Stat5. *J Immunol* 164: 2533-2541.
39. Sadlack, B., J. Löhler, H. Schorle, G. Klebb, H. Haber, E. Sickel, R. J. Noelle, and I. Horak. 1995. Generalized autoimmune disease in interleukin-2-deficient mice is triggered by an uncontrolled activation and proliferation of CD4+ T cells. *Eur J Immunol* 25: 3053-3059.
40. Gravano, D. M., M. Al-Kuhlani, D. Davini, P. D. Sanders, J. O. Manilay, and K. K. Hoyer. 2016. CD8(+) T cells drive autoimmune hematopoietic stem cell dysfunction and bone marrow failure. *J Autoimmun* 75: 58-67.
41. Willerford, D. M., J. Chen, J. A. Ferry, L. Davidson, A. Ma, and F. W. Alt. 1995. Interleukin-2 receptor alpha chain regulates the size and content of the peripheral lymphoid compartment. *Immunity* 3: 521-530.
42. Sadlack, B., H. Merz, H. Schorle, A. Schimpl, A. C. Feller, and I. Horak. 1993. Ulcerative colitis-like disease in mice with a disrupted interleukin-2 gene. *Cell* 75: 253-261.
43. Barron, L., H. Dooks, K. K. Hoyer, W. Kuswanto, J. Hofmann, W. E. O'Gorman, and A. K. Abbas. 2010. Cutting edge: mechanisms of IL-2-dependent maintenance of functional regulatory T cells. *J Immunol* 185: 6426-6430.
44. Rahimy, E., J. D. Pitcher, S. B. Pangelinan, W. Chen, W. J. Farley, J. Y. Niederkorn, M. E. Stern, D. Q. Li, S. C. Pflugfelder, and C. S. De Paiva. 2010. Spontaneous autoimmune dacryoadenitis in aged CD25KO mice. *Am J Pathol* 177: 744-753.
45. Pelegriño, F. S., E. A. Volpe, N. B. Gandhi, D. Q. Li, S. C. Pflugfelder, and C. S. de Paiva. 2012. Deletion of interferon- $\gamma$  delays onset and severity of dacryoadenitis in CD25KO mice. *Arthritis Res Ther* 14: R234.
46. Brunkow, M. E., E. W. Jeffery, K. A. Hjerrild, B. Paeper, L. B. Clark, S. A. Yasayko, J. E. Wilkinson, D. Galas, S. F. Ziegler, and F. Ramsdell. 2001. Disruption of a new forkhead/winged-helix protein, scurf, results in the fatal lymphoproliferative disorder of the scurfy mouse. *Nat Genet* 27: 68-73.
47. Malek, T. R., A. Yu, V. Vincek, P. Scibelli, and L. Kong. 2002. CD4 regulatory T cells prevent lethal autoimmunity in IL-2Rbeta-deficient mice. Implications for the nonredundant function of IL-2. *Immunity* 17: 167-178.

48. Parackova, Z., J. Kayserova, K. Danova, K. Sismova, E. Dudkova, Z. Sumnik, S. Kolouskova, J. Lebl, K. Stechova, and A. Sediva. 2016. T regulatory lymphocytes in type 1 diabetes: Impaired CD25 expression and IL-2 induced STAT5 phosphorylation in pediatric patients. *Autoimmunity* 49: 523-531.
49. Lieberman, L. A., and G. C. Tsokos. 2010. The IL-2 defect in systemic lupus erythematosus disease has an expansive effect on host immunity. *J Biomed Biotechnol* 2010: 740619.
50. Goropevšek, A., M. Gorenjak, S. Gradišnik, K. Dai, I. Holc, R. Hojs, I. Krajnc, A. Pahor, and T. Avčin. 2017. STAT5 phosphorylation in CD4 T cells from patients with SLE is related to changes in their subsets and follow-up disease severity. *J Leukoc Biol* 101: 1405-1418.
51. Cerosaletti, K., A. Schneider, K. Schwedhelm, I. Frank, M. Tatum, S. Wei, E. Whalen, C. Greenbaum, M. Kita, J. Buckner, and S. A. Long. 2013. Multiple autoimmune-associated variants confer decreased IL-2R signaling in CD4<sup>+</sup> CD25(hi) T cells of type 1 diabetic and multiple sclerosis patients. *PLoS One* 8: e83811.
52. Crotty, S. 2015. A brief history of T cell help to B cells. *Nat Rev Immunol* 15: 185-189.
53. King, C., S. G. Tangye, and C. R. Mackay. 2008. T follicular helper (TFH) cells in normal and dysregulated immune responses. *Annu Rev Immunol* 26: 741-766.
54. Ramiscal, R. R., and C. G. Vinuesa. 2013. T-cell subsets in the germinal center. *Immunol Rev* 252: 146-155.
55. Crotty, S. 2014. T follicular helper cell differentiation, function, and roles in disease. *Immunity* 41: 529-542.
56. Alberts B, J. A., Lewis J, et al. 2002. *Molecular Biology of the Cell*. 4th ed. Garland Science, New York.
57. Forthall, D. N. 2014. Functions of Antibodies. *Microbiol Spectr* 2: 1-17.
58. Choi, J., S. T. Kim, and J. Craft. 2012. The pathogenesis of systemic lupus erythematosus-an update. *Curr Opin Immunol* 24: 651-657.
59. Vinuesa, C. G., and J. G. Cyster. 2011. How T cells earn the follicular rite of passage. *Immunity* 35: 671-680.
60. Crotty, S. 2011. Follicular helper CD4 T cells (TFH). *Annu Rev Immunol* 29: 621-663.
61. Vinuesa, C. G., M. A. Linterman, C. C. Goodnow, and K. L. Randall. 2010. T cells and follicular dendritic cells in germinal center B-cell formation and selection. *Immunol Rev* 237: 72-89.
62. Wu, Y., N. M. van Besouw, Y. Shi, M. J. Hoogduijn, L. Wang, and C. C. Baan. 2016. The Biological Effects of IL-21 Signaling on B-Cell-Mediated Responses in Organ Transplantation. *Front Immunol* 7: 319.
63. Ersching, J., A. Efeyan, L. Mesin, J. T. Jacobsen, G. Pasqual, B. C. Grabiner, D. Dominguez-Sola, D. M. Sabatini, and G. D. Victora. 2017. Germinal Center Selection and Affinity Maturation Require Dynamic Regulation of mTORC1 Kinase. *Immunity* 46: 1045-1058.e1046.
64. Finkin, S., H. Hartweger, T. Y. Oliveira, E. E. Kara, and M. C. Nussenzweig. 2019. Protein Amounts of the MYC Transcription Factor Determine Germinal Center B Cell Division Capacity. *Immunity* 51: 324-336.e325.
65. Zarnegar, B., J. Q. He, G. Oganessian, A. Hoffmann, D. Baltimore, and G. Cheng. 2004. Unique CD40-mediated biological program in B cell activation requires both type 1 and type 2 NF-kappaB activation pathways. *Proc Natl Acad Sci U S A* 101: 8108-8113.
66. Qian, Y., Z. Zhao, Z. Jiang, and X. Li. 2002. Role of NF kappa B activator Act1 in CD40-mediated signaling in epithelial cells. *Proc Natl Acad Sci U S A* 99: 9386-9391.

67. Luo, W., F. Weisel, and M. J. Shlomchik. 2018. B Cell Receptor and CD40 Signaling Are Rewired for Synergistic Induction of the c-Myc Transcription Factor in Germinal Center B Cells. *Immunity* 48: 313-326.e315.
68. Snapper, C. M., and J. J. Mond. 1993. Towards a comprehensive view of immunoglobulin class switching. *Immunol Today* 14: 15-17.
69. Purkerson, J., and P. Isakson. 1992. A two-signal model for regulation of immunoglobulin isotype switching. *FASEB J* 6: 3245-3252.
70. Gigoux, M., J. Shang, Y. Pak, M. Xu, J. Choe, T. W. Mak, and W. K. Suh. 2009. Inducible costimulator promotes helper T-cell differentiation through phosphoinositide 3-kinase. *Proc Natl Acad Sci U S A* 106: 20371-20376.
71. Pedros, C., Y. Zhang, J. K. Hu, Y. S. Choi, A. J. Canonigo-Balancio, J. R. Yates, A. Altman, S. Crotty, and K. F. Kong. 2016. A TRAF-like motif of the inducible costimulator ICOS controls development of germinal center TFH cells via the kinase TBK1. *Nat Immunol* 17: 825-833.
72. Jogdand, G. M., S. Mohanty, and S. Devadas. 2016. Regulators of Tfh Cell Differentiation. *Front Immunol* 7: 520.
73. Papillion, A., M. D. Powell, D. A. Chisolm, H. Bachus, M. J. Fuller, A. S. Weinmann, A. Villarino, J. J. O'Shea, B. León, K. J. Oestreich, and A. Ballesteros-Tato. 2019. Inhibition of IL-2 responsiveness by IL-6 is required for the generation of GC-T. *Sci Immunol* 4.
74. Yu, D., S. Rao, L. M. Tsai, S. K. Lee, Y. He, E. L. Sutcliffe, M. Srivastava, M. Linterman, L. Zheng, N. Simpson, J. I. Ellyard, I. A. Parish, C. S. Ma, Q. J. Li, C. R. Parish, C. R. Mackay, and C. G. Vinuesa. 2009. The transcriptional repressor Bcl-6 directs T follicular helper cell lineage commitment. *Immunity* 31: 457-468.
75. Tubo, N. J., A. J. Pagán, J. J. Taylor, R. W. Nelson, J. L. Linehan, J. M. Ertelt, E. S. Huseby, S. S. Way, and M. K. Jenkins. 2013. Single naive CD4+ T cells from a diverse repertoire produce different effector cell types during infection. *Cell* 153: 785-796.
76. DiToro, D., C. J. Winstead, D. Pham, S. Witte, R. Andargachew, J. R. Singer, C. G. Wilson, C. L. Zindl, R. J. Luther, D. J. Silberger, B. T. Weaver, E. M. Kolawole, R. J. Martinez, H. Turner, R. D. Hatton, J. J. Moon, S. S. Way, B. D. Evavold, and C. T. Weaver. 2018. Differential IL-2 expression defines developmental fates of follicular versus nonfollicular helper T cells. *Science* 361.
77. Baumjohann, D., S. Preite, A. Reboldi, F. Ronchi, K. M. Ansel, A. Lanzavecchia, and F. Sallusto. 2013. Persistent antigen and germinal center B cells sustain T follicular helper cell responses and phenotype. *Immunity* 38: 596-605.
78. Deenick, E. K., A. Chan, C. S. Ma, D. Gatto, P. L. Schwartzberg, R. Brink, and S. G. Tangye. 2010. Follicular helper T cell differentiation requires continuous antigen presentation that is independent of unique B cell signaling. *Immunity* 33: 241-253.
79. Valentine, K. M., D. Davini, T. J. Lawrence, G. N. Mullins, M. Manansala, M. Al-Kuhlani, J. M. Pinney, J. K. Davis, A. E. Beaudin, S. S. Sindi, D. M. Gravano, and K. K. Hoyer. 2018. CD8 Follicular T Cells Promote B Cell Antibody Class Switch in Autoimmune Disease. *The Journal of Immunology*.
80. E, J., F. Yan, Z. Kang, L. Zhu, J. Xing, and E. Yu. 2018. CD8 CXCR5 T cells in tumor-draining lymph nodes are highly activated and predict better prognosis in colorectal cancer. *Hum Immunol* 79: 446-452.
81. Jin, Y., C. Lang, J. Tang, J. Geng, H. K. Song, Z. Sun, and J. Wang. 2017. CXCR5+CD8+ T cells could induce the death of tumor cells in HBV-related hepatocellular carcinoma. *Int Immunopharmacol* 53: 42-48.

82. Xing, J., C. Zhang, X. Yang, S. Wang, Z. Wang, X. Li, and E. Yu. 2017. CXCR5+ CD8+ T cells infiltrate the colorectal tumors and nearby lymph nodes, and are associated with enhanced IgG response in B cells. *Exp Cell Res* 356: 57-63.
83. Bai, M., Y. Zheng, H. Liu, B. Su, Y. Zhan, and H. He. 2017. CXCR5+ CD8+ T cells potently infiltrate pancreatic tumors and present high functionality. *Exp Cell Res* 361: 39-45.
84. Jiang, H., L. Li, J. Han, Z. Sun, Y. Rong, and Y. Jin. 2017. CXCR5+ CD8+ T cells indirectly offer B cell help and are inversely correlated with viral load in chronic hepatitis B infection. *DNA Cell Biol* 36: 321-327.
85. Leong, Y. A., Y. Chen, H. S. Ong, D. Wu, K. Man, C. Deleage, M. Minnich, B. J. Meckiff, Y. Wei, Z. Hou, D. Zotos, K. A. Fenix, A. Atnerkar, S. Preston, J. G. Chipman, G. J. Beilman, C. C. Allison, L. Sun, P. Wang, J. Xu, J. G. Toe, H. K. Lu, Y. Tao, U. Palendira, A. L. Dent, A. L. Landay, M. Pellegrini, I. Comerford, S. R. McColl, T. W. Schacker, H. M. Long, J. D. Estes, M. Busslinger, G. T. Belz, S. R. Lewin, A. Kallies, and D. Yu. 2016. CXCR5(+) follicular cytotoxic T cells control viral infection in B cell follicles. *Nat Immunol* 17: 1187-1196.
86. Ye, L., Y. Li, H. Tang, W. Liu, Y. Chen, T. Dai, R. Liang, M. Shi, S. Yi, G. Chen, and Y. Yang. 2019. CD8+CXCR5+T cells infiltrating hepatocellular carcinomas are activated and predictive of a better prognosis. *Aging (Albany NY)* 11: 8879-8891.
87. Le, K. S., P. Amé-Thomas, K. Tarte, F. Gondois-Rey, S. Granjeaud, F. Orlanducci, E. D. Foucher, F. Broussais, R. Bouabdallah, T. Fest, D. Leroux, S. Yadavilli, P. A. Mayes, L. Xerri, and D. Olive. 2018. CXCR5 and ICOS expression identifies a CD8 T-cell subset with Tfh features in Hodgkin lymphomas. *Blood Adv* 2: 1889-1900.
88. Jiang, H., L. Li, J. Han, Z. Sun, Y. Rong, and Y. Jin. 2017. CXCR5+CD8+ T cells infiltrate the colorectal tumors and nearby lymph nodes, and are associated with enhanced IgG response in B cells. *DNA Cell Biol* 36: 321-327.
89. Allen, C. D., K. M. Ansel, C. Low, R. Lesley, H. Tamamura, N. Fujii, and J. G. Cyster. 2004. Germinal center dark and light zone organization is mediated by CXCR4 and CXCR5. *Nat Immunol* 5: 943-952.
90. Elsner, R. A., D. N. Ernst, and N. Baumgarth. 2012. Single and coexpression of CXCR4 and CXCR5 identifies CD4 T helper cells in distinct lymph node niches during influenza virus infection. *J Virol* 86: 7146-7157.
91. Odegard, J. M., B. R. Marks, L. D. DiPlacido, A. C. Poholek, D. H. Kono, C. Dong, R. A. Flavell, and J. Craft. 2008. ICOS-dependent extrafollicular helper T cells elicit IgG production via IL-21 in systemic autoimmunity. *J Exp Med* 205: 2873-2886.
92. Zhang, N., and M. J. Bevan. 2011. CD8(+) T cells: foot soldiers of the immune system. *Immunity* 35: 161-168.
93. Gravano, D. M., and K. K. Hoyer. 2013. Promotion and prevention of autoimmune disease by CD8+ T cells. *J Autoimmun* 45: 68-79.
94. He, R., S. Hou, C. Liu, A. Zhang, Q. Bai, M. Han, Y. Yang, G. Wei, T. Shen, X. Yang, L. Xu, X. Chen, Y. Hao, P. Wang, C. Zhu, J. Ou, H. Liang, T. Ni, X. Zhang, X. Zhou, K. Deng, Y. Chen, Y. Luo, J. Xu, H. Qi, Y. Wu, and L. Ye. 2016. Follicular CXCR5- expressing CD8(+) T cells curtail chronic viral infection. *Nature* 537: 412-428.
95. Huang, Q., Q. Zhou, H. Zhang, Z. Liu, H. Zeng, Y. Chen, Y. Qu, Y. Xiong, J. Wang, Y. Chang, Y. Xia, Y. Wang, L. Liu, Y. Zhu, L. Xu, B. Dai, J. Guo, Z. Wang, Q. Bai, and W. Zhang. 2020. Identification and validation of an excellent prognosis subtype of muscle-invasive bladder cancer patients with intratumoral CXCR5. *Oncoimmunology* 9: 1810489.

96. Nurieva, R. I., Y. Chung, G. J. Martinez, X. O. Yang, S. Tanaka, T. D. Matskevitch, Y. H. Wang, and C. Dong. 2009. Bcl6 mediates the development of T follicular helper cells. *Science* 325: 1001-1005.
97. Johnston, R. J., A. C. Poholek, D. DiToro, I. Yusuf, D. Eto, B. Barnett, A. L. Dent, J. Craft, and S. Crotty. 2009. Bcl6 and Blimp-1 are reciprocal and antagonistic regulators of T follicular helper cell differentiation. *Science* 325: 1006-1010.
98. Valentine, K. M., and K. K. Hoyer. 2019. CXCR5+ CD8 T Cells: Protective or Pathogenic? *Front Immunol* 10: 1322.
99. Yu, D., and L. Ye. 2018. A Portrait of CXCR5 Follicular Cytotoxic CD8 T cells. *Trends Immunol* 39: 965-979.
100. Im, S. J., M. Hashimoto, M. Y. Gerner, J. Lee, H. T. Kissick, M. C. Burger, Q. Shan, J. S. Hale, T. H. Nasti, A. H. Sharpe, G. J. Freeman, R. N. Germain, H. I. Nakaya, H. H. Xue, and R. Ahmed. 2016. Defining CD8+ T cells that provide the proliferative burst after PD-1 therapy. *Nature* 537: 417-421.
101. Xu, L., Y. Cao, Z. Xie, Q. Huang, Q. Bai, X. Yang, R. He, Y. Hao, H. Wang, T. Zhao, Z. Fan, A. Qin, J. Ye, X. Zhou, L. Ye, and Y. Wu. 2015. The transcription factor TCF-1 initiates the differentiation of T(FH) cells during acute viral infection. *Nat Immunol* 16: 991-999.
102. Miyazaki, M., R. R. Rivera, K. Miyazaki, Y. C. Lin, Y. Agata, and C. Murre. 2011. The opposing roles of the transcription factor E2A and its antagonist Id3 that orchestrate and enforce the naive fate of T cells. *Nat Immunol* 12: 992-1001.
103. Chen, Y., M. Yu, Y. Zheng, G. Fu, G. Xin, W. Zhu, L. Luo, R. Burns, Q. Z. Li, A. L. Dent, N. Zhu, W. Cui, L. Malherbe, R. Wen, and D. Wang. 2019. CXCR5+ PD-1+ follicular helper CD8 T cells control B cell tolerance. *Nat Commun* 10: 4415.
104. Yang, R., A. R. Masters, K. A. Fortner, D. P. Champagne, N. Yanguas-Casás, D. J. Silberger, C. T. Weaver, L. Haynes, and M. Rincon. 2016. IL-6 promotes the differentiation of a subset of naive CD8+ T cells into IL-21-producing B helper CD8+ T cells. *J Exp Med* 213: 2281-2291.
105. de Goër de Herve, M. G., M. Abdoh, S. Jaafoura, D. Durali, and Y. Taoufik. 2019. Follicular CD4 T Cells Tutor CD8 Early Memory Precursors: An Initiatory Journey to the Frontier of B Cell Territory. *iScience* 20: 100-109.
106. Hofland, T., A. W. J. Martens, J. A. C. van Bruggen, R. de Boer, S. Schetters, E. B. M. Remmerswaal, F. J. Bemelman, M. D. Levin, A. D. Bins, E. Eldering, A. P. Kater, and S. H. Tonino. 2021. Human CXCR5+ PD-1+ CD8 T cells in healthy individuals and patients with hematologic malignancies. *Eur J Immunol* 51: 703-713.
107. Verdon, D. J., M. Mulazzani, and M. R. Jenkins. 2020. Cellular and Molecular Mechanisms of CD8+ T cell differentiation, dysfunction and exhaustion. *Int J Mol Sci* 21.
108. Herndler-Brandstetter, D., H. Ishigame, R. Shinnakasu, V. Plajer, C. Stecher, J. Zhao, M. Lietzenmayer, L. Kroehling, A. Takumi, K. Kometani, T. Inoue, Y. Kluger, S. M. Kaech, T. Kurosaki, T. Okada, and R. A. Flavell. 2018. KLRG1+ Effector CD8+ T cells Lose KLRG1, Differentiate into All Memory T Cell Lineages, and Convey Enhanced Protective Immunity. *Immunity* 48: 716-729.e718.
109. Im, S. J., B. T. Konieczny, W. H. Hudson, D. Masopust, and R. Ahmed. 2020. PD-1+ stemlike CD8 T cells are resident in lymphoid tissues during persistent LCMV infection. *Proc Natl Acad Sci U S A* 117: 4292-4299.
110. Fousteri, G., and M. Kuka. 2020. The elusive identity of CXCR5 CD8 T cell in viral infection and autoimmunity: Cytotoxic, regulatory, or helper cells? *Mol Immunol* 119: 101-105.

111. Quigley, M. F., V. D. Gonzalez, A. Granath, J. Andersson, and J. K. Sandberg. 2007. CXCR5+ CCR7- CD8 T cells are early effector memory cells that infiltrate tonsil B cell follicles. *Eur J Immunol* 37: 3352-3362.
112. Hofland, T., A. W. J. Martens, J. A. C. van Bruggen, R. de Boer, S. Schetters, E. B. M. Remmerswaal, F. J. Bemelman, M. D. Levin, A. D. Bins, E. Eldering, A. P. Kater, and S. H. Tonino. 2021. Human CXCR5. *Eur J Immunol* 51: 703-713.

## FIGURES AND FIGURE LEGENDS

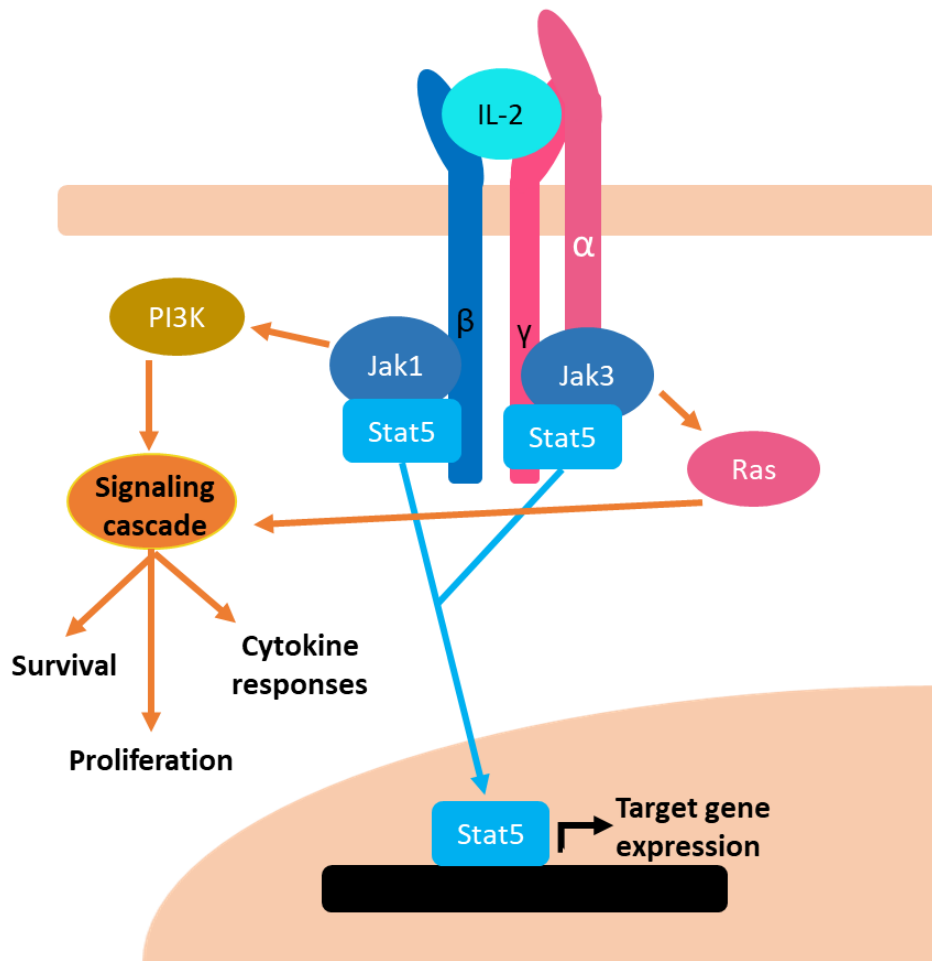


**Figure 1-1: IL-2 signaling pathways.** Upon binding of IL-2 to the IL-2R, Jak-1 and -3 become activated and further activate STAT5, PI3K, and Ras/MEK/Erk pathways to mediate survival, proliferation, cytokine responses, and gene expression.

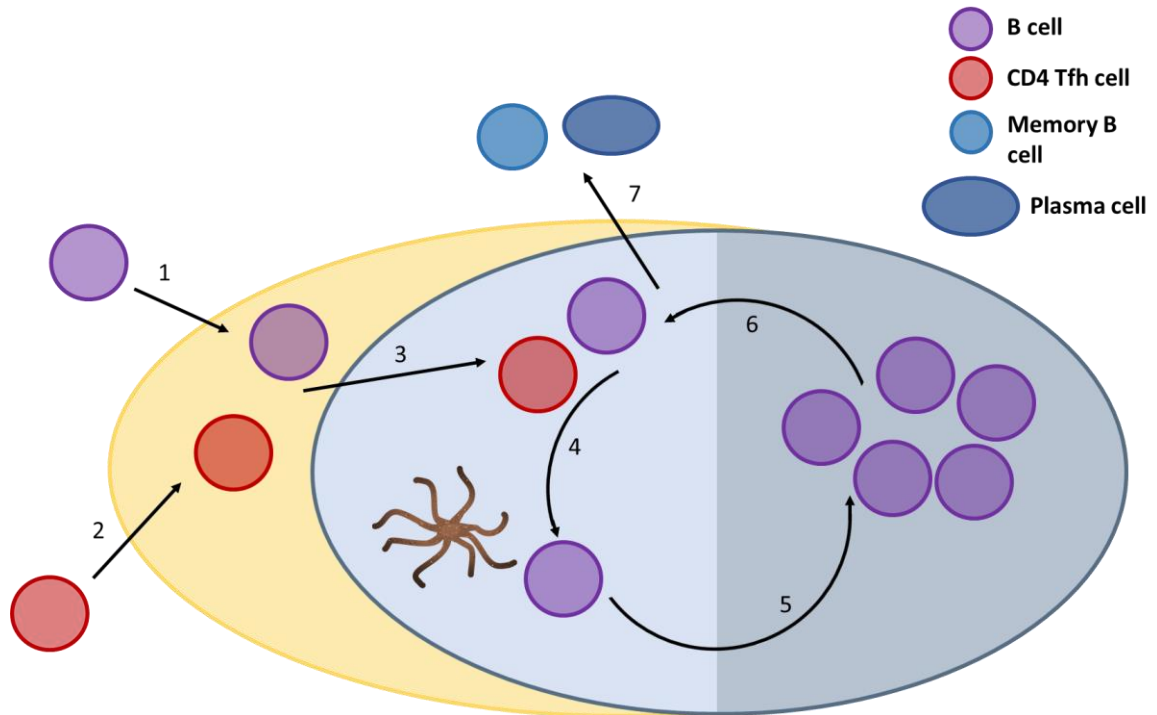


**Figure 1-2: Germinal center reaction.** When B cells become activated, they migrate into the germinal center (blue region). Differentiating CD4 Tfh cells will also migrate into the B cell follicle (yellow region) and then the germinal center, where they provide signals to germinal center B cells to promote the cycling of germinal center B cells between the light zone (light blue region) and dark zone (dark blue region). In the dark zone germinal center B cells will undergo rounds of proliferation and somatic hypermutation before returning to the light zone to receive further antigen and CD4 Tfh cell stimulation. Germinal center B cells eventually leave the germinal center as memory B cells and plasma cells.

## CHAPTER 2

### **T cell signaling and Treg dysfunction correlate to disease kinetics in IL-2R $\alpha$ -KO autoimmune mice**



## OPEN T cell signaling and Treg dysfunction correlate to disease kinetics in IL-2R $\alpha$ -KO autoimmune mice

Genevieve N. Mullins<sup>1,3</sup>, Kristen M. Valentine<sup>1,3</sup>, Mufadhal Al-Kuhlani<sup>2</sup>, Dan Davini<sup>2</sup>, Kirk D. C. Jensen<sup>1,2,3</sup> & Katrina K. Hoyer<sup>1,2,3</sup>✉

IL-2R $\alpha$ , in part, comprises the high affinity receptor for IL-2, a cytokine important in immune proliferation, activation, and regulation. IL-2R $\alpha$  deficient mice (IL-2R $\alpha$ -KO) develop systemic autoimmune disease and die from severe anemia between 10 and 80 days of age. These mice develop kinetically distinct autoimmune progression, with approximately a quarter dying by 21 days of age and half dying after 30 days. This research aims to define immune parameters and cytokine signaling that distinguish cohorts of IL-2R $\alpha$ -KO mice that develop early- versus late-stage autoimmune disease. To investigate these differences, we evaluated complete blood counts (CBC), antibody binding of RBCs, T cell numbers and activation, hematopoietic progenitor changes, and signaling kinetics, during autoimmune hemolytic anemia (AIHA) and bone marrow failure. We identified several alterations that, when combined, correlate to disease kinetics. Early onset disease correlates with anti-RBC antibodies, lower hematocrit, and reduced IL-7 signaling. CD8 regulatory T cells (Tregs) have enhanced apoptosis in early disease. Further, early and late end stage disease, while largely similar, had several differences suggesting distinct mechanisms drive autoimmune disease kinetics. Therefore, IL-2R $\alpha$ -KO disease pathology rates, driven by T cell signaling, promote effector T cell activation and expansion and Treg dysfunction.

IL-2 is a cytokine important for proliferation of activated T cells, and survival and function of Tregs<sup>1–4</sup>. The receptor for IL-2 is comprised of three chains—IL-2R $\alpha$  (CD25), IL-2R $\beta$  (CD122), and the common gamma chain ( $\gamma_c$ ; CD132)<sup>5,6</sup>. IL-2 binding to its receptor activates three signaling pathways, MAPK, PI3K, and JAK1/3-STAT5 pathways<sup>4–6</sup>. These pathways promote cell survival and proliferation, and STAT5-mediated gene expression. IL-2 signaling is strongest and most stable when IL-2R $\alpha$  is present<sup>1,5</sup>. IL-15, a common-gamma cytokine, also utilizes the same  $\beta$  and  $\gamma$  receptor chains, while IL-7 shares the  $\gamma$  chain<sup>6,7</sup>. Mice deficient in IL-2 (IL-2-KO) or its receptor (IL-2R $\alpha$ -KO or IL-2R $\beta$ -KO) develop spontaneous, multi-organ autoimmune disease, including autoimmune hemolytic anemia (AIHA), bone marrow (BM) failure (BMF), inflammatory bowel disease, and dacryoadenitis<sup>8–15</sup>. Decreased IL-2 signaling reduces survival and suppressive function of regulatory T cells (Tregs) that primarily drives disease<sup>1,3,14,15</sup>.

Signaling through IL-2 lowers the threshold of TCR signaling required to initiate proliferation in CD8 T cells, but not in CD4 T cells<sup>16</sup>. In CD8 T cells, IL-2 signaling strength is important in memory development, with lower signaling strength associated with central memory development rather than effector memory<sup>7,17</sup>. Due to the shared IL-2R $\beta$  subunit, these differentiation signals occur in response to both IL-2 and IL-15<sup>7</sup>. In CD4 Tregs, IL-2 signaling stabilizes STAT5-mediated gene expression of FoxP3 promoting suppressive function<sup>3,14</sup>.

We set out to evaluate the mechanisms underlying differences in disease kinetics in IL-2R $\alpha$ -KO mice. IL-2R $\alpha$ -KO mice develop severe autoimmune disease at different rates with some succumbing to disease rapidly and others progressing more slowly<sup>10</sup>. AIHA, thought to be the primary cause of death in IL-2 and IL-2R $\alpha$ -KO mice is caused by autoantibodies against RBC antigens and is measured by the frequency of antibodies bound to RBCs in combination with anemia severity. RBC life span is thus reduced by Fc-mediated phagocytosis and complement-mediated lysis. Conventional AIHA therapy includes splenectomy and general immunosuppressive

<sup>1</sup>Quantitative and Systems Biology Graduate Program, University of California Merced, Merced, CA 95343, USA. <sup>2</sup>Department of Molecular and Cell Biology, School of Natural Sciences, University of California Merced, Merced, CA 95343, USA. <sup>3</sup>Health Sciences Research Institute, University of California Merced, Merced, CA 95343, USA. ✉email: khoyer2@ucmerced.edu

and anti-inflammatory regimens. As IL-2Ra-KO T cells do not proliferate in response to low-dose IL-2<sup>10</sup>, but may still signal with high IL-2 availability, we explored potential differences in IL-2 signaling cascades affecting disease progression. At day 19, we found that symptoms associated with AIHA were more severe in mice that develop early disease versus late disease, and the frequency of common lymphoid progenitors (CLP) and peripheral CD4 and CD8 T cells was increased in early disease. TCR signaling kinetics in the lymph node differed between early and late disease mice and T cells from early disease were more apoptotic. IL-2Ra-KO CD8 T cells from both early and late disease mice responded normally to IL-2, but IL-7 and IL-15 responses differed between early and late disease IL-2Ra-KO T cells. Alterations in signaling responsiveness may drive changes in Treg suppression and T cell differentiation, skewing disease kinetics.

## Results

**Early RBC characteristics predict disease kinetics.** To assess general survival and disease progression in IL-2Ra-KO mice, survival was monitored. IL-2Ra-KO mice die due to anemia-induced hypoxia from 18 to 79 days, with a median survival of 26 days (Fig. 1A). Twenty-six percent of IL-2Ra-KO mice die between 19 and 21 days of age and 38% die after 30 days. Given the rapid disease in IL-2Ra-KO mice, where 100% of mice die by 25 days in our colony, this larger window of disease kinetics was surprising<sup>8,19</sup>. Separation of mice into distinct early and late disease categories based on the age of death may allow an evaluation of early disease drivers.

To assess disease progression in relation to disease outcome, we first sought a biomarker to predict IL-2Ra-KO age of death. Peripheral blood was collected from IL-2Ra-KO and WT mice at 19 days and evaluated by CBC and bound red blood cell (RBC) antibodies. Mice were monitored for survival, and the age of death was recorded and correlated to the parameters from CBC and RBC antibody detection. The strongest Pearson correlations were RBC concentration ( $R^2 = 0.4856$ ), hematocrit ( $R^2 = 0.4807$ ), and percentage RBC bound by IgM antibodies ( $R^2 = 0.5294$ ) (Fig. 1B). While these showed clear correlations, the 95% prediction interval was  $\pm 10$  days, indicating each variable alone does not allow for accurate predictions.

Linear correlation tests alone were not strong enough to predict the age of death but did suggest that blood parameter measurements were strongly correlated with disease outcome; we therefore sought to improve the prediction strength by combining variables together. PCA was performed on variables from CBC and RBC antibody detection. Initial PCA performed on a total of 14 blood variables separated 96.9% of mice into two groups by age of death with 65.1% of variance explained within the first two principal components (Fig. 1C). Regression tree analysis on these data revealed four variables—RBC concentration, hematocrit, white blood cell numbers, and mean platelet volume—as being most important in separating mice by age of death. PCA performed using these four variables split IL-2Ra-KO mice into two groups by age of death, a group of mice that die early (between 19 and 24 days) and a group of mice that die late (24 days or older) with 83.65% of variance explained within the first two principal components (Fig. 1D). Using the four blood parameters, the death could be predicted in 93.8% of mice at 19 days. Furthermore, PC1 in the 4-variable PCA was more highly correlated to the age of death than the 14-variable PC1 (Fig. 1E,F). Together our results reveal a diagnostic tool to predict disease outcome in IL-2Ra-KO mice using blood samples collected early in disease progression.

To assess AIHA disease in relation to disease kinetics, IL-2Ra-KO mice at day 19 were categorized into predicted early (PE) with rapid disease progression or predicted late (PL) with delayed disease progression groups using the four-parameter PCA analysis. Endpoints in the middle time frame (22–26 days) had higher variability, thus a more stringent breakdown of PE (19–21 days) and PL ( $\geq 27$  days) disease groups was utilized for subsequent disease analysis. RBCs collected from these mice were evaluated for binding of IgM and IgG antibodies to evaluate warm (IgM) and cold (IgG) AIHA, each with unique and overlapping etiology, although warm AIHA tends to induce more severe hemolysis<sup>20,21</sup>. Mice in the PE disease group have significantly more RBCs bound by IgM and IgG antibodies than PL mice at day 19 (Fig. 1G). However, PL mice eventually develop high RBC frequencies bound by antibody at disease endpoint (Fig. 1G). At disease endpoint for both groups, day 19–21 PE mice and day 27+ late disease mice show similar signs of advanced anemia, including pale extremities, hunched appearance, and dyspnea (Fig. 1H, Supplementary Table S1). This indicates that early AIHA development leads to early death in IL-2Ra-KO mice, and that several blood parameters, including antibody-binding to RBCs, can be highly predictive of early disease onset.

Given that class-switched IgG antibodies bind to RBCs, we assessed whether this was concomitant to a difference in follicular T cells that mediate B cell class-switching<sup>19,22</sup>. We found that splenic CD4 T follicular helper and CD8 T follicular cell populations were significantly increased in IL-2Ra-KO mice (Supplementary Fig. S1A). CD8 Tfc was also mildly increased in PE compared to PL groups, but the difference didn't reach significance. These observations may account for the difference in frequency of anti-RBC IgG at the same timepoint (Fig. 1G), although a direct comparison between T follicular cells and RBC antibodies did not correlate. By disease endpoint, PL IL-2Ra-KO mice also exhibited significantly increased CD8 Tfc and CD4 Tfh frequency and total number, contributing to endpoint levels of anti-RBC IgG (Supplementary Fig. S1A,B).

**Altered T cell ratio and activation/memory profiles in IL-2Ra-KO mice.** Lymphoproliferation and T cell activation occur in IL-2-KO and IL-2Ra-KO mice<sup>8,10</sup>, however the preceding events and immune parameters that correlate with early disease onset are unknown. To identify such immune phenotypes, mice were evaluated early in disease onset (day 19) and separated into predicted PE or PL disease groups based on four-parameter PCA and assessed for T cell numbers and activation by flow cytometry. CD4:CD8 ratio in the spleen and BM of both disease groups shifted from an expected ratio of ~2:1 to 1:1, although PL mice had a lower frequency of splenic CD4 and CD8 T cells than PE mice, which was not associated with a similar change in total number (Fig. 2A, Supplementary Figs. S2A, S3A). The shift in CD4:CD8 T cell ratio is not a consequence of thymic development, as thymic T cell ratios were normal (Supplementary Fig. S2B).

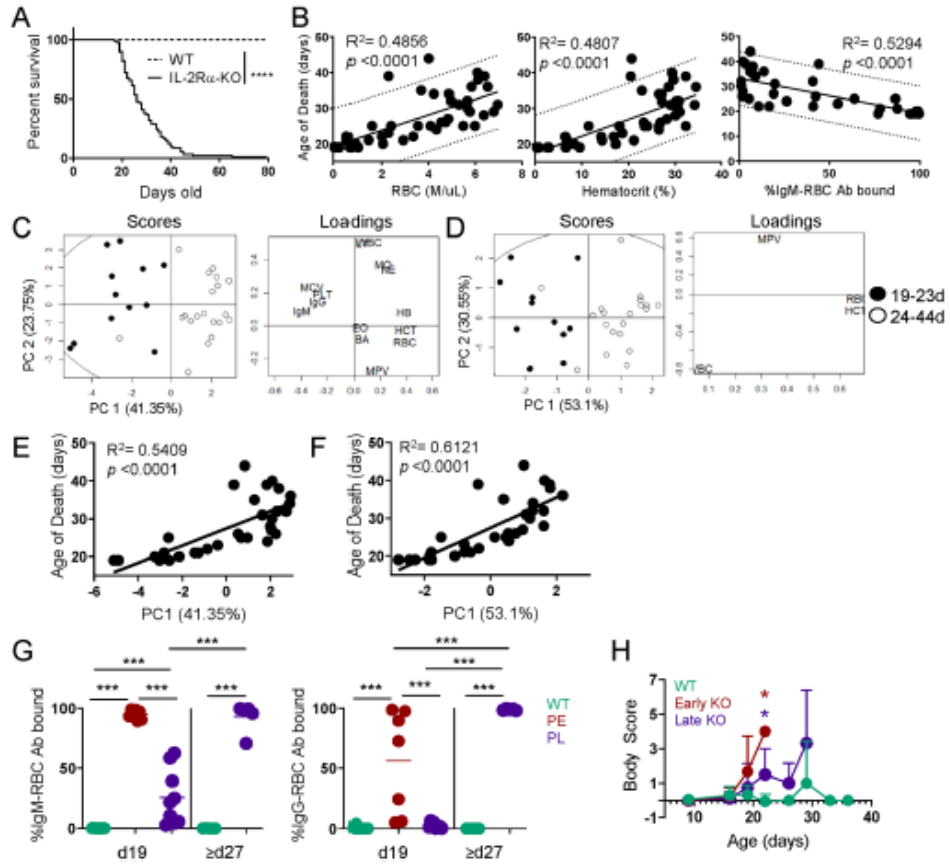


**Figure 1.** Early RBC characteristics predict IL-2Ra-KO disease kinetics. (A) Kaplan-Meier survival curves for WT and IL-2Ra-KO mice. Statistics: log-rank (Mantel-Cox) test, \*\*\*\* $p < 0.001$ ;  $n = 90$  IL-2Ra-KO and 47 WT mice. (B) Dot plots and linear correlations for data collected from day 19 CBC and RBC Ab binding were tested against the age of death of IL-2Ra-KO mice. Pearson correlations with the highest  $R^2$  values are shown. Dotted lines indicate the 95% prediction interval. Statistics:  $p$  values shown on graphs indicate whether the slope of the linear regression is significantly non-zero;  $n = 44$  (RBC and HCT),  $n = 36$  (IgM). (C,E) PCA by singular value decomposition was performed on peripheral blood collected from 19-day old IL-2Ra-KO using 14 variables or (D,F) 4 variables. Percentage on the axis indicate the amount of variance in the data that the principal component explains. (E,F) PC1 is shown against the age of death of the mice. Pearson  $R^2$  values are shown. Statistics:  $p$  values shown on graphs indicate whether the slope of the linear regression is significantly non-zero.  $n = 32$  mice. (G) The frequency of RBC bound by IgM or IgG antibodies at day 19 and late endpoint (d27+).  $n = 7-15$  mice per group for day 19,  $n = 5$  mice per group for day 27 or older. Statistics: one-way ANOVA with multiple comparisons \*\*\*\* $p < 0.001$ . (H) Body score of IL-2KO and WT mice are shown from day 9 onward.  $n = 4$  (PE), 11 (PL), 36 (WT) mice. Statistics: multiple t tests with Benjamini-Hochberg FDR correction; \* $p < 0.001$ . Standard CBC abbreviations are used<sup>37</sup>.

PE and PL IL-2Ra-KO disease groups demonstrated increased T cell activation based on reduced CD62L and elevated CD44 expression, as previously observed in IL-2-KO mice (Fig. 2B,C, Supplementary Fig. S2C). CD8 T cells exhibited markers indicative of an expanded developing central memory population (CD62L<sup>hi</sup>CD44<sup>hi</sup>), and expansion of this CD8 T cell memory population in the spleen associated with late disease kinetics (Fig. 2B,C). Strikingly, splenic CD4 and CD8 T cell central memory was significantly decreased in mice at late disease endpoint (Fig. 2C). These results indicate that a fairly normal splenic T cell frequency and memory T expansion

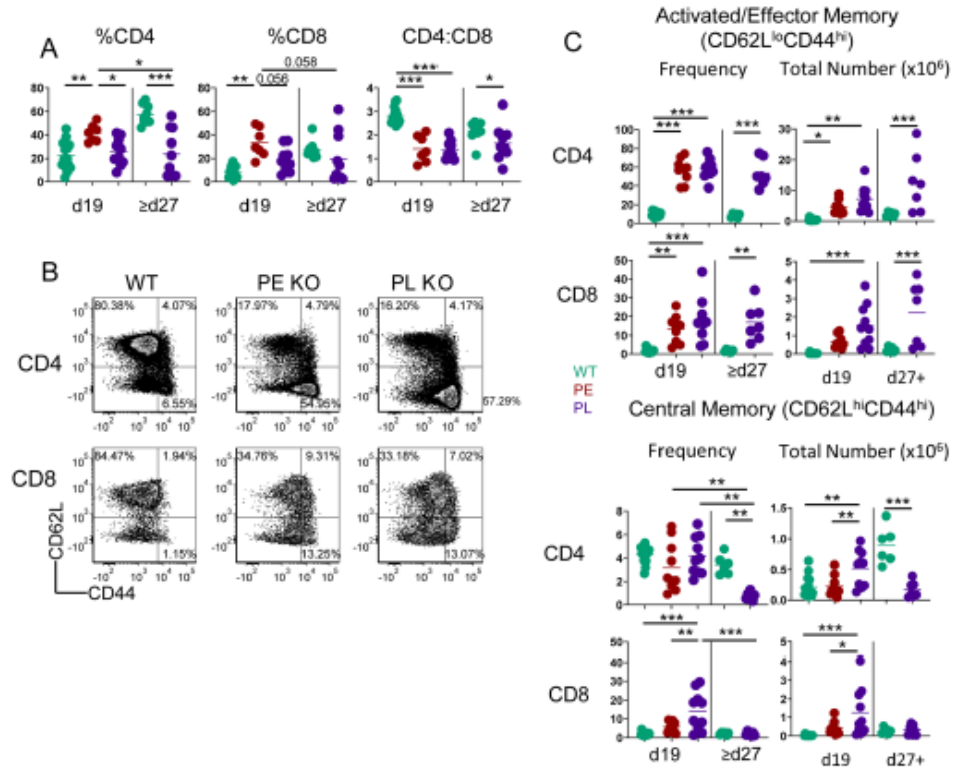


**Figure 2.** IL-2R $\alpha$ -KO T cells express markers indicative of developing memory. (A) CD4 and CD8 T cell frequency of live B220-CD11b-CD11c-Gr-1-cells and the ratio of CD4:CD8 T cells in spleen are shown for 19-day-old and late endpoint (d27+) WT and IL-2R $\alpha$ -KO mice. (B) Representative flow plots of CD44 and CD62L expression on spleen CD4 and CD8 T cells in 19-day-old WT and IL-2R $\alpha$ -KO mice. (C) Frequency and total number of CD4 and CD8 T cell activation state in 19-day-old and late endpoint (d27+) WT and IL-2R $\alpha$ -KO mice. Statistics: one-way ANOVA with Benjamini–Hochberg FDR correction; \* $p < 0.05$ , \*\* $p < 0.01$ , \*\*\* $p < 0.001$ ;  $n = 5–10$  mice per experimental group. Non-significant comparisons are not shown. For total number, comparisons between mice of different ages are not shown due to differences in mouse size.

are associated with slower disease development. Conversely, increased T cell splenic frequencies with normal frequencies of memory T cell populations are associated with rapid disease progression.

**IL-2R $\alpha$ -KO mice exhibit kinetic-dependent differences in CLP frequency.** Mice lacking IL-2 also develop severe BMF contributing to anemia development<sup>11,23</sup>. We evaluated whether there were differences in BM stem cell and progenitor populations between PE and PL IL-2R $\alpha$ -KO mice. Since IL-2R $\alpha$ -KO mice die from hypoxia, dysregulated RBC development is critical to disease endpoint<sup>11</sup>. As such, we assessed RBC precursor populations, which gain Ter119 and lose CD71 expression as they mature, moving from precursor I (Ter119<sup>int</sup>CD71<sup>high</sup>) progressively to the precursor IV stage (Ter119<sup>hi</sup>CD71<sup>neg</sup>)<sup>24</sup>. At day 19, no deficiencies in RBC development and maturation were observed, although there is an increase in precursor IV cells in some PE mice (Fig. 3A, Supplementary Fig. S3B), that does not translate to changes in the megakaryocyte-erythrocyte progenitors (MEP; Fig. 3D). In contrast to IL-2-KO disease, we observe no major alteration in IL-2R $\alpha$ -KO BM erythrocyte precursors during early endpoint disease, although some changes were observed in late stage endpoints, despite similar physical signs of anemia, which includes an increase in precursors I/II, but a decrease in later-stage RBC progenitors (precursor IV) (Fig. 3A, Supplementary Fig. S3B). These data suggest that early disease is not driven by RBC progenitor defects but may be important in late end-stage disease.

Next, PE and PL IL-2R $\alpha$ -KO and WT BM was evaluated for hematopoietic progenitors (Fig. 3B,C). IL-2R $\alpha$ -KO mice in both groups exhibited increased LSK frequency and total number and decreased common myeloid

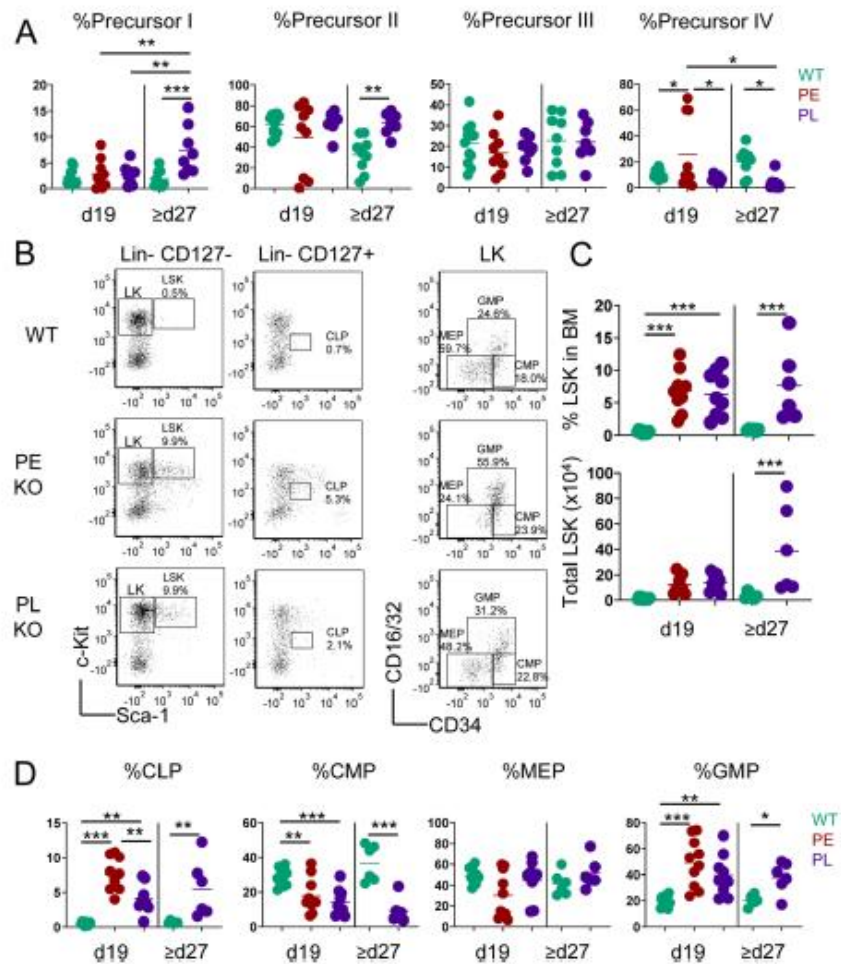


**Figure 3.** IL-2Ra-KO mice exhibit kinetic-dependent differences in CLP and RBC precursor frequency. **(A)** Frequency of RBC precursor analysis by expression of CD71 and Ter119 in WT and IL-2Ra-KO mice at day 19 and day  $\geq 27$ . **(B)** Representative flow plots for hematopoietic progenitor populations in BM of 19-day-old WT and IL-2Ra-KO mice. **(C)** Frequency and total number of LSK cells in 19-day-old and late endpoint (d27+) WT and IL-2Ra-KO mice. **(D)** Frequency of hematopoietic progenitor populations in 19-day-old and late endpoint (d27+) WT and IL-2Ra-KO mice. Statistics: one-way ANOVA with Benjamini–Hochberg FDR correction; \* $p < 0.05$ , \*\* $p < 0.01$ , \*\*\* $p < 0.001$ ;  $n = 9–12$  mice per experimental group. Non-significant comparisons are not shown. For total number, comparisons between mice of different ages are not shown to due differences in mouse size.

progenitors (CMP) compared to WT (Fig. 3C,D, Supplementary Fig. S3C). Common lymphoid progenitors (CLP) and granulocyte monocyte progenitor (GMP) frequency, but not total number, was increased compared to WT (Fig. 3D, Supplementary Fig. S3C). In IL-2-KO mice, expanded LSKs were less competitive relative to WT LSKs, driving a BMF phenotype<sup>11</sup>. Similar to IL-2-KO mice, BM progenitor frequency is altered in IL-2Ra-KO mice. Importantly, CLP frequency was higher in PE versus PL mice, perhaps contributing to increased splenic CD4 and CD8 T cell frequency in these mice.

**Unchanged thymic development in IL-2R $\alpha$ -KO mice.** To determine whether changes in BM CLP frequency translated to changes in thymic T cell development, we assessed thymic T cell populations and thymic CLP frequency in WT and IL-2R $\alpha$ -KO mice. Despite increases in BM CLP, thymic CLP frequencies and numbers were unchanged at both day 19 and late endpoint (Supplementary Fig. S4A). In agreement with previous work on IL-2R $\alpha$ -KO mice<sup>10</sup>, there were no significant changes to developing T cell populations, including single-positive, double-positive, and double-negative (Supplementary Fig. S4B,C). This data suggests that all changes to peripheral T cell population frequencies are due to changes in the periphery, not from changes during development.

**IL-2R $\alpha$ -KO Tregs acquire effector functionality.** A major defect in IL-2-KO and IL-2 signaling deficient mice is a reduction in CD4 Treg frequency and function, so we assessed whether disease outcome was associated with Treg frequency<sup>25–27</sup>. Surprisingly, splenic IL-2R $\alpha$ -KO CD4 and CD8 Treg frequency was comparable to WT (Fig. 4A, Supplementary Fig. S5A)<sup>5</sup>.

We next evaluated whether disease kinetics was determined by cytokine production or differential signaling in response to cytokines. Elevated serum IL-2 levels have been observed in C57BL/6 IL-2R $\alpha$ -KO mice<sup>28</sup>, and IFN $\gamma$  is critical for early autoimmune disease in IL-2-KO mice<sup>11,12,23,29,30</sup>. A significant frequency of IL-2R $\alpha$ -KO CD4 and CD8 T cells produced IL-2, IFN $\gamma$ , and a combination of both cytokines, however this frequency was similar between PE and PL IL-2R $\alpha$ -KO mice (Fig. 4B1,B2). A higher frequency of PE IL-2R $\alpha$ -KO CD4 and CD8 Treg cells also expressed IFN $\gamma$  compared to WT, suggesting a gain of effector function (Fig. 4C, Supplementary Fig. S5B,C). FoxP3+ Tregs conversion into effector cells has been demonstrated under inflammatory conditions, including autoimmune disease<sup>31–33</sup>. To determine whether IL-2R $\alpha$ -KO CD4 Treg cells retain a suppressive phenotype, we assessed IL-10 production and CTLA-4 expression. WT and IL-2R $\alpha$ -KO mice had similar IL-10+ CD4 Treg frequencies (Fig. 4D), but CTLA-4 expression was slightly elevated in PE compared to WT CD4 Treg cells (Fig. 4E). Together this data suggests that IL-2R $\alpha$ -KO CD4 Treg cells have acquired effector capacity while largely retaining CTLA-4 expression. Strikingly, CTLA-4 was primarily expressed on FoxP3– CD4 T cells in IL-2R $\alpha$ -KO (Fig. 4E). Additionally, we found an increase in IL-10 producing CD8 T and CD8 Treg cells in PE mice and PL mice compared to WT (Fig. 4G), although PL increases were not significant due to the larger spread of the data.

**Elevated IL-2R $\beta$  expression on IL-2R $\alpha$ -KO CD8 T cells.** Cytokines IL-2, IL-7, and IL-15 provide necessary survival signals to T cells<sup>34,35</sup>. Elevated IL-7R $\alpha$  expression on IL-2-KO CD4 T cells promotes autoimmunity<sup>36,37</sup>. To assess whether disease outcome was associated with differences in T cell capacity to respond to these cytokines, IL-2R $\beta$  and IL-7R $\alpha$  expression on T cells was evaluated. IL-2R $\beta$  expression was elevated on IL-2R $\alpha$ -KO CD4, CD8, and CD8 Treg cells in the spleen compared to WT (Fig. 5A). Differences in PE and PL CD8 T cell expression of IL-2R $\beta$  were clearly observed in naive and central memory T cells, but not in activated/effector memory cells (Fig. 5C). IL-7R $\alpha$  expression was mildly decreased on splenic CD4 Tregs from PL mice (Fig. 5B). Differences in IL-2R $\beta$  expression observed in CD4 and CD8 T cells in IL-2R $\alpha$ -KO mice were not explained by disease kinetics. Cytokine receptor expression levels indicate a differing capacity for CD4 and CD8 T cell responses to IL-2 and IL-15 in the absence of IL-2R $\alpha$  signaling, suggesting a possible mechanism for disease kinetics.

**IL-2R $\alpha$ -KO T cells are differentially capable of responding to IL-2.** IL-2 signaling in T cells lowers the threshold of TCR stimulation needed for CD8 T cell proliferation, and higher CD8 T cell basal IL-2R $\beta$  expression allows for sustained IL-2 signaling, leading CD8 T cells to proliferate earlier than CD4 T cells<sup>16,38</sup>. Since IL-2R $\alpha$ -KO CD8 T cells have two-fold higher IL-2R $\beta$  expression than WT CD8 T cells (Fig. 5A), we evaluated the signaling capacity of IL-2R $\alpha$ -KO T cells. To assess whether the lack of IL-2R $\alpha$  would impact TCR signaling, we measured ribosomal protein S6 phosphorylation following TCR stimulation in splenocytes. We found no significant differences in response to TCR stimulation (Fig. 6A). IL-2R $\alpha$ -KO T cell response to IL-2 was assessed by STAT5 phosphorylation. High IL-2 levels utilized for these stimulations exist in IL-2R $\alpha$ -KO mice<sup>28</sup>. IL-2R $\alpha$ -KO CD4 Treg cells were less capable of signaling in response to IL-2 regardless of disease kinetics (Fig. 6B). However, STAT5 phosphorylation in response to IL-2 was similar between WT and IL-2R $\alpha$ -KO CD8 T cells at all doses, perhaps because elevated IL-2R $\beta$  compensates for absence of IL-2R $\alpha$  on IL-2R $\alpha$ -KO cells (Fig. 6B). WT and IL-2R $\alpha$ -KO CD4 T and CD8 Treg cells were non-responsive to IL-2, as previously observed for CD4 T cells in *ex vivo* re-stimulations<sup>16</sup>. Since IL-15 shares receptor subunits with IL-2, we assessed whether IL-2R $\alpha$ -KO T cells respond differentially to IL-15 via STAT5. CD8 T, and CD4 and CD8 Treg cells responded similarly to IL-15 stimulation between WT and IL-2R $\alpha$ -KO mice, while IL-2R $\alpha$ -KO CD4 T cells were more responsive to IL-15 stimulation than their WT counterparts (Fig. 6C). PL IL-2R $\alpha$ -KO CD8 T, CD4 Treg, and CD8 Treg cells were also more responsive than PE counterparts (Fig. 6C), although these differences were smaller and non-significant.

Splenic IL-2R $\alpha$ -KO CD4 Treg cells had increased IL-7R $\alpha$  surface expression compared to WT (Fig. 5B). To determine whether this receptor difference resulted in a differential response to IL-7, we assessed pSTAT5 levels. Surprisingly, given similar IL-7R $\alpha$  expression, PE IL-2R $\alpha$ -KO CD8 T and CD8 Treg cells exhibited reduced IL-7 responsiveness (Fig. 6D). Despite differences in IL-7R $\alpha$  expression on splenic CD4 Treg cells, responsiveness to IL-7 was unchanged (Fig. 6D).

To evaluate whether differential signaling outcomes impact T cell proliferation and apoptosis, Ki67 and Annexin V expression was assessed directly *ex vivo*. IL-2R $\alpha$ -KO CD4 T and CD8 Treg cells proliferated more than WT T cells (Fig. 7A,B). Further, PE IL-2R $\alpha$ -KO CD4 T and CD8 Treg cells exhibited enhanced apoptosis (Fig. 7A,B). The increased apoptosis seen in PE IL-2R $\alpha$ -KO CD4 T cells may account for the greater frequency

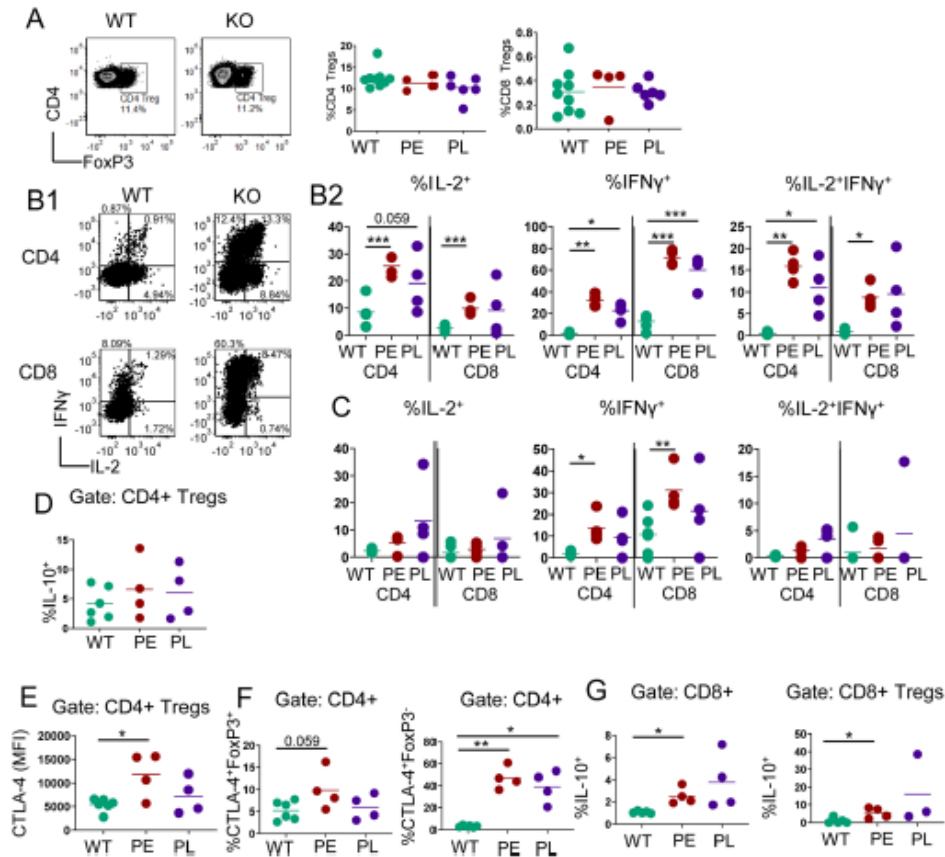


**Figure 4.** IL-2Ra-KO Tregs acquire effector functionality. (A) Representative flow plots, and frequency of CD4 and CD8 Tregs in the spleen in 19-day-old WT and IL-2Ra-KO mice.  $n = 4-11$  mice per experimental group. Representative flow plots and frequency of T cells producing IL-2 and IFN $\gamma$  in 19-day-old WT and IL-2Ra-KO LN T cells (B1,B2) or Tregs (C) post 5-h PMA and ionomycin stimulation.  $n = 4-6$  mice per experimental group. (D) CTLA-4 expression on CD4 Treg cells at day 19 by mean fluorescent intensity (MFI). (E) Frequency of IL-10+ 19-day-old WT and IL-2Ra-KO CD4 Treg cells post 5-h PMA and ionomycin stimulation. (F) Frequency of CTLA-4+FoxP3+CD4 T cells or CTLA-4+FoxP3- CD4 T cells are shown for 19-day-old WT and IL-2Ra-KO mice. (G) Frequency of IL-10+ 19-day-old WT and IL-2Ra-KO CD8 T and CD8 Treg cells post 5-h PMA and ionomycin stimulation.  $n = 4-6$  mice per experimental group over 4 independent experiments. Statistics: unpaired Student's t test; \* $p < 0.05$ , \*\* $p < 0.01$ , \*\*\* $p < 0.001$ . Non-significant comparisons are not shown.

of PE IL-2Ra-KO CD8 T cells. Increased apoptosis of PE IL-2Ra-KO CD8 Treg cells may contribute to more rapid disease kinetics.

While the primary site of hemolytic anemia is the spleen, we also performed staining and functional assessments on lymphocytes as disease in IL-2Ra-KO and IL-2-KO mice is systemic and lymph nodes are a site of T cell activation. While much of what we found in the lymph nodes mirrored that seen in the spleen, there were distinct changes that were present in the lymph nodes that were not present in the spleen. A higher frequency of IL-2Ra-KO lymph node CD4 T cells from PL mice exhibited an emerging memory population (CD62L<sup>hi</sup>CD44<sup>hi</sup>) relative to PE mice, as is seen with CD8 T cells in the spleen (Fig. 2C, Supplementary Fig. S6A). As is expected in this model, CD4 and CD8 Tregs are reduced in frequency in the lymph node, contrasting what is seen in the spleen (Fig. 4A, Supplementary Fig. S6B)<sup>5</sup>. IL-10-producing CD8 T and CD8 Treg cells were reduced in PE IL-2Ra-KO mice compared to PL and WT, suggesting reduced suppression at these sites of T cell activation

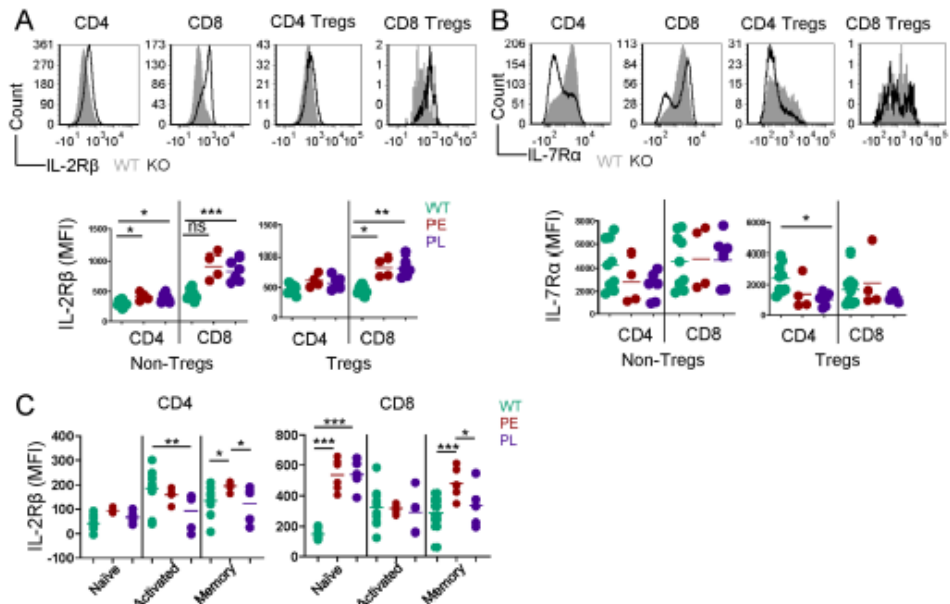


**Figure 5.** IL-2Ra-KO CD8 T cells express two-fold higher levels of IL-2R $\beta$  than WT CD8 T cells. Representative histograms showing the expression and summary of mean fluorescent intensity (MFI) of (A) IL-2R $\beta$  and (B) IL-7R $\alpha$  on CD4, CD8, CD4 Treg, and CD8 Treg cells in spleen of 19-day-old WT and IL-2Ra-KO mice.  $n=5-10$  mice per experimental group. (C) MFI of IL-2R $\beta$  on LN cells from 19-day-old WT and IL-2Ra-KO mice based on activation state as defined in Fig. 2B.  $n=5-10$  mice per experimental group. Statistics: unpaired Student's t test; \* $p < 0.05$ , \*\* $p < 0.01$ , \*\*\* $p < 0.001$ . Non-significant comparisons are not shown.

(Supplementary Fig. S6C). While TCR responses were unchanged in the spleen, PE lymphocytes had less sustained and weaker peak phosphorylation and PL lymphocytes had slower kinetics and drastically reduced maximum phosphorylation (Supplementary Fig. S6D).

Finally, to assess how different PE and PL disease are from each other, PCA was performed on 35 parameters gathered from the same mice, including data from the spleen, bone marrow, peripheral blood, and lymph nodes. WT and IL-2Ra-KO mice clearly separate, as expected; however, PE and PL IL-2Ra-KO mice did not (Fig. 8A). Following regression tree analysis to identify the most useful separating variables, PCA was performed again. As before, WT and IL-2Ra-KO mice were separated, but importantly PE and PL IL-2Ra-KO mice were also distinct (Fig. 8A). In the refined PCA analysis PE, PL, and late endpoint IL-2Ra-KO mice separated from each other. Interestingly, PL on day 19 and PL endpoint (end stage disease) overlap almost completely in PC1, but separate in PC2, suggesting that some factors (PC1) drive disease induction while other factors (PC2) change during late stages of autoimmunity. This demonstrates that the disease in early and late kinetics have many overlapping features, but when most significant variables are assessed, PE and PL disease are distinct even through to disease endpoint when signs of anemia are similar (Fig. 1H).

## Discussion

Several perturbations combine to delay or accelerate disease in the absence of appropriate IL-2 signals. This study identified several small alterations that together may contribute to differences in disease kinetics. IL-2Ra-KO mice with delayed disease kinetics (PL) had increased central memory T cells and some maintained CD8 Treg IL-10 expression. In contrast, PE IL-2Ra-KO T cells displayed reduced IL-7 signaling. Increased CLP output in PE mice along with elevated proliferation, normal TCR signals, and reduced suppression from CD8 Tregs may provide an environment that more rapidly induces disease onset and progression. As the spleen is the primary site of AIHA, higher memory T cell frequency, expanded Treg effector responses, and enhanced proliferation may further contribute to accelerated death in PE IL-2Ra-KO mice. Importantly end stage disease is not identical for early and late death. While anemia pathologies were similar, several differences remained in the underlying mechanisms driving disease kinetics and endpoint pathologies (Fig. 8A).

Follicular CD4 and CD8 T cells promote antibody production in autoimmune disease<sup>36,40</sup>. In IL-2 KO mice, CD8 T follicular cells increase dramatically shortly before disease endpoint<sup>49</sup>. Like CD4 T helper cells, CD8

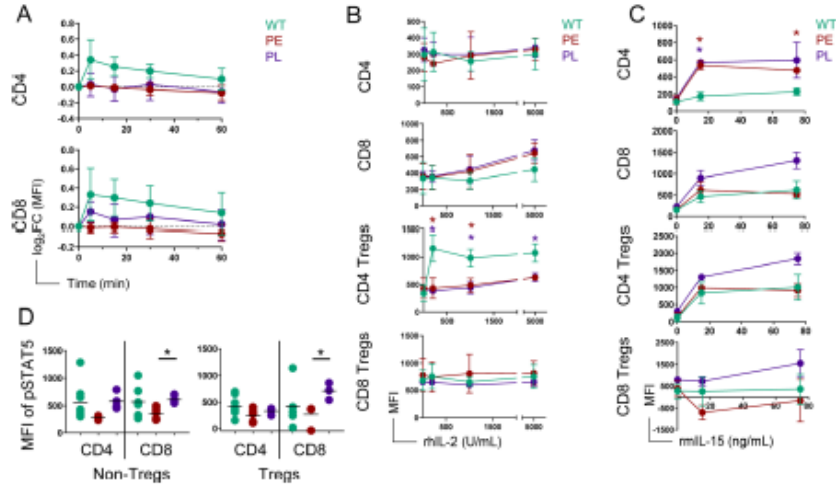


**Figure 6.** IL-2R $\alpha$ -KO T cells respond differentially to cytokine stimulation. (A) Log<sub>2</sub> fold change of pSTAT5 phosphorylation by mean fluorescent intensity (MFI) from unstimulated over time following TCR stimulation comparing WT versus IL-2R $\alpha$ -KO mice for CD4 and CD8 T cells. *n* = 2–4 mice per experimental group from 5 independent experiments. (B) MFI of phosphorylated STAT5 in 19-day-old WT and IL-2R $\alpha$ -KO splenic T cells stimulated with rhIL-2 for 15 min with the indicated dosage. *n* = 2–3 mice per experimental group. (C) MFI of phosphorylated STAT5 in 19-day-old WT and IL-2R $\alpha$ -KO splenic T cells stimulated with rmIL-15 for 15 min with the indicated dosage. *n* = 2–4 mice per experimental group from 2 independent experiments. (D) MFI of STAT5 phosphorylation in 19-day-old WT and IL-2R $\alpha$ -KO T cells following 10 ng/mL rmIL-7 stimulation for 15 min. *n* = 4–8 mice per experimental group. Statistics: unpaired Student's *t* test; \**p* < 0.05, \*\**p* < 0.01, \*\*\**p* < 0.001. Non-significant comparisons are not shown. Statistics in (B) and (C) are compared to WT and colored by which IL-2R $\alpha$ -KO group is being compared.

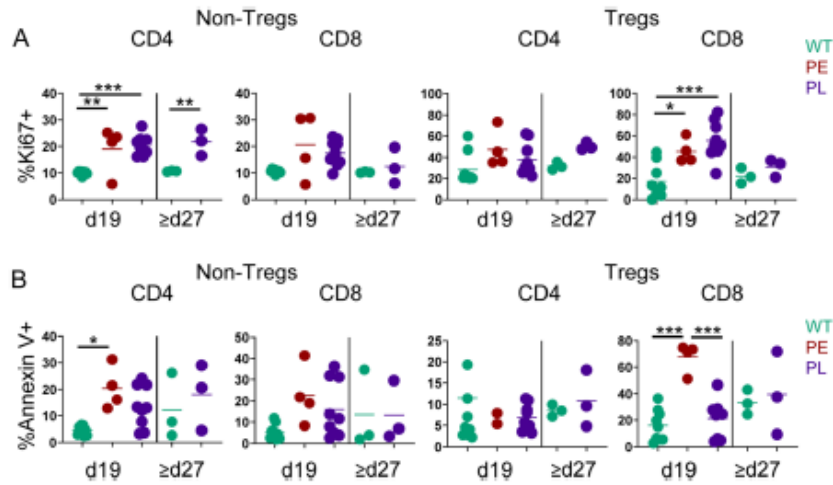


**Figure 7.** IL-2R $\alpha$ -KO T cells exhibit differential proliferation and apoptosis. Frequency of (A) Ki67+ or (B) annexin V+ 19-day-old and late endpoint ( $\geq$ d27+) WT and IL-2R $\alpha$ -KO T cells from the spleen are shown. *n* = 3–9 mice per experimental group. Statistics: one-way ANOVA with Benjamini–Hochberg FDR correction; \**p* < 0.05, \*\**p* < 0.01, \*\*\**p* < 0.001. Non-significant comparisons are not shown.

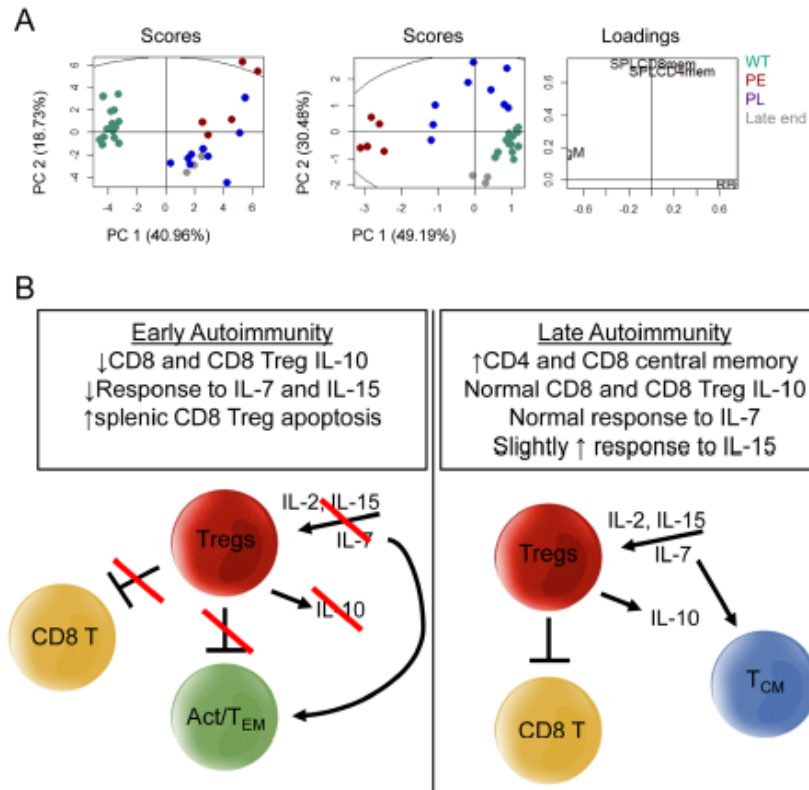


**Figure 8.** PE and PL IL-2Ra-KO disease are distinct. (A) PCA was performed on 35 variables (left) collected from the same mice including RBC, hemoglobin, hematocrit, RBC-bound IgM and IgG, and data shown in Figs. 2, 3 and Supplementary Fig. S1. IL-2Ra-KO mice at day 19 and late endpoint, along with correspondingly aged WT controls were used for PCA. Following regression tree analysis PCA was performed on five variables: RBC, RBC-bound IgM, splenic CD4 central memory T cells, and CD8 central memory T cells (right). Percentage shown on axes refers to the amount of variance in the data that is explained by the given principal component. (B) Summary of PE vs PL disease progression; all changes are relative to WT activities. In PE IL-2Ra-KO mice, lowered T cell responsiveness to IL-2, IL-7, and IL-15 leads to reduced function of Tregs (reduced IL-10 production) and increased apoptosis of CD8 Tregs, allowing T cell effector activation (act/T<sub>EM</sub>). In PL IL-2Ra-KO mice, normal to slightly elevated IL-2, IL-7, and IL-15 responsiveness allows for prolonged Treg function. Enhanced responsiveness to IL-15 and IL-2 may be driving central memory (T<sub>CM</sub>) differentiation in mice with delayed disease.

T follicular cells promote plasma cell differentiation, antibody production and class-switching<sup>19,41–43</sup>. CD8 T follicular cells were mildly elevated but non-significant in PE compared to PL IL-2Ra-KO mice. This CD8 T follicular cell increase near disease endpoint in IL-2Ra-KO mice may accelerate endpoint disease progression by contributing to elevated anti-RBC antibody production. Differentiation signals for CD8 T follicular cells are currently unknown, however, these cells express high IL-7Rα<sup>44</sup>, and thus their expansion in PE mice may be due to altered IL-2 and IL-7 signaling.

In addition to AIHA, IL-2-KO mice develop severe BMF that contributes to severe anemia<sup>11,23</sup>. We observed defects in IL-2Ra-KO BM indicative of BMF, including increased frequencies of LSK, CLP, and GMP, and reduced CMPs. Surprisingly these alterations did not translate into early RBC precursor defects in IL-2Ra-KO mice, regardless of disease kinetics. RBC precursor defects only became apparent in older IL-2Ra-KO mice, suggesting that BMF only mildly contributes to early anemia but may be relevant to late disease kinetics, despite BMF contribution to rapid anemia in IL-2-KO mice. This delayed contribution of BMF to overall anemia in PL mice is likely due to normal MEP frequency during early stages of IL-2Ra-KO disease. The reversed CD4:CD8 ratio in IL-2Ra-KO mice could be due to increases in CLPs. However, thymic CD4:CD8 T cell ratio is normal indicating

that this shift is likely due to peripheral influences. CD8 T cells with higher IL-2R $\beta$  might out-compete CD4 T cells for cytokine signals, thus surviving more and skewing the CD4:CD8 T cell ratio.

Activated and developing central memory CD4 and CD8 T cells were found in PL disease similar to C57BL/6 mice that develop autoimmunity with delayed kinetics<sup>28,45–47</sup>. However, a corresponding increase in the memory marker, IL-7R $\alpha$ , on CD4 or CD8 T cells was not consistently seen, contrasting IL-2-KO mice, perhaps due to difference in signaling when IL-2 is absent rather than highly expressed<sup>18,45</sup>. Although elevated IL-2R $\beta$  expression did not correspond to disease kinetics, this pattern is indicative of memory CD8 T cells, which were increased in IL-2Ra-KO mice. IL-2Ra-KO Tregs receive reduced IL-2 signals, in spite of elevated IL-2 availability, lymph node Tregs, although Treg frequency is normal in the spleen<sup>28</sup>. Increased IL-2R $\beta$  expression on CD8 T cells may provide an edge on responding to IL-2 over CD4 T cells. However, normal IL-2 signaling in CD8 T cells along with elevated IL-2 production would indicate an environment that inhibits differentiation of CD8 T cells into central memory, and favors effector and effector memory differentiation<sup>7,28</sup>. Yet, our results and previous studies phenotypically indicate that IL-2Ra-KO CD8 T cells are developing into central memory-like cells<sup>28</sup>. This apparent contradiction could be due to the timeframe in which we assessed IL-2 signaling. CD8 T cells can maintain IL-2 signaling over several hours, a trait that CD4 T cells do not share<sup>38</sup>. It is possible that if assessed at later timepoints of IL-2 signaling, IL-2Ra-KO CD8 T cells may be defective and permissive for memory differentiation, or constant exposure to elevated IL-2 in vivo may skew T cell differentiation or signaling feedback. Increased frequency of central memory-like T cells in PL IL-2Ra-KO mice may contribute to delayed disease progression, as these cells are thought to have a lower effector function than other activated T cells<sup>45,47</sup>.

Elevated serum IL-2 likely contributes to an increased memory CD8 T cell population in IL-2Ra-KO mice<sup>28</sup>. Supporting this, a higher frequency of IL-2Ra-KO T cells produce IL-2 than WT T cells and mice maintain normal splenic CD4 and CD8 Treg frequencies. IL-2Ra-KO CD4 Tregs expressed normal IL-2R $\beta$  and were less responsive to IL-2 but maintained normal responsiveness to IL-15. Tostek et al. suggested that CD4 Treg responsiveness to IL-15 allows survival in tissues with lower IL-2 accessibility<sup>48</sup>, such as the spleen<sup>49</sup>, possibly contributing to increased IL-2Ra-KO splenic Treg proliferation and frequency. Alternatively, maintenance of normal Treg frequency may be due to expansion of Tregs that acquired effector function, including IFN $\gamma$  production. Disease in IL-2Ra-KO and IL-2-KO mice is IFN $\gamma$ -mediated<sup>11,12,30</sup>, thus IL-2Ra-KO Tregs may be actively contributing to disease pathology.

IL-2 is required for the maintenance and survival of CD4 Tregs<sup>50,51</sup> and IL-2 or receptor loss leads to reduced Tregs and autoimmunity onset<sup>13–10,17</sup>. CD4 Treg transfer before autoimmunity onset prevents autoimmune development, including autoimmunity within IL-2R $\beta$ -KO mice<sup>27,23</sup>, which speaks to the importance of CD4 Tregs in preventing autoimmunity. However, these studies did not test CD8 Treg transfer or assess how CD4 Tregs affect autoimmune disease progression after onset. CD8 Tregs function in suppressing CD8 T cell responses, memory T cell responses, autoantibody production from CD4 T follicular helper cells, and multiple organ immune infiltration causing autoimmunity<sup>44–52</sup>. We observed that PL IL-2Ra-KO CD8 Tregs respond better to IL-7 and produce more IL-10 than their PE counterparts, perhaps allowing for maintenance of suppressive control. Additionally, in EAE and collagen-induced arthritis models, transfer of regulatory B cells, CD4 Tregs, or CD8 Tregs, prevents autoimmunity<sup>53–54</sup>. In EAE, the *in vivo* role of regulatory B cells and CD4 Tregs differs by the stage of disease progression. These suggest that defects in suppression from multiple regulatory cells may lead to more severe autoimmunity as layers of control on T and B cell activation are lost. Gain of IFN $\gamma$  production and reduction in IL-10 production by CD8 Tregs in PE IL-2Ra-KO mice may allow earlier advancement of autoimmunity.

Rapid disease in IL-2Ra-KO mice is likely driven by disruption of T effector and Treg balance. PE and PL IL-2Ra-KO CD4 and CD8 Tregs acquire effector cytokine expression. PE CD8 Tregs have increased apoptosis, and reduced IL-10 expression in lymph node CD8 T cells and Tregs, resulting in reduced Treg suppressive capacity at the site of T cell activation. As there are several CD8 Treg subsets (some not defined by Foxp3 expression)<sup>65,66</sup>, IL-10 production by CD8+ Foxp3– could represent expression by other subsets, or by conventional CD8 T cells. This data suggests that CD8 T cell IL-10 production may contribute to disease kinetics although CD4 Tregs are critical for overall autoimmune development. As effector T cells and Tregs compete for survival signals, changes in receptor abundance and signaling strength, and local cytokine encounters, may tip the balance between Treg suppression and effector expansion, leading to rapid, early disease in PE IL-2Ra-KO mice.

IL-2 reduces the threshold of TCR signaling needed to induce proliferation in CD8 T cells, but not CD4 T cells<sup>16</sup>. Increased IL-2R $\beta$  expression on CD8 T cells leads to sustained IL-2 signaling and earlier proliferation induction<sup>38</sup>. IL-2Ra-KO lymph node CD4 and CD8 T cells were significantly less responsive to TCR signaling than WT CD4 and CD8 T cells respectively, but with differing kinetics between PE and PL mice, perhaps suggesting that PL T cells maintain a less responsive state delaying disease. STAT5 phosphorylation in IL-2Ra-KO T cells following IL-2 stimulation indicated that while CD4 Tregs were less responsive to lower IL-2 than their WT counterparts, IL-2Ra-KO CD4 and CD8 T cells were not impaired in their ability to respond to IL-2. IL-2Ra-KO CD8 T cells express higher IL-2R $\beta$  than WT CD8 T cells, perhaps allowing higher IL-2 sensitivity and responsiveness. Indicative of an effector CD8 phenotype that promotes rapid disease kinetics, PL CD4 and CD8 T cells responded normally following IL-7 stimulation, while PE T cells were less responsive. Altered cytokine signaling, from IL-2R $\beta$  upregulation and increased IL-2 production, along with increased apoptosis and reduced IL-10 production in CD8 Tregs, may in turn promote elevated CD8 T cells and effector/memory fate choices that skew disease kinetics (Fig. 8B). Meanwhile in WT mice, self-reactive T cells would be suppressed by normal Treg function, preventing massive proliferation and autoimmune manifestation.

## Materials and methods

**Mice.** All animal procedures and protocols were approved by the UC Merced Animal Care and Use Committee (protocol number AUP18-0005). Animal euthanasia followed the Guide for the Care and Use of Laboratory, and humane endpoints were used in survival studies. BALB/c IL-2R $\alpha$ -KO or control littermate mice (wildtype and heterozygous; WT) were bred and maintained in our specific pathogen-free facility in an Animal Barrier Facility in accordance with the guidelines of the Laboratory Animal Resource Center of the University of California Merced and under approval by the Institutional Animal Care and Use Committee with appropriate training for all animal husbandry and experimentation. Disease manifestation and survival of IL-2R $\alpha$ -KO and littermate controls was monitored daily from day 9 onward, with a subset assigned body scores based on signs of anemia (Supplementary Table S1), with 80 days being the longest an animal was monitored before endpoint reached. Signs of severe autoimmune disease include hunched appearance, lethargy, ruffled hair, and hypoxia, and are indicative of endpoint within 4–8 h. Mice displaying these signs of autoimmune disease manifestation were euthanized and age of death presumed to be within the day.

**Complete blood count (CBC).** Blood samples used for predictions were collected from mice aged 19 days via the submandibular vein. Endpoint blood collection was performed via terminal eye bleeds immediately following carbon dioxide asphyxiation into heparinized tubes<sup>65</sup>. CBC were evaluated within 8 h on a Hemavet 950 Veterinary Hematology System (Ibex Diagnostics). Standard CBC medical abbreviations are used in all figures and text<sup>67</sup>.

**RBC Ab detection.** Abs bound to RBCs were detected using flow cytometry as previously described<sup>18</sup>. RBCs were freshly isolated from mice by terminal bleed or submandibular vein puncture, washed three times in room-temperature PBS, and resuspended to 1% RBCs. 10  $\mu$ l of 1% RBCs were incubated with either anti-mouse IgM-FITC (1:100 dilution; on Ice; Jackson ImmunoResearch) or anti-mouse IgG-FITC (1:50 dilution; at 37 °C; Jackson ImmunoResearch) for 20–30 min. The percentage of RBCs bound by Ab was determined by flow cytometry.

**Flow cytometry.** Abs were purchased from eBioscience and staining was performed in PBS/1%FBS (Omega Scientific) for 30 min at 4 °C unless otherwise noted. Cell viability was determined using eFluor506 viability dye (eBioscience). To evaluate cytokine receptor expression on T cells, both Treg and non-Treg, lymph node and splenic cells were incubated with surface antibodies prior to fixation. Cells were fixed using the FoxP3/Transcription Factor Staining Buffer Kit (Invitrogen) according to manufacturer's instructions. Following fixation cells were stained intracellularly for FoxP3 (FJK-16s). To evaluate hematopoietic progenitor populations in the BM and thymus, RBC-lysed BM and thymic cells were first incubated with biotinylated lineage/dump markers without Fc-block, washed, then stained for surface markers and streptavidin. To evaluate RBC precursors, whole BM cells were incubated with anti-Ter119 (TER-119) and anti-CD71 (R17217). To assess proliferation, cells were incubated with surface antibodies and annexin V in binding buffer prior to fixation. Cells were fixed using the FoxP3/Transcription Factor Staining Buffer Kit (Invitrogen) according to manufacturer's instructions. Following fixation cells were stained intracellularly for Ki67 and FoxP3. To assess T follicular cells, staining was performed as previously described using a two-step CXCR5 staining protocol<sup>19</sup>. Flow cytometry was performed on a Becton Dickinson LSR-II and data analyzed using FCS Express with Diva Version 4 (DeNovo Software) or FlowJo Version 7.6.5 (FlowJo). Antibodies are outlined by staining panel in Supplementary Table S2.

**Intracellular cytokine stains.** For evaluation of cytokine production, intracellular cytokine staining was performed as previously described<sup>24,68</sup>. Lymphocytes and splenocytes were stimulated for 5 h at 37 °C with 70 ng/mL phorbol 12-myristate 13-acetate (PMA; Fisher Scientific) and 700 ng/mL ionomycin (MP-Biomedicals) and treated with 5  $\mu$ g/mL brefeldin A (MP-Biomedicals)<sup>30</sup>. Cells were then surface stained with anti-CD4 (RM4-5), anti-CD8 $\alpha$  (53-6.7), and for exclusion of non-relevant cells [anti-CD45R (B220; RA3-6B2), anti-CD11b (MI/70), anti-CD11c (N418), and anti-Ly-6G (Gr-1; RB6-8C5)]. Cells were fixed in BD Cytotfix/CytoPerm (BD Biosciences) according to manufacturer's instructions. Next, cells were incubated for 45 min at 4 °C in 0.5% saponin/PBS with anti-IL-2 (JES6-5H4) and anti-IFN $\gamma$  (XMG1.2), or IL-10 (JES5-16E3) and CTLA-4 (UC10-4F10-11; BD Pharmingen).

**T cell stimulations and phospho-flow cytometry.** For all signaling assays, non-sorted splenocytes or lymph node cells were serum-starved for 1 h at 37 °C before stimulation in complete media without serum. For evaluation of TCR signaling, splenocytes and lymphocytes were stimulated with 20  $\mu$ g/mL anti-CD3 $\epsilon$  (145-2C11; Biolegend) and 50  $\mu$ g/mL anti-IgG (polyclonal,  $\alpha$ -Armentan hamster, Jackson ImmunoResearch) for the indicated times<sup>69,70</sup>. For evaluation of pSTAT5 signaling, cells were stimulated for 15 min with recombinant human IL-2 (rhIL-2; NIH AIDS Reagent Program) at indicated concentrations, recombinant mouse IL-15 (rmIL-15; Peprotech) at indicated concentrations, or 10 ng/mL recombinant IL-7 (rmIL-7; Peprotech). Immediately following stimulation cells were fixed with a final concentration of 1.5% methanol-free formaldehyde (Fisher Scientific; Cat. PI28906) for 15 min, and permeabilized with 500  $\mu$ l of ice-cold methanol per  $1 \times 10^6$  cells for 30 min<sup>69,71</sup>. Cells were washed twice with PBS/2%FBS (Omega Scientific) then stained for 60 min in anti-CD4 (RM4-5), anti-CD8 $\alpha$  (53-6.7), anti-FoxP3 (FJK-16s), anti-pSTAT5 (Y694; C71E5; Cell Signaling Technologies) or anti-pS6 (S235/236; D57.2.2E; Cell Signaling Technologies), and, for exclusion of non-relevant cells, anti-CD45R (B220; RA3-6B2), anti-CD11b (MI/70), anti-CD11c (N418), and anti-Ly-6G (Gr-1; RB6-8C5).

**Flow cytometry gating strategies.** In all analysis, leukocytes were gated on forward and side scatter with doublets excluded, then for viability by exclusion of eFluor506 viability dye. For T cell analysis, non-relevant cells were excluded then CD4 or CD8 T cells were gated for feature characterization. Treg cells were defined as Foxp3+ cells within either CD4+ or CD8+ gates. Hematopoietic cell populations were analyzed by the indicated surface expression following exclusion of lineage positive cells—Lineage-negative, Sca-1-positive, c-Kit-positive progenitors (LSK; CD127<sup>+</sup> Sca-1<sup>+</sup> c-Kit<sup>+</sup>), CLP (CD127<sup>+</sup> Sca-1<sup>int</sup> c-Kit<sup>int</sup>), megakaryocyte-erythrocyte progenitor (MEP; CD127<sup>+</sup> Sca-1<sup>+</sup> c-Kit<sup>+</sup> CD34<sup>+</sup> CD16/32<sup>-</sup>), common myeloid progenitor (CMP; CD127<sup>+</sup> Sca-1<sup>+</sup> c-Kit<sup>+</sup> CD34<sup>+</sup> CD16/32<sup>-</sup>), and granulocyte-monocyte progenitor (GMP; CD127<sup>+</sup> Sca-1<sup>+</sup> c-Kit<sup>+</sup> CD34<sup>+</sup> CD16/32<sup>+</sup>). RBC precursors in the BM were analyzed by expression of CD71 and Ter119 following exclusion of CD71<sup>+</sup> Ter119<sup>-</sup> cells—RBC I (CD71<sup>+</sup> Ter119<sup>-</sup>), RBC II (CD71<sup>+</sup> Ter119<sup>+</sup>), RBC III (Ter119<sup>+</sup> CD71<sup>int</sup>), RBC IV (Ter119<sup>+</sup> CD71<sup>+</sup>)<sup>11,24</sup>. Thymic T cell subsets were gated based on CD4 and CD8 expression following elimination of non-relevant cells based on CD11b, CD11c, CD49e, CD45R, and Ly6-G. Double-negative T cells were further divided into subsets 1–4 by CD25 and CD44 expression (1: CD44+CD25<sup>-</sup>; 2: CD44+CD25<sup>+</sup>; 3: CD44<sup>-</sup>CD25<sup>+</sup>; 4: CD44<sup>-</sup>CD25<sup>-</sup>). Combined subsets 1 and 2, and 3 and 4 were defined by expression of CD44 alone.

**Principal component analysis (PCA).** PCA was performed using singular value decomposition in RStudio using R version 3.4.0 through the Bioconductor “pcaMethods” package. PCA was initially performed on 14 parameters acquired from CBC and RBC Ab detection, including frequencies of RBC-bound IgM and RBC-bound IgG, and concentrations of RBC, white blood cells, platelets, neutrophils, hemoglobin, lymphocytes, monocytes, eosinophils, and basophils, hematocrit, mean platelet volume, and mean corpuscular volume. To determine which of these 14 parameters most contributed to separation between early and late disease mice, regression tree analysis via Chi-square automatic interaction detection was performed using XLSTAT-Base Version 19.4.46344 with Bonferroni correction, excluding observations with missing data. This identified four parameters that contributed the most to the variance, and these four parameters—WBC, RBC, hematocrit, and mean platelet volume—were used for subsequent principal component analyses. R script used for 14-variable PCA shown below, with annotation. Script for 4-variable PCA only differs by file name. To evaluate causes of overall disease kinetics, PCA was performed similarly on 35 parameters that were all collected from the same mice, including RBC, hemoglobin, hematocrit, and frequencies of RBC-bound IgM, RBC-bound IgG, LN naive CD4 T cells, LN CD4 activated/effector memory T cells, LN CD4 central memory T cells, LN CD8 central memory T cells, SPL CD4 T cells, SPL CD8 T cells, SPL CD4:CD8 ratio, SPL naive CD4 T cells, SPL CD4 activated/effector memory T cells, SPL CD4 central memory T cells, SPL naive CD8 T cells, SPL CD8 activated/effector memory T cells, SPL CD8 central memory T cells, SPL CD4 T follicular helper, SPL CD8 T follicular cell, BM LSK, BM CLP, BM CMP, BM GMP, BM MEP, and BM RBC precursors 1–4. Following regression tree analysis, four parameters were identified as most useful in separating the data—RBC, RBC-bound IgM, splenic CD4 central memory T cells, and splenic CD8 central memory T cells—which were then used alone for PCA analysis.

**Statistics.** All statistics were performed in GraphPad Prism Version 7 or 8 or RStudio with R version 3.4.0. For evaluations with five group comparisons, one-way ANOVA with multiple comparisons test and Benjamini–Hochberg FDR correction was performed. For data with only three group comparisons, student's t tests were performed. When standard deviations were significantly different between groups, Welch's correction was applied to the student's t test. Grubb's test for outliers was utilized to determine whether significant outliers were present to exclude. Log-rank (Mantel-Cox) test was performed to compare Kaplan–Meier survival curves. Pearson's correlations were used to assess linear regressions for peripheral blood data. F tests were performed as part of linear regression analyses to determine whether the slopes are significantly non-zero.

Received: 16 March 2020; Accepted: 23 November 2020

Published online: 15 December 2020

## References

- Malek, T. R. & Castro, I. Interleukin-2 receptor signaling: At the interface between tolerance and immunity. *Immunity* 33, 153–165. <https://doi.org/10.1016/j.immuni.2010.08.004> (2010).
- Hoyer, K. K., Dooms, H., Barron, L. & Abbas, A. K. Interleukin-2 in the development and control of inflammatory disease. *Immunol. Rev.* 226, 19–28. <https://doi.org/10.1111/j.1600-065X.2008.00697.x> (2008).
- Barron, L. et al. Cutting edge: Mechanisms of IL-2-dependent maintenance of functional regulatory T cells. *J. Immunol.* 185, 6426–6430. <https://doi.org/10.4049/jimmunol.0903940> (2010).
- Schmandt, R. et al. T-lymphocyte proliferation: Tyrosine kinases in interleukin 2 signal transduction. *Baillieres Clin. Haematol.* 5, 551–573 (1992).
- Lan, R. Y., Selmi, C. & Gershwin, M. E. The regulatory, inflammatory, and T cell programming roles of interleukin-2 (IL-2). *J. Autoimmun.* 31, 7–12. <https://doi.org/10.1016/j.jaut.2008.03.002> (2008).
- Liao, W., Lin, J. X. & Leonard, W. J. IL-2 family cytokines: New insights into the complex roles of IL-2 as a broad regulator of T helper cell differentiation. *Curr. Opin. Immunol.* 23, 598–604. <https://doi.org/10.1016/j.coi.2011.08.003> (2011).
- Castro, I., Yu, A., Dee, M. J. & Malek, T. R. The basis of distinctive IL-2- and IL-15-dependent signaling: Weak CD122-dependent signaling favors CD8+ T central-memory cell survival but not T effector-memory cell development. *J. Immunol.* 187, 5170–5182. <https://doi.org/10.4049/jimmunol.1003961> (2011).
- Sadlack, B. et al. Ulcerative colitis-like disease in mice with a disrupted interleukin-2 gene. *Cell* 75, 253–261 (1993).
- Sadlack, B. et al. Generalized autoimmune disease in interleukin-2-deficient mice is triggered by an uncontrolled activation and proliferation of CD4+ T cells. *Eur. J. Immunol.* 25, 3053–3059. <https://doi.org/10.1002/eji.1830251111> (1995).
- Wallerford, D. M. et al. Interleukin-2 receptor alpha chain regulates the size and content of the peripheral lymphoid compartment. *Immunity* 3, 521–530 (1995).

11. Gravano, D. M. et al. CD8(+) T cells drive autoimmune hematopoietic stem cell dysfunction and bone marrow failure. *J. Autoimmun.* **75**, 58–67. <https://doi.org/10.1016/j.jaut.2016.07.007> (2016).
12. Pelegrino, F. S. et al. Deletion of Interferon- $\gamma$  delays onset and severity of dacryoadenitis in CD25KO mice. *Arthritis Res. Ther.* **14**, R234. <https://doi.org/10.1186/ar4077> (2012).
13. Rahimy, E. et al. Spontaneous autoimmune dacryoadenitis in aged CD25KO mice. *Am. J. Pathol.* **177**, 744–753. <https://doi.org/10.2353/ajpath.2010.091116> (2010).
14. Goldstein, J. D., Balderas, R. S. & Marodon, G. Continuous activation of the CD122/STAT-5 signaling pathway during selection of antigen-specific regulatory T cells in the murine thymus. *PLoS One* **6**, e19038. <https://doi.org/10.1371/journal.pone.0019038> (2011).
15. Malek, T. R. The biology of Interleukin-2. *Annu. Rev. Immunol.* **26**, 453–479. <https://doi.org/10.1146/annurevimmunol.26.021607.090357> (2008).
16. Au-Yeung, B. B. et al. IL-2 modulates the TCR signaling threshold for CD8 but not CD4 T cell proliferation on a single-cell level. *J. Immunol.* **198**, 2445–2456. <https://doi.org/10.4049/jimmunol.1601453> (2017).
17. Feau, S., Arens, R., Togher, S. & Schoenberger, S. P. Autocrine IL-2 is required for secondary population expansion of CD8(+) memory T cells. *Nat. Immunol.* **12**, 908–913. <https://doi.org/10.1038/ni.2079> (2011).
18. Hoyer, K. K., Wolslegel, K., Dooms, H. & Abbas, A. K. Targeting T cell-specific costimulators and growth factors in a model of autoimmune hemolytic anemia. *J. Immunol.* **179**, 2844–2850 (2007).
19. Valentine, K. M. et al. CD8 follicular T cells promote B cell antibody class switch in autoimmune disease. *J. Immunol.* **20**, 20 (2018).
20. Bass, G. F., Tuscano, E. T. & Tuscano, J. M. Diagnosis and classification of autoimmune hemolytic anemia. *Autoimmun. Rev.* **13**, 560–564. <https://doi.org/10.1016/j.autrev.2013.11.010> (2014).
21. Cermak, J. & Pisacka, M. Autoimmune hemolytic anemia. *Vnitr. Lek.* **64**, 514–519 (2018).
22. Crotty, S. A brief history of T cell help to B cells. *Nat. Rev. Immunol.* **15**, 185–189. <https://doi.org/10.1038/nri3803> (2015).
23. Chopra, M., Langenhorst, D., Bellhack, A., Serfling, E. & Patra, A. K. Interleukin-2 critically regulates bone marrow erythropoiesis and prevents anemia development. *Eur. J. Immunol.* **45**, 3362–3374. <https://doi.org/10.1002/ej.201545396> (2015).
24. Soclovisky, M. et al. Ineffective erythropoiesis in Stat3<sup>-/-</sup>/Jsb<sup>-/-</sup> mice due to decreased survival of early erythroblasts. *Blood* **98**, 3261–3273 (2001).
25. Almeida, A. R., Legrand, N., Papiernik, M. & Freitas, A. A. Homeostasis of peripheral CD4+ T cells: IL-2R $\alpha$  and IL-2 shape a population of regulatory cells that controls CD4+ T cell numbers. *J. Immunol.* **169**, 4850–4860 (2002).
26. Papiernik, M., de Moraes, M. L., Pontoux, C., Vasseur, F. & Pénit, C. Regulatory CD4 T cells: Expression of IL-2R $\alpha$  chain, resistance to clonal deletion and IL-2 dependency. *Int. Immunol.* **10**, 371–378 (1998).
27. Malek, T. R., Yu, A., Vincek, V., Scheibel, P. & Kong, L. CD4 regulatory T cells prevent lethal autoimmunity in IL-2R $\beta$ -deficient mice. Implications for the nonredundant function of IL-2. *Immunity* **17**, 167–178 (2002).
28. Sharma, R. et al. A regulatory T cell-dependent novel function of CD25 (IL-2R $\alpha$ ) controlling memory CD8(+) T cell homeostasis. *J. Immunol.* **178**, 1251–1255 (2007).
29. De Patva, C. S. et al. Age-related T-cell cytokine profile parallels corneal disease severity in Sjogren's syndrome-like keratoconjunctivitis sicca in CD25KO mice. *Rheumatology (Oxford)* **49**, 246–258. <https://doi.org/10.1093/rheumatology/kep357> (2010).
30. Hoyer, K. K., Kuswanto, W. F., Gallo, E. & Abbas, A. K. Distinct roles of helper T-cell subsets in a systemic autoimmune disease. *Blood* **113**, 389–395. <https://doi.org/10.1182/blood-2008-04-153346> (2009).
31. Zhou, X. et al. Instability of the transcription factor Foxp3 leads to the generation of pathogenic memory T cells in vivo. *Nat. Immunol.* **10**, 1000–1007. <https://doi.org/10.1038/ni.1774> (2009).
32. Hori, S. Lineage stability and phenotypic plasticity of Foxp3+ regulatory T cells. *Immunity* **259**, 159–172. <https://doi.org/10.1111/immr.12175> (2014).
33. Hua, J. et al. Pathological conversion of regulatory T cells is associated with loss of allotolerance. *Sci. Rep.* **8**, 7059. <https://doi.org/10.1038/s41598-018-25384-x> (2018).
34. Boyman, O., Létourneau, S., Krieg, C. & Sprent, J. Homeostatic proliferation and survival of naive and memory T cells. *Eur. J. Immunol.* **39**, 2088–2094. <https://doi.org/10.1002/eji.200939444> (2009).
35. Lodolce, J. P. et al. IL-15 receptor maintains lymphoid homeostasis by supporting lymphocyte homing and proliferation. *Immunity* **9**, 669–676 (1998).
36. Dooms, H., Wolslegel, K., Lin, P. & Abbas, A. K. Interleukin-2 enhances CD4+ T cell memory by promoting the generation of IL-7R $\alpha$  expressing cells. *J. Exp. Med.* **204**, 547–557. <https://doi.org/10.1084/jem.20062381> (2007).
37. Katzman, S. D. et al. Opposing functions of IL-2 and IL-7 in the regulation of immune responses. *Cytokine* **56**, 116–121. <https://doi.org/10.1016/j.cyto.2011.07.005> (2011).
38. Smith, G. A., Taunton, J. & Weiss, A. IL-2R $\beta$  abundance differentially tunes IL-2 signaling dynamics in CD4. *Sci. Signal.* <https://doi.org/10.1126/scisignal.aan4931> (2017).
39. Valentine, K. M. & Hoyer, K. K. CXCR5+ CD8 T cells: Protective or pathogenic? *Front. Immunol.* **10**, 1322. <https://doi.org/10.3389/fimmu.2019.01322> (2019).
40. Crotty, S. T follicular helper cell differentiation, function, and roles in disease. *Immunity* **41**, 529–542. <https://doi.org/10.1016/j.immuni.2014.10.004> (2014).
41. Xing, J. et al. CXCR5+ CD8+ T cells indirectly offer B cell help and are inversely correlated with viral load in chronic hepatitis B infection. *Exp. Cell. Res.* **356**, 57–63. <https://doi.org/10.1016/j.yexcr.2017.04.014> (2017).
42. Jiang, H. et al. CXCR5+ CD8+ T cells infiltrate the colorectal tumors and nearby lymph nodes, and are associated with enhanced IgG response in B cells. *DNA Cell Biol.* **36**, 321–327. <https://doi.org/10.1089/dna.2016.3571> (2017).
43. Yang, R. et al. IL-6 promotes the differentiation of a subset of naive CD8+ T cells into IL-21-producing B helper CD8+ T cells. *J. Exp. Med.* **213**, 2281–2291. <https://doi.org/10.1084/jem.20160417> (2016).
44. Outgley, M. F., Gonzalez, V. D., Granath, A., Andersson, J. & Sandberg, J. K. CXCR5+ CCR7- CD8 T cells are early effector memory cells that infiltrate tonsil B cell follicles. *Eur. J. Immunol.* **37**, 3352–3362. <https://doi.org/10.1002/eji.200636746> (2007).
45. Mueller, S. N., Gebhardt, T., Carbone, F. R. & Heath, W. R. Memory T cell subsets, migration patterns, and tissue residence. *Annu. Rev. Immunol.* **31**, 137–161. <https://doi.org/10.1146/annurev-immunol-032712-095954> (2013).
46. Sprent, J. & Surh, C. D. Normal T cell homeostasis: The conversion of naive cells into memory-phenotype cells. *Nat. Immunol.* **12**, 478–484 (2011).
47. Ratajczak, W., Niedzwiedzka-Rystwej, P., Tokarz-Deptuła, B. & Deptuła, W. Immunological memory cells. *Cent. Eur. J. Immunol.* **43**, 194–203. <https://doi.org/10.5114/cej.2018.77390> (2018).
48. Tostek, M. J., Plette, L., El Daker, S., Eberl, G. & Freitas, A. A. IL-15-dependent balance between Foxp3 and ROR $\gamma$ t expression impacts inflammatory bowel disease. *Nat. Commun.* **7**, 10888. <https://doi.org/10.1038/ncomms10888> (2016).
49. Smitgel, K. S. et al. CCR7 provides localized access to IL-2 and defines homeostatically distinct regulatory T cell subsets. *J. Exp. Med.* **211**, 121–136. <https://doi.org/10.1084/jem.20131142> (2014).
50. Fontenot, J. D., Rasmussen, J. P., Gavin, M. A. & Rudensky, A. Y. A function for interleukin 2 in Foxp3-expressing regulatory T cells. *Nat. Immunol.* **6**, 1142–1151. <https://doi.org/10.1038/ni1263> (2005).
51. Setoguchi, R., Hori, S., Takahashi, T. & Sakaguchi, S. Homeostatic maintenance of natural Foxp3(+) CD25(+) CD4(+) regulatory T cells by interleukin (IL)-2 and induction of autoimmune disease by IL-2 neutralization. *J. Exp. Med.* **201**, 723–735. <https://doi.org/10.1084/jem.20041982> (2005).

52. Isakson, S. H., Katzman, S. D. & Hoyer, K. K. Spontaneous autoimmunity in the absence of IL-2 is driven by uncontrolled dendritic cells. *J. Immunol.* **189**, 1585–1593. <https://doi.org/10.4049/jimmunol.1200342> (2012).
53. Sakaguchi, S., Sakaguchi, N., Asano, M., Itoh, M. & Toda, M. Immunologic self-tolerance maintained by activated T cells expressing IL-2 receptor  $\alpha$ -chains (CD25). Breakdown of a single mechanism of self-tolerance causes various autoimmune diseases. *J. Immunol.* **155**, 1151–1164 (1995).
54. Long, X. *et al.* Memory CD4 T cells are suppressed by CD8 regulatory T cells in vitro and in vivo. *Am. J. Transl. Res.* **9**, 63–78 (2017).
55. Yang, I. *et al.* Allograft rejection mediated by memory T cells is resistant to regulation. *Proc. Natl. Acad. Sci. USA* **104**, 19954–19959. <https://doi.org/10.1073/pnas.0704397104> (2007).
56. Zou, Q. *et al.* CD8<sup>+</sup> Treg cells suppress CD8<sup>+</sup> T cell-responses by IL-10-dependent mechanism during H5N1 influenza virus infection. *Eur. J. Immunol.* **44**, 103–114. <https://doi.org/10.1002/ejlt.201343583> (2014).
57. Kim, H. J. *et al.* CD8<sup>+</sup> T regulatory cells express the Ly49 Class I MHC receptor and are defective in autoimmune prone B6-Yaa mice. *Proc. Natl. Acad. Sci. USA* **108**, 2010–2015. <https://doi.org/10.1073/pnas.1018974108> (2011).
58. Nakagawa, H., Wang, L., Cantor, H. & Kim, H. J. New insights into the biology of CD8 regulatory T cells. *Adv. Immunol.* **140**, 1–20. <https://doi.org/10.1016/bbs.2018.09.001> (2018).
59. Yoshitaki, A. *et al.* Regulatory B cells control T-cell autoimmunity through IL-21-dependent cognate interactions. *Nature* **491**, 264–268. <https://doi.org/10.1038/nature11501> (2012).
60. Evans, J. G. *et al.* Novel suppressive function of transitional 2 B cells in experimental arthritis. *J. Immunol.* **178**, 7868–7878. <https://doi.org/10.4049/jimmunol.178.12.7868> (2007).
61. Park, M. K. *et al.* Amelioration of autoimmune arthritis by adoptive transfer of Foxp3-expressing regulatory B cells is associated with the Treg/Th17 cell balance. *J. Transl. Med.* **14**, 191. <https://doi.org/10.1186/s12967-016-0940-7> (2016).
62. Matsushita, T., Horiyama, M., Iwata, Y. & Tedder, T. F. Regulatory B cells (B10 cells) and regulatory T cells have independent roles in controlling experimental autoimmune encephalomyelitis initiation and late-phase immunopathogenesis. *J. Immunol.* **185**, 2240–2252. <https://doi.org/10.4049/jimmunol.1001307> (2010).
63. Feltenloben, I. *et al.* Adoptively transferred Tregs accumulate in a site-specific manner and ameliorate signs of less advanced collagen-induced arthritis progress in rats. *Immunotherapy* **7**, 215–228. <https://doi.org/10.2217/itm.14.121> (2015).
64. Chen, M. L., Yan, B. S., Kozorz, D. & Wetner, H. L. Novel CD8<sup>+</sup> Treg suppress EAE by TGF- $\beta$ - and IFN- $\gamma$ -dependent mechanisms. *Eur. J. Immunol.* **39**, 3423–3435. <https://doi.org/10.1002/ejt.200939441> (2009).
65. Vieyra-Lobato, M. R., Vela-Ojeda, I., Montiel-Cervantes, L., López-Santiago, R. & Moreno-Lafont, M. C. Description of CD8. *J. Immunol. Res.* **2018**, 3758713. <https://doi.org/10.1155/2018/3758713> (2018).
66. Yu, Y. *et al.* Recent advances in CD8. *Oncol. Lett.* **15**, 8187–8194. <https://doi.org/10.3892/ol.2018.8378> (2018).
67. Survey, N. H. & N. E. 4–9 (Center for Disease Control and Prevention, 2013).
68. Katzman, S. D., Gallo, E., Hoyer, K. K. & Abbas, A. K. Differential requirements for Th1 and Th17 responses to a systemic self-antigen. *J. Immunol.* **186**, 4668–4673. <https://doi.org/10.4049/jimmunol.1003786> (2011).
69. Krutzik, P. O., Trejo, A., Schulz, K. R. & Nolan, G. P. Phospho flow cytometry methods for the analysis of kinase signaling in cell lines and primary human blood samples. *Methods Mol. Biol.* **699**, 179–202. [https://doi.org/10.1007/978-1-61737-950-5\\_9](https://doi.org/10.1007/978-1-61737-950-5_9) (2011).
70. Tan, Y. X. *et al.* Inhibition of the kinase Cdk in thymocytes reveals a requirement for actin remodeling in the initiation of full TCR signaling. *Nat. Immunol.* **15**, 186–194. <https://doi.org/10.1038/ni.2772> (2014).
71. O’Gorman, W. E. *et al.* The initial phase of an immune response functions to activate regulatory T cells. *J. Immunol.* **183**, 332–339. <https://doi.org/10.4049/jimmunol.0900691> (2009).

### Acknowledgements

The authors thank Roy Hoglund and staff of the UC Merced Department of Animal Research Services for animal husbandry care, Dr. David Gravano and the UC Merced Stem Cell Instrumentation Foundry for critical evaluation of the manuscript and their assistance running flow cytometry and advice with gating schemes, and Dr. Jonathan Boyajian and the HSRI Biostats and Data Support Core for statistical consultation and guidance. We also thank our undergraduate researchers, Karely Barajas, Kendrick Nguyen, Nicole Quiroz Lumbe, and Lek Wet Seow for mouse genotyping and experimental support. Finally, we thank Anh Dtep and Oscar Davalos for assistance with Fig. 8.

### Author contributions

The project was designed by G.N.M. and K.K.H. Experiments were performed by G.N.M. and supervised by K.K.H., G.N.M., K.M.V., M.A.K., D.D., K.D.C.J., K.K.H. contributed to the experiment methodology. Data preparation and analysis was performed by G.N.M. The manuscript was written by G.N.M. and K.K.H. with input from all other authors.

### Funding

This work was supported by the National Institutes of Health Grants R00HL090706 and R15HL146779 to K.K.H., and an Aplastic Anemia and MDS International Foundation Grant to K.M.V.

### Competing interests

The authors declare no competing interests.

### Additional information

**Supplementary Information** The online version contains supplementary material available at <https://doi.org/10.1038/s41598-020-78975-y>.

**Correspondence** and requests for materials should be addressed to K.K.H.

**Reprints and permissions information** is available at [www.nature.com/reprints](http://www.nature.com/reprints).

**Publisher’s note** Springer Nature remains neutral with regard to jurisdictional claims in published maps and institutional affiliations.

## **CHAPTER 3**

**CD8 follicular T cells localize throughout the follicle during germinal center reactions and maintain cytolytic and helper properties**

## **CHAPTER 3: CD8 follicular T cells localize throughout the follicle during germinal center reactions and maintain cytolytic and helper properties.**

### **Introduction**

CXCR5+ CD8 T cells arise during situations of chronic antigen and inflammation; including models of chronic viral infection, multiple cancer types, and antibody mediated autoimmune disease (1-3). In some conditions CXCR5 expression facilitates CXCR5+ CD8 T cell homing to CXCL13 expressed in B cell follicles, while some studies find persistent expression of CCR7 on CXCR5+ CD8 T cells prevents follicle entry (4-7). Irrespective of disease condition, CXCR5+ CD8 T cells express the transcriptional repressor Bcl-6 associated with CD8 T effector memory differentiation and CXCR5 expression (7-16). CXCR5+ CD8 T cells also demonstrate a gene profile associated with Bcl-6 function including TCF-1, E2A, and e-related proteins Id2 and Id3 expression (13, 17). Despite recent research that explores CXCR5+ CD8 T cells, variance in tissue localization, expression profiles, inflammatory conditions and developmental stages limit comparisons between existing studies.

Functionally, CXCR5+ CD8 T cells respond in an antigen determined manner. In situations of chronic viral infection CXCR5+ CD8 T cells maintain an effector memory phenotype, capable of reseeding the CD8 T cell niche and controlling viral infection (7, 13). CXCR5+ CD8 T cells isolated from patients with colon cancer promote antibody mediated immune responses, whereas cells isolated from hepatocellular carcinoma promote antibody mediated immune responses and exhibit cytolytic capacity towards tumor cells (9, 18, 19). CXCR5+ CD8 T cells generated during inflammation also maintain cytolytic function (5). In the context of autoimmunity, we have previously shown that a subset of CXCR5+ CD8 T cells that co-express PD-1 and CXCR5, localize to the germinal center and mediate antibody class switching (10). Despite the emergence of comprehensive and robust research a consistent description of CXCR5+ CD8 T cell development and function remains elusive.

As the priming cues for CXCR5+ CD8 T cells are similar to those for CD4 T follicular helper (Tfh) cells, the recruitment and entry of CXCR5+ CD8 T cells into the follicle and germinal center are likely also similar (3). CD4 Tfh entry into the germinal center begins upon antigen encounter and migration to the T-B border. Once there, interactions with B cells re-enforce key migratory protein expression, such as CXCR5 upregulation and CCR7 downregulation, which progresses as the CD4 Tfh cells move first into the follicle and then the germinal center (20). Once in the germinal center, CD4 Tfh and CXCR5+ CD8 T cells interact via cell:cell contact and cytokine secretion to influence B cell differentiation, antibody class switch and memory (21). The interaction between self-reactive CXCR5+

CD8 T cells or CD4 Tfh cells and self-reactive B cells that arise during autoimmune disease may promote disease.

We aim to define the function of CXCR5+ CD8 T cells within autoimmune disease, particularly in regards to their interaction with B cells. Here we show that autoimmune CXCR5+PD-1+ CD8 T cells (CD8 Tfc) develop despite IL-2 concentration but instead expand with inflammation and the absence of T regulatory (Treg) cells. Similar to data described for CXCR5+ CD8 T cells in viral infection and cancer, CD8 Tfc maintain cytolytic capacity while, within the germinal center CD8 Tfc employ multiple cytokine and direct cell:cell mechanisms to manipulate B cell responses. These data provide further evidence that CD8 Tfc development requires exposure to chronic antigen and perhaps chronic inflammation and can promote autoimmune disease progression.

## Methods

**Mice, antibody depletions, and immunizations.** BALB/c IL-2 knockout (KO), CD25 (IL-2R $\alpha$ )-KO, IL-2.IFN $\gamma$ -double KO (dKO), and IL-2.CD28-dKO were used with littermate IL-2 wildtype or heterozygous (WT) controls (22, 23). IL-2 mediated autoimmune disease is not gender specific such that only age is used to determine disease and is indicated for each experiment. CD4 or CD8 depletions were performed in WT and IL-2-KO mice by 5 intraperitoneal (i.p.) injections from day 8-16 of 20 $\mu$ g anti-CD4 (GK1.5; BioXcell) or anti-CD8 (2.43; BioXcell) Ab per gram weight. BALB/c hemizygous male Foxp3sf/Y (scurfy) mice and HET female FoxPsf/+ (scurfy-HET) littermate controls were used as previously described (10). Scurfy and scurfy-HET mice were depleted of IL-2 by 5 i.p. injections from day 7-16 of age using 20 $\mu$ g/g mouse of anti-IL-2 (JES6-1A12; BioXcell) or PBS (Omega). Male Scurfy mutant containing IL-2-KO (scurfy x IL-2) mice we generated by crossing scurfy heterozygous, IL-2 heterozygous females to IL-2-heteozygous scurfy WT males for F1 progeny that contained both scurfy and IL-2-KO. MRL/MpJ-*Fas*<sup>lpr</sup>/J (Mrl.lpr) mice (JAX000485) and MRL/MpJ mice, as controls for Mrl.lpr mice, aged 17 weeks or more were generously donated by Dr. Gabriela Loots at Lawrence Livermore National Laboratory. NOD mice generously donated by Dr. Hans Doms at Boston University were used at 11 weeks of age after urine testing as glucose positive. Collagen-induced arthritis mice were generated as described (24) using 6–8-week-old C57BL/6 mice (JAX000664) injected intradermally with 100 $\mu$ g type II chicken collagen in complete freund's adjuvant (CFA) containing 200 $\mu$ g tuberculosis mycobacterium supplemented by a collagen boost of 50 $\mu$ g type II chicken collagen in incomplete freund's adjuvant (IFA). B6N.129-*Il21*<sup>tm1Kopf</sup>/J (IL-21R-KO mice; JAX019115) were used to isolate B cells. All mice were housed and bred in specific-pathogen free conditions in accordance with UC Merced's

Department of Animal Research Services and approved by the UC Merced Institutional Animal Care and Use Committee.

**Flow cytometry and cell sorting.** All antibodies were purchased from eBioscience at Fisher Scientific unless otherwise specified. Lymphocytes and/or splenocytes were processed and stained in 1% fetal bovine serum (FBS; Omega) phosphate buffered saline (PBS; Omega). Splenocyte red blood cell (RBC) lysis was performed in 3mL of 1x ammonium chloride lysis buffer for 1 minute at room temperature (RT). CXCR5<sup>+</sup> PD-1<sup>+</sup> CD4 Tfh or CD8 Tfc were identified as previously described (10). In brief, lymphocytes and splenocytes were stained first for CXCR5-biotin for 1 hour at RT, then stained for CD4, CD8, PD-1 (Biolegend), ICOS, fixable viability 506, streptavidin (BD Biosciences), CD11c, CD11b, Ly6G (Gr-1), and B220 for 30 min at 4°C. CD4 Tfh and CD8 Tfc are described as live CXCR5<sup>+</sup>PD-1<sup>+</sup>B220<sup>-</sup>CD11c<sup>-</sup>CD11b<sup>-</sup>GR-1<sup>-</sup> and were gated by fluorescence minus one for CXCR5<sup>+</sup>PD-1<sup>+</sup> cells. Non-CD4 Tfh and Non-CD8 Tfc were determined as CXCR5<sup>-</sup>PD-1<sup>-</sup>. CD8 Tfc cells were evaluated for Treg markers by staining with CD122, CD44, and ICOSL or were fixed after CD8 Tfc surface staining with the FoxP3 fixation/permeabilization kit (Thermofisher/Invitrogen) following manufacturer instructions for intracellular staining then stained with Foxp3 and Helios. To assess B cell expression of activation induced deaminase (AID), cultured cells were surface stained for B220, CD19, and viability dye 506 for 30 min at 4°C. Cells were then fixed using the FoxP3 fixation/permeabilization kit prior to intracellular staining for AID (mAID-2) and fluorochrome-conjugated streptavidin for 45 min at RT for each.

To isolate CD4 Tfh and CD8 Tfc, splenocytes and lymphocytes were processed and negatively selected for T cells using a murine PE-selection kit (Stem Cell Technologies) using CD11c, CD11b, Ly6G (Gr-1) and B220 in PE. T cells were then stained for CXCR5 and PD-1 and sorted at greater than 85% purity. Naïve WT or IL-21R-KO B cells were isolated from splenocytes by staining for CD19, TCR $\beta$ , CD11c, CD11b, Gr-1 and fixable viability dye 506 for 30 min at 4°C. B cells were sorted at greater than 95% purity. All flow cytometry and cell sorting were performed on Becton Dickinson LSR-II and BD Biosciences Aria II cell sorter, respectively. Flow cytometric analysis was performed using FCS Express with Diva Version 4.07.005 (DeNovo Software) or FlowJo Version 10.1 (FlowJo).

**T cell stimulations.** Processed cells were stimulated with 50ng/ml Phorbol 12-myristate 13-acetate (PMA) and 500ng/ml ionomycin with brefeldin A (BFA) for 5 hours at 37°C 5% CO<sub>2</sub>. Post-stimulation staining was categorized into multiple panels. For all panels cells were surface stained with follicular cell markers above except streptavidin (SA), then fixed using the Foxp3 fixation and permeabilization kit and stained for intracellular cytokines. In panel 1, CD8 Tfc were stained with

SA, perforin, granzyme B, and IFN $\gamma$  or SA, CD95L (FasL), granzyme B and IFN $\gamma$  for 45 minutes at RT. In panel 2, CD8 Tfc were stained tertiary with IL-21R-chimeria for 1 hour at RT then with SA, IL-10, IL-4, and IL-21R for 45 minutes at RT. In panel 3, CD8 Tfc follicular cells were stained tertiary with IL-21R-chimeria for 1 hour at RT then with SA, IL-21R, and IFN $\gamma$  for 45 minutes at RT. To stain for CD107a, 5 $\mu$ l in 200 $\mu$ l stimuli was used during the 5-hour stimulation without BFA for the first hour.

***In vitro T cell and B cell culture assays.*** Indirect co-culture of T and B cells by supernatant was performed as described previously (10, 25). In brief, FACS isolated T cell populations were plated at 5x10<sup>4</sup> cells per well and activated with 5 $\mu$ g/mL soluble anti-CD3 $\epsilon$  (17A2; BioXCell) and 1 $\mu$ g/mL soluble anti-CD28 (37.51; BioLegend) for 72 hours. Supernatant from activated T cells was plated with 5x10<sup>4</sup> sorted WT or IL-21R-KO B cells per well and with 1 $\mu$ g/ml anti-CD40 (IC10) and 5 $\mu$ g/ml F(ab')<sub>2</sub> goat anti-mouse IgM $\mu$  (Jackson ImmunoResearch Laboratories) for 3 days for assessment of AID expression or 6 days for assessment of B cell Ab production by ELISA as described (10). For IL-4 depleted co-culture, T cells were plated with stimuli and 2 $\mu$ g/mL anti-IL-4 (11B11) for 72 hours. Co-culture then proceeded as described.

***RNA isolation and analysis of RNA next generation sequencing.*** RNA sequencing (RNAseq) of 4 IL-2-KO CD8 T cell samples are available at NCBI GEO (accession number GSE112540) and as previously published (10). IL-2-KO CD4 and CD8 Tfc cells were sorted from at least 6 pooled 15–16-day old lymph node (LN) and spleens. Samples were quick frozen and shipped to Expression Analysis for total RNA isolation and TruSeq stranded mRNA sequencing. Four samples were sequenced with 2 biological replicates each for IL-2-KO CD4 Tfh and IL-2-KO CD8 Tfc. Raw reads were used for the expression analysis. Quality and adapter content of raw reads were analyzed using FastQC (version 0.11.8). Adapter removal and quality trimming were performed using trimmomatic (version 0.38) (26). Read pairs were mapped to the patch assembly (C57BL/6J) of GRCm38/mm10 NCBI build 38.p6 (GCF\_000001635.26) using Rsubread (version 1.34.7) reporting up to ten mapping locations with equal MAPQ scores (27). Read summarization was performed on the gene level using featureCounts using annotations from a modified version of the annotations for GRCm38/mm10 containing only protein coding genes (28). Multi-mapping reads were counted but not treated as fractional counts when mapping to several genes, reads mapping across more than one gene. Genes with less than one count per million in at least three samples were removed. To account for varying sequencing depths, read counts were normalized using trimmed mean of M-values (TMM) in edgeR (version 3.26.8) (29). Read counts were voom transformed using the voomWithQualityWeights function for differential expression analysis in limma (version 3.40.6) (30-32). Genes were considered differentially expressed if their

p-value was less than 0.05 after adjusting for false positive rate using Benjamini-Hochberg correction (33). Heatmaps were generated with log<sub>2</sub> count per million (log-CPM) using package pheatmap (version 1.0.12) (34). T cells were grouped in the heatmap by subtype: follicular, effector, exhaustion, and memory. Expression (log-CPM) of IL-2-KO CD8 Tfc and IL-2-KO CD4 Tfh expression was merged with prior RNAseq of day 12 IL-2-KO CD8 T cells and generated a heatmap to visualize gene expression differences using the different sub-type groupings (GSE112540) (10). Comparisons were conducted between IL-2-KO CD8 Tfc and IL-2-KO CD4 Tfh. Differentially expressed genes were annotated with their biological process using enrichGO from clusterProfiler (version 3.12.0) using the org.Mm.eg.db (version 3.8.2) database (35, 36). All analysis for read mapping, summarization, and differential expression analysis were performed using R versions v3.5.1 and v3.6.0(37). Tidyverse (version 1.2.1) functions were used throughout the analysis for plotting and data wrangling (38).

***Microscopy and Immunofluorescence.*** Spleens from d18-21 IL-2KO, WT, and 6-8-week-old WT mice 7-days post-keyhole limpet hemocyanin (KLH) with IFA injection were collected and frozen in OCT. 10 μm sections were sliced from spleens on a Leica CM1860 cryostat. Sections were fixed in ice-cold acetone prior to staining. For chemokine receptor staining, CXCR5 (2G8, BD Biosciences) was performed as a 3-step stain (39), CXCR4 (SPRCL5, Invitrogen) as a 2-step stain (40), and CD4 (GK1.5, Invitrogen) or CD8β (eBioH35-17.2, Invitrogen), IgD (11-26C, Invitrogen), and PNA (Vector Laboratories) as a one-step 30 min stain. For cytokine staining, IL-4 (11B11, BD Bioscience) was performed as a 3-step stain (41), IL-21 (149204, R&D Systems) as a 2-step stain (39), and CD4 or CD8β, IgD, and PNA (Sigma-Aldrich) as a one-step 30 min stain. After staining, slides were treated with Fluoromount G (Southern Biotech) before a glass coverslip was sealed over it. The sections were visualized with a Zeiss LSM 880 confocal system. Images were taken at 10x (10x/0.45 Plan Apochromat; 420640-9900) and 40x (40x/1.2 LC LCI Plan Apochromat; 420862-9970-799) objectives. Images were saved in three ways: 1) all 5 color channels; 2) only CD4/CD8, IgD, and PNA; and 3) CD4/CD8, CXCR5 or IL-4, and CXCR4 or IL-21. The latter two are used for counting analysis.

Before counting, all images were assigned blinded names and counted independently by two individuals and averaged to determine final counts. Images were counted in ImageJ (version 1.52a) using the cell counter plugin. Outlines around germinal centers were drawn using the polygon tool and determined by PNA+IgD- areas. T cells (either CD4 or CD8) were counted first, then presence of other markers (CXCR4, CXCR5, IL-4, or IL-21) on counted cells was determined. Cells were defined by round shapes with clear CD4 or CD8 staining along the outer edge with no staining on the interior. Cells were considered positive for surface markers if the stain was present along the outer edge of the

cell. Cells were positive for cytokine if stain was present either on the cell edge and/or as puncta of stain on the interior. The same counting procedure was performed for the neighboring non-germinal center follicle.

**Statistics.** All statistics, except for RNAseq, were performed on GraphPad Prism (Version 8.0.0). Differences between two means was assessed by Student's T test with a Welsh correction if indicated. Differences between multiple groups was performed by ordinary 1-way or 2-way ANOVA with a Bonferroni correction. ELISA protein concentrations from a standard protein curve were interpolated using a sigmoidal four parameter logistic standard curve analysis. Statistical measurements were indicated in each figure legend and described as NS= not significant, \*  $p < 0.05$ , \*\*  $p < 0.01$ , or \*\*\*  $p \leq 0.001$ .

## Results

### *CD8 Tfc arise in multiple models of autoimmune disease.*

Recent variability in the functional role of CXCR5+ CD8 T cells may be attributed to differences in nomenclature and potential subpopulations, thus we sought to understand CXCR5+ CD8 T cell function as it relates to PD-1 co-expression. During severe autoimmune disease, IL-2-KO CD4 and CD8 T cells have similar total CXCR5+ T cell frequencies, 7.32% and 6.4% respectively. Yet, when compared to CXCR5+ CD4 T cells, CD8 T cells have reduced CXCR5+ CD8 T cell total numbers. IL-2-KO CXCR5+PD-1+ CD4 Tfh cells comprise 50% of the total CXCR5+ CD4 T cell population while IL-2-KO CXCR5+PD-1+ CD8 T cells (here termed T follicular cells [Tfc]) comprise only 37% of total CXCR5+ CD8 T cells (Fig 3-1A). These, IL-2-KO CD8 Tfc express more ICOS costimulatory molecules (Fig 3-1B) and bcl-6 transcription factor (Fig 3-1C) than their IL-2-KO CXCR5+PD-1- CD8 T cell, IL-2-KO CXCR5-PD-1- CD8 T cell (non Tfc), and WT naïve CD8 T cell counterparts. Specific analysis of the PD-1+ subset of CXCR5+CD8 T cells (CXCR5+PD-1+ CD8 Tfc versus CXCR5+ CD8 T cells) may explain reported differences in function and development between disease models and cell subsets.

CD8 Tfc function in response to systemic autoantigen may drive antibody production to exacerbate autoimmune disease. To determine which autoimmune conditions facilitate CD8 Tfc responses, we assessed models of systemic and tissue-specific autoimmunity. As previously determined, IL-2-KO and scurfy CD8 Tfc frequency and total numbers were elevated when compared to WT naïve mice (Fig 3-2) (10). Autoimmunity in Fas<sup>lpr</sup> mice presents as severe lymphoproliferation and antibody-mediated systemic lupus erythematosus (SLE) that is associated with an expanded Tfh population (42). During SLE in Fas<sup>lpr</sup> mice splenic CD8 Tfc are also expanded, if less than CD4 Tfh, by frequency (10.84+/-5.4%) and total number ( $0.3 \times 10^6$ +/-  $0.2 \times 10^6$  cells) when compared to aged MRL.MpJ control mice (Fig 3-2). However, when we assessed tissue-

specific models of autoimmunity, non-obese diabetic (NOD) and collagen induced arthritis (CIA), CD8 Tfc did not arise despite a detectable CD4 Tfh population (Fig 3-2). It is possible that CD8 Tfc may instead be restricted to ectopic germinal centers or draining lymph nodes during tissue-specific autoimmunity. Together these data suggest that CD8 Tfc predominately arise in response to systemic antigen and expand by lymphoproliferation to impact autoantibody responses.

*CD8 Tfc have distinct germinal center populations in systemic autoimmunity.*

CD4 Tfh cells can function in the extrafollicular region to influence plasma cell development (43) and within the germinal center during B cell cycling and somatic hypermutation (44). To determine if CD8 Tfc can similarly promote regionalized B cell responses during autoimmune disease, we sought to understand CD8 Tfc localization in and around the B cell follicle. Extrafollicular CD4 T cells express increased CXCR4 and decreased CCR7. Further license to enter the germinal center requires the addition of CXCR5 and decreased CXCR4 (40, 45). We first evaluated CXCR4 and CCR7 expression on IL-2-KO CD8 Tfc by flow cytometry. Unlike WT CD8 T cells (59.98 +/-9.08% CCR7+) or IL-2-KO CD8 non Tfc (58.16 +/-15.5% CCR7+) only a small population of CCR7+ CD8 Tfc exist (11.89 +/-10.51% CCR7+) (Fig 3-3A). Instead, IL-2-KO CD8 Tfc have significantly higher frequency of CCR7- cells, of which, 58% are CXCR4- and 29% are CXCR4+, significantly more than observed in IL-2-KO non Tfc or WT naive CD8 T cells. The dominance of CD8 Tfc populations that express less CXCR4 and CCR7 suggest CXCR5+ is used to enter the light zone of the germinal center, while another CXCR4+CXCR5+ population likely populates the extrafollicular space (Fig 3-3B).

To further determine CD8 Tfc localization within the tissue structure, we used immunohistochemistry to evaluate germinal centers, defined by PNA and IgD staining, during intermediate to late disease in IL-2-KO mice or in KLH-immunized WT controls (Fig 3-3C, Fig 3-4A). As expected, germinal centers and follicles in KLH-immunized WT mice contained no CD8 T cells (Fig 3-4B) (10). We found that IL-2-KO mice had a significantly greater total number of CD4 (1012.86 +/-364.55 per mm<sup>2</sup>, 1046.39 +/-340.0 per mm<sup>2</sup>) than CD8 (168.90 +/-259.53 per mm<sup>2</sup>, 421.06 +/-173.61 per mm<sup>2</sup>) T cells when normalized to the GC and follicle area. Unsurprisingly, of the CD8 T cells counted, an equal number of CD8 T cells were identified within the follicle and the GC area, similar to CD4 T cells (Fig 3-3D). When germinal center IL-2-KO CD4 T cells were evaluated based on CXCR5 and CXCR4 expression, were split between CXCR5 expression alone (25.58 +/-20.63%) and no expression (47.02 +/-25.80%) (Fig 3-3E). In contrast, CD8 T cells tended to co-express more CXCR5 and CXCR4 (86.28 +/-18.01%) than CXCR4 (3.13 +/-8.84%) or CXCR5 (2.95 +/-5.48%)

alone. This was also true of follicular localized CD8 T cells, although more follicular localized CD8 T cells expressed CXCR5 (12.98 +/-14.55%) or CXCR4 (22.87 +/-16.33%) alone than their germinal center localized counterparts (Fig 3-3F). Differences between confocal and flow results may be explained by differences between CXCR5+ PD-1+ CD8 Tfc cells and CXCR5+ PD-1- CD8 T cells. These data suggest that CD8 T cells, like CD4 T cells, are capable of localizing to the B cell follicle and germinal center. The high co-expression of CXCR5 and CXCR4 on germinal center CD8 T cells suggests that CD8 T cells may localize preferentially to the dark zone of the germinal center, rather than the light zone where CD4 T follicular helper cells generally reside.

*T cell regulation and not inflammation control CD8 Tfc differentiation.*

CD4 T cell responsiveness to IL-2 dictates CD4 Tfh development (46, 47). To begin interrogating how IL-2 deficiency and Treg cell function influence CD8 Tfc development, we manipulated IL-2 availability in IL-2 sufficient, Treg deficient scurfy mice (10). We first depleted IL-2 in scurfy mice using anti-IL-2 antibodies. Splenocytes from scurfy depleted of IL-2 maintain a similar CD8 Tfc frequency (1.3+/-0.71%) to untreated scurfy controls (0.6+/-0.15%), both of which are significantly reduced in comparison to IL-2-KO mice (Fig 3-5A). Then, to determine if germline IL-2 deficiency plays a greater role in CD8 Tfc development, we generated scurfy and IL-2-KO mice (scurfy x IL-2 mice). Scurfy x IL-2 splenocytes have slightly elevated CD8 Tfc compared to scurfy CD8 Tfc yet, scurfy CD8 Tfc (0.6+/-0.15%) and scurfy x IL-2 CD8 Tfc (6.01+/-2.71%) are significantly reduced in comparison to IL-2-KO CD8 Tfc (5.45+/-3.75%) (Fig 3-5B). Further, the total number of splenocytes in scurfy, and scurfy depleted of IL-2 but not scurfy x IL-2 mice were reduced compared to IL-2-KO mice (Fig 3-5C). The splenic CD8 Tfc expansion in IL-2-KO or scurfy x IL-2-KO mice compared to scurfy mice is likely due to differences in lymphoproliferation caused by lack of bioavailable IL-2 and not due to presence or absence of the Treg compartment (48).

To test the possible influence of paracrine T cell interactions we depleted IL-2-KO mice of either CD4 or CD8 T cells before disease onset and evaluated CD4 Tfh or CD8 Tfc development at late-stage disease for PBS-treated IL-2-KO control mice. The frequency of IL-2-KO CD4 Tfh or CXCR5+PD-1<sup>lo</sup> CD4+ does not change in the absence of total CD8 T cells. However, in the absence of CD4 T cells, including CD4 Tfh, activated T cells and remaining Tregs, only CD8 Tfc (1.3+/-0.87%) are significantly reduced compared to IL-2-KO control CD8 Tfc (4.43+/-3.1%) (Figure 3-5E). Further suggesting that unstable or dysfunctional CD4 Treg, T follicular regulatory cells (Tfreg) and/or T effectors may drive CD8 Tfc development during autoimmune disease.

However, this CD8 Tfc population likely does not arise from Foxp3+ Treg or Qa-1 restricted CD8 Treg populations previously defined in autoimmune disease (49, 50). CD8 Tfc cannot be identified similarly to CD4 Tfh expressing Foxp3, although a significant population of CD8 Tfc can express Helios compared to non CD8 Tfc (Fig 3-6A). Helios expression is required for stable Treg and CD8 Qa-1-specific Treg to function but is also a marker of T cell activation and proliferation (51, 52). CD8 Tfc cells do not express significantly different levels of ICOSL despite significantly elevated CD122 and CD44 co-expression (Fig 3-6B), suggesting that helios expression by CD8 Tfc is an indication of activation rather than Treg differentiation. These data suggest that CD8 Tfc development is likely due to the absence of functional Tregs allowing for excessive T co-stimulation and signaling within the B cell follicle and enhanced by the absence of IL-2 signaling. CD8 Tfc cells then continue to expand during situations of lymphoproliferation promoted by IL-2 deficiency.

*CD8 Tfc cell transcriptional expression indicates cytotoxic and B cell helper functionality, and a memory-like profile.*

In autoimmune disease CD8 Tfc cells upregulate genes associated with a CD4 Tfh phenotype (10) but is also distinct from both naïve CD8 T and CXCR5- CD8 T cell transcriptional profiles (7). To determine how closely autoimmune CD8 Tfc cells resemble CD4 Tfh cells we performed RNAseq on IL-2-KO CD4 Tfh and IL-2-KO CD8 Tfc cells sorted from day 15-16 spleens. Differential expression analysis yielded 1118 genes (479 upregulated; 639 downregulated) that are differentially expressed between CD4 Tfh and CD8 Tfc (Fig 3-7A). IL-2-KO CD8 Tfc cells upregulated T cell activation genes *Sema4a*, *Crtam*, *Tnfrsf4*, and CD8 effector genes *Ctsw*, *Nkg7*, *Klrd1*, and *Perf1* (Figure 4A). In line with trends observed in gene expression, differential gene expression categorized by gene ontology indicate cytokine production, cell:cell adhesion and T cell activation as top biological processes eluding to dynamic IL-2-KO CD8 Tfc function (Fig 3-7B).

To further evaluate CD8 Tfc functional capacity we compared IL-2-KO CD4 Tfh and CD8 Tfc expression for known select genes associated with CD4 Tfh and CD8 effector T cells. As a visual comparison without direct analysis, we added our prior RNAseq of IL-2-KO day 12 total CD8 T cells (GSE112540) (Figure 3-7C) (10). Consistent with prior observations, IL-2-KO CD8 Tfc upregulate genes associated with CD4 Tfh, including *Icos*, *Bcl-6*, and *Cd28*, especially when assessed against IL-2-KO total CD8 T cells. Although, CD4 Tfh-associated genes upregulated in IL-2-KO CD8 Tfc are expressed at lower levels than in IL-2-KO CD4 Tfh, suggesting that IL-2-KO CD8 Tfc may not function as efficiently as traditional CD4 Tfh and may instead maintain diverse functional capacity (10). In fact, *Vdr*, *Sosdc1*, *Ii21*, and *Cd40lg* expression is lower in IL-2-KO CD8 Tfc relative to IL-2-KO CD4 Tfh. In contrast to CXCR5+ CD8 T cells identified in chronic viral infection, IL-2-KO CD8 Tfc maintain effector gene expression via

upregulated *Perf1* but not *Gzmb* or *Ctla4* compared to IL-2-KO CD4 Tfh cells and also upregulate exhaustion markers such as *Lag3*, *Havcr2* (*Tim3*) and *Cd160*. Strikingly both IL-2-KO CD8 Tfc and CD4 Tfh express this exhaustion pattern suggesting a potential feedback mechanism for slowing antibody production during autoimmune disease. Together these data demonstrate that CD8 Tfc cells maintain a unique transcriptional profile incorporating CD4 Tfh associated cytotoxic CD8 T cell gene patterns permitting diverse functional potential.

### *CD8 Tfc maintain diverse functional capacity*

In chronic viral infection and some cancer settings CXCR5+CD8 T cells maintain the capacity for cytolytic function by perforin and granzyme B protein expression (4, 53, 54). Our RNAseq analysis reveals that IL-2-KO CD8 Tfc transcriptionally express cytolytic genes so we investigated whether CD8 Tfc have cytolytic capacity during autoimmune disease. We examined the production of CD107a, granzyme B, perforin, and TNF. A significantly higher frequency of IL-2-KO CD8 Tfc produce CD107a, granzyme B, perforin, and TNF than IL-2-KO CD8 non Tfc. However, by mean fluorescent intensity (MFI) only CD107a and TNF are significantly higher in IL-2-KO CD8 Tfc than IL-2-KO CD8 non Tfc and naïve WT CD8 T cells (Fig 3-8A). Further, as a cytolytic population IL-2-KO CD8 Tfc are more likely to be polyfunctional producing two or more cytolytic proteins (57.39% double; 5.46% triple) than IL-2-KO CD8 non Tfc (13.96% double; 0.43% triple) (Fig 3-8B). IL-2-KO CD8 Tfc co-produce granzyme B and IFN $\gamma$  (9.80%) or IFN $\gamma$  and TNF (47.0%), but can also produce granzyme B (1.34%), IFN $\gamma$  (25.8%) or TNF (2.45%) alone (Fig 3-8B). Thus, individual CD8 Tfc maintain lytic capacity via CD107a and TNF but as a population could mediate a lytic environment during autoimmune disease. CD8 Tfc maintain diversity as a population, producing somewhat different cytokines and cytolytic proteins in individual cells. Whether this represents different stages of differentiation and function, or a limitation on detection remains unknown.

IL-2-KO CD8 Tfc also transcribe genes associated with CD4 Tfh function (Fig 3-7) and can promote IgG class switch in vitro (10). CD8 T cells expressing IL-21 in human nasal polyps co-express IL-17 and IFN $\gamma$  promote IgG class switch in vitro (55) suggesting a role for CD8 T cell cytokine mediated antibody class switch. To evaluate mechanisms by which CD8 Tfc promote antibody class switch we measured cytokines associated with germinal center reactions. A population of IL-2-KO CD8 Tfc produced significantly more IFN $\gamma$ , IL-21 and IL-17 with an elevated frequency producing IL-4 than naïve CD8 T cells or CD8 non Tfc. By MFI, only IFN $\gamma$  and IL-4 were significantly produced by IL-2-KO CD8 Tfc cells compared to naïve CD8 T cells and IL-2-KO CD8 non Tfc (Fig 3-9A). Similar to cytolytic protein production in IL-2-KO CD8 Tfc, Tfh-associated cytokines are co-produced (4.77% double; 0.44% triple) compared to IL-2-KO non Tfc (0.51%

double, 0.01% triple) (Fig 3-9B). While IL-2-KO CD8 Tfc can co-produce IL-21 and IL-4 (3.40 %), a greater frequency express IL-21 (3.16%) or IL-4 (20.0%) alone (Fig 3-8D). CD8 Tfc maintain a diverse repertoire of cytokine expression with the capacity to be both lytic and promote helper-like responses.

Since CD8 Tfc maintain a broad diversity of effector cytokine production within the population, we next assess where CD8 Tfc cytokine-mediated function localizes within lymphoid tissue using immunohistochemistry. Splenic tissue sections were stained for IL-21 and IL-4, and IgD and PNA to determine germinal center position (Fig 3-10A). Both CD4 and CD8 T cells in the germinal center and follicle have a large and significant frequency of IL-4 and IL-21 double-negative cells (50.39 +/-15.03%, 29.49 +/-32.28%), suggesting that these cells are potentially producing other cytokines not examined here (Fig 3-10B and 3-10C). CD4 T cells in the germinal center and follicle produced a mix of these cytokines, equally producing IL-4 (18.93 +/-15.85%), IL-21 (11.56 +/-5.93%), and the two in combination (19.12 +/-14.66%) (Fig 3-10B). CD8 T cells present in the germinal center and follicle of IL-2-KO primarily and significantly produce IL-4, similar to what is seen by flow cytometry (Fig 3-9B and 3-10C). Further, fairly equal amounts of IL-4+ CD8 T cells were found in IL-2-KO germinal center (49.27 +/-39.0%) and follicle (43.02 +/-15.29%), suggesting that CD8 T cells may provide cytokine-mediated B cell help equally in both locations, potentially affecting B cell responses as they enter or leave the germinal center.

#### *B cell class switch and AID induction directed by CD8 Tfc*

B cell responses to cytokine often initiate in the extrafollicular region of the B cell follicle for plasma cell development (43) followed by somatic hypermutation and B cell cycling within the germinal center (44). Presence of CD8 T cells in the follicle, germinal center and extrafollicular region, and demonstrated capacity for producing B cell acting cytokines, led us to next evaluate B cell responses induced by CD8 Tfc cytokines.

CD4 Tfh through cytokines like IL-21 and surface proteins CD40L promote the expression of AID, responsible for antibody class-switching and somatic mutation, in GC B cells (20, 21). To assess CD8 Tfc-produced cytokine contribution to B cell AID expression, WT or IL-21R-KO B cells were stimulated using supernatant from cultured CD8 Tfc and CD4 Tfh then assessed for intracellular AID. As expected, the inability of IL-21R-KO B cells to respond to CD4 Tfh-produced IL-21 reduced B cell AID expression. However, this was not the case for CD8 Tfc; AID induction by CD8 Tfc occurred independent of IL-21 responsiveness by the B cells (Fig 3-10D). Given the majority of CD8 Tfc cells produce primarily IL-4, we also assessed the contribution of CD8 Tfc cell IL-4 on

B cell function. To address this, IL-4 was depleted from T cell supernatant before addition to sorted WT B cells. In contrast to IL-21, when IL-4 was removed from CD4 Tfh and CD8 Tfc cell supernatant B cell expression of AID was reduced (Fig 3-10E). This suggests that while IL-21 is a key cytokine for mediating CD4 Tfh function, it may not play as significant a role for CD8 Tfc function. Together these data demonstrate that CD8 Tfc mediate B cell responses, at least in part, via cytokine secretion within the germinal center. To facilitate autoantibody responses CD8 Tfc likely work in synergy with CD4 Tfh cells.

## Discussion

Together, these data demonstrated that CD8 Tfc comprise a functionally non-redundant subset of CXCR5+ CD8 Tfc in systemic autoimmune disease. CD8 Tfc develop in the absence of functional Tregs and expand in the context of lymphoproliferation. CD8 Tfc maintain significant effector cytokine levels to function as B cell helpers in germinal center and follicular reactions, although their function is not limited to CD4 Tfh activities. By transcriptional profile and protein expression, CD8 Tfc resemble CD4 Tfh cells. IL-2-KO CD8 Tfc acquire the capacity to produce helper cytokines including the co-expression of IL-21 and IL-4. However, CD8 Tfc maintain the capacity for cytolytic function and express granzyme B and TNF $\alpha$ , suggesting the potential for functional mechanisms that diverge from CD4 Tfh cells. Although, gene profiling (Fig 3-7) indicates that IL-2-KO CD4 Tfh cells also acquire substantial cytotoxic gene expression perhaps due to reduced Tregs in the absence of IL-2.

While both IL-2-KO CD4 Tfh and CD8 Tfc promote cytokine-mediated B cell AID induction, CD8 Tfc do not utilize IL-21 to mediate B cell responses. This is in contrast to CD4 Tfh cells that utilize IL-21 for AID induction and antibody class switching (43). Instead CD8 Tfc may use IL-4 or combinatorial interactions to mediate B cell responses. It is possible that direct cell:cell interactions such as CD40L known to be elevated on CD8 Tfc or mechanisms unique to CD8 Tfc are responsible for CD8 Tfc helper activity (10). In this study we cannot rule out a role for IL-2-KO CD8 Tfc cytolytic responses in antibody generation or in driving autoimmunity. However, CD8 Tfc position coupled with cytokine production in the germinal center and follicle, along with AID induction suggest a dominant helper-like role. A cytotoxic role for CD8 Tfc can also be imagined for promoting apoptosis within the affinity maturation process, although this has not been assessed in any models of CXCR5+ CD8 T cell generation. T cells interact with B cells at the follicular border, begin the germinal center reaction. CD8 Tfc localization within the follicle places these cells spatially within this interaction. IL-4+ CD8 Tfc broad localization throughout the follicle and germinal center suggest that CD8 Tfc may promote B cell activities in either location during autoimmune disease. Whether this holds true will likely require live imaging studies between

CD8 Tfc and B cells. The types of B cell activities that CD8 Tfc cells influence are not fully defined such as regulating somatic mutation, memory and short-lived or long-lived plasma cell differentiation, and movement within the germinal center. However, we know that CD8 T cells promote plasma cell differentiation and antibody class switch, but do not alter germinal center B cell numbers (10).

Differences in the helper function we define in autoimmune CD8 Tfc as compared to the cytolytic function of CD8 Tfc in chronic viral infection may be in part related to different CXCR5+ CD8 T cell subset definitions. Studies of CXCR5+ CD8 T cells in chronic viral infection and cancer have not separated CD8 Tfc from the total CXCR5+ CD8 T cell population. However, we show that IL-2-KO CXCR5+PD-1+ CD8 Tfc maintain a higher capacity for co-stimulatory and Bcl-6 transcription factor expression than CXCR5+PD-1- CD8 T cells in autoimmune disease. A consistent description of CXCR5+ CD8 T cells may resolve remaining conflicts in function and classification across different immune reactions. Although it is still probable that CD8 Tfc function is dictated by antigen type, prevalence, and localization.

CD8 Tfc in autoimmune disease appear in multiple models of systemic autoimmune disease, including IL-2 sufficient autoimmunity, promoting the hypothesis that CD8 Tfc development is associated with Treg dysfunction and not IL-2 regulation. Yet, some questions remain regarding the contribution of Treg deficiency or IL-2 signaling to CD8 Tfc development. IL-2 inhibits CD4 Tfh cell differentiation via STAT5 (56, 57). Yet, when IL-2 is depleted in scurfy mice CD8 Tfc fail to expand but IL-2-KO x scurfy mice have an increased frequency of CD8 Tfc. This contradictory data can be explained, in part, by the lymphoproliferation exhibited by IL-2 x scurfy (48) that is absent in IL-2 depleted scurfy. Together, this supports the hypothesis that Treg deficiency releases CD8 Tfc function while IL-2 deficiency promotes lymphoproliferation associated with CD8 Tfc expansion. As CD8 Tfc can still develop even in the absence of CD4 T cells, including Tregs, albeit much less than in the presence of CD4 cells, it reasons that alternative mechanisms may initiate CD8 Tfc differentiation. To fully clarify the role of Treg control on CD8 Tfc development additional studies are needed.

CD8 Tfc are an effector T cell population closely associated with late-stage autoimmune disease that present with lymphoproliferation, autoantibodies and systemic activation, germinal center development including SLE and AIHA. As such CD8 Tfc represent a promising avenue for autoimmune treatment.

## References

1. Valentine, K. M., and K. K. Hoyer. 2019. CXCR5+ CD8 T Cells: Protective or Pathogenic? *Front Immunol* 10: 1322.
2. Yu, D., and L. Ye. 2018. A Portrait of CXCR5 Follicular Cytotoxic CD8 T cells. *Trends Immunol* 39: 965-979.
3. Foustieri, G., and M. Kuka. 2020. The elusive identity of CXCR5 CD8 T cell in viral infection and autoimmunity: Cytotoxic, regulatory, or helper cells? *Mol Immunol* 119: 101-105.
4. Petrovas, C., S. Ferrando-Martinez, M. Y. Gerner, J. P. Casazza, A. Pegu, C. Deleage, A. Cooper, J. Hataye, S. Andrews, D. Ambrozak, P. M. Del Rio Estrada, E. Boritz, R. Paris, E. Moysi, K. L. Boswell, E. Ruiz-Mateos, I. Vagios, M. Leal, Y. Ablanado-Terrazas, A. Rivero, L. A. Gonzalez-Hernandez, A. B. McDermott, S. Moir, G. Reyes-Teran, F. Docobo, G. Pantaleo, D. C. Douek, M. R. Betts, J. D. Estes, R. N. Germain, J. R. Mascola, and R. A. Koup. 2017. Follicular CD8 T cells accumulate in HIV infection and can kill infected cells in vitro via bispecific antibodies. *Science translational medicine* 9.
5. Quigley, M. F., V. D. Gonzalez, A. Granath, J. Andersson, and J. K. Sandberg. 2007. CXCR5+ CCR7- CD8 T cells are early effector memory cells that infiltrate tonsil B cell follicles. *European journal of immunology* 37: 3352-3362.
6. Hardtke, S., L. Ohl, and R. Forster. 2005. Balanced expression of CXCR5 and CCR7 on follicular T helper cells determines their transient positioning to lymph node follicles and is essential for efficient B-cell help. *Blood* 106: 1924-1931.
7. Im, S. J., M. Hashimoto, M. Y. Gerner, J. Lee, H. T. Kissick, M. C. Burger, Q. Shan, J. S. Hale, T. H. Nasti, A. H. Sharpe, G. J. Freeman, R. N. Germain, H. I. Nakaya, H. H. Xue, and R. Ahmed. 2016. Defining CD8+ T cells that provide the proliferative burst after PD-1 therapy. *Nature* 537: 417-421.
8. Mylvaganam, G. H., D. Rios, H. M. Abdelaal, S. Iyer, G. Tharp, M. Mavigner, S. Hicks, A. Chahroudi, R. Ahmed, S. E. Bosinger, I. R. Williams, P. J. Skinner, V. Velu, and R. R. Amara. 2017. Dynamics of SIV-specific CXCR5+ CD8 T cells during chronic SIV infection. *Proc Natl Acad Sci U S A* 114: 1976-1981.
9. Xing, J., C. Zhang, X. Yang, S. Wang, Z. Wang, X. Li, and E. Yu. 2017. CXCR5(+)CD8(+) T cells infiltrate the colorectal tumors and nearby lymph nodes, and are associated with enhanced IgG response in B cells. *Exp Cell Res*.
10. Valentine, K. M., D. Davini, T. J. Lawrence, G. N. Mullins, M. Manansala, M. Al-Kuhlani, J. M. Pinney, J. K. Davis, A. E. Beaudin, S. S. Sindi, D. M. Gravano, and K. K. Hoyer. 2018. CD8 Follicular T Cells Promote B Cell Antibody Class Switch in Autoimmune Disease. *J Immunol* 201: 31-40.
11. Le, K. S., P. Amé-Thomas, K. Tarte, F. Gondois-Rey, S. Granjeaud, F. Orlanducci, E. D. Foucher, F. Broussais, R. Bouabdallah, T. Fest, D. Leroux, S. Yadavilli, P. A. Mayes, L. Xerri, and D. Olive. 2018. CXCR5 and ICOS expression identifies a CD8 T-cell subset with T. *Blood Adv* 2: 1889-1900.
12. Chen, Y., M. Yu, Y. Zheng, G. Fu, G. Xin, W. Zhu, L. Luo, R. Burns, Q. Z. Li, A. L. Dent, N. Zhu, W. Cui, L. Malherbe, R. Wen, and D. Wang. 2019. CXCR5+ PD-1+ follicular helper CD8 T cells control B cell tolerance. *Nat Commun* 10: 4415.
13. Leong, Y. A., Y. Chen, H. S. Ong, D. Wu, K. Man, C. Deleage, M. Minnich, B. J. Meckiff, Y. Wei, Z. Hou, D. Zotos, K. A. Fenix, A. Atnerkar, S. Preston, J. G. Chipman, G. J. Beilman, C. C. Allison, L. Sun, P. Wang, J. Xu, J. G. Toe, H. K. Lu, Y. Tao, U. Palendira, A. L. Dent, A. L. Landay, M. Pellegrini, I. Comerford, S. R. McColl, T. W. Schacker, H. M. Long, J. D. Estes, M. Busslinger, G.

- T. Belz, S. R. Lewin, A. Kallies, and D. Yu. 2016. CXCR5(+) follicular cytotoxic T cells control viral infection in B cell follicles. *Nature immunology* 17: 1187-1196.
14. Nurieva, R. I., Y. Chung, G. J. Martinez, X. O. Yang, S. Tanaka, T. D. Matskevitch, Y. H. Wang, and C. Dong. 2009. Bcl6 mediates the development of T follicular helper cells. *Science* 325: 1001-1005.
  15. Johnston, R. J., A. C. Poholek, D. DiToro, I. Yusuf, D. Eto, B. Barnett, A. L. Dent, J. Craft, and S. Crotty. 2009. Bcl6 and Blimp-1 are reciprocal and antagonistic regulators of T follicular helper cell differentiation. *Science* 325: 1006-1010.
  16. Yu, D., S. Rao, L. M. Tsai, S. K. Lee, Y. He, E. L. Sutcliffe, M. Srivastava, M. Linterman, L. Zheng, N. Simpson, J. I. Ellyard, I. A. Parish, C. S. Ma, Q. J. Li, C. R. Parish, C. R. Mackay, and C. G. Vinuesa. 2009. The transcriptional repressor Bcl-6 directs T follicular helper cell lineage commitment. *Immunity* 31: 457-468.
  17. He, R., S. Hou, C. Liu, A. Zhang, Q. Bai, M. Han, Y. Yang, G. Wei, T. Shen, X. Yang, L. Xu, X. Chen, Y. Hao, P. Wang, C. Zhu, J. Ou, H. Liang, T. Ni, X. Zhang, X. Zhou, K. Deng, Y. Chen, Y. Luo, J. Xu, H. Qi, Y. Wu, and L. Ye. 2016. Follicular CXCR5-expressing CD8+ T cells curtail chronic viral infection. *Nature* 537: 412-428.
  18. Jin, Y., C. Lang, J. Tang, J. Geng, H. K. Song, Z. Sun, and J. Wang. 2017. CXCR5(+)CD8(+) T cells could induce the death of tumor cells in HBV-related hepatocellular carcinoma. *International immunopharmacology* 53: 42-48.
  19. Ye, L., Y. Li, H. Tang, W. Liu, Y. Chen, T. Dai, R. Liang, M. Shi, S. Yi, G. Chen, and Y. Yang. 2019. CD8+CXCR5+T cells infiltrating hepatocellular carcinomas are activated and predictive of a better prognosis. *Aging (Albany NY)* 11: 8879-8891.
  20. Crotty, S. 2014. T follicular helper cell differentiation, function, and roles in disease. *Immunity* 41: 529-542.
  21. Crotty, S. 2011. Follicular helper CD4 T cells (TFH). *Annual review of immunology* 29: 621-663.
  22. Hoyer, K. K., K. Wolslegel, H. Doms, and A. K. Abbas. 2007. Targeting T cell-specific costimulators and growth factors in a model of autoimmune hemolytic anemia. *J Immunol* 179: 2844-2850.
  23. Mullins, G. N., K. M. Valentine, M. Al-Kuhlani, D. Davini, K. D. C. Jensen, and K. K. Hoyer. 2020. T cell signaling and Treg dysfunction correlate to disease kinetics in IL-2R $\alpha$ -KO autoimmune mice. *Scientific reports* 10: 21994.
  24. Rosloniec, E. F., M. Cremer, A. H. Kang, L. K. Myers, and D. D. Brand. 2010. Collagen-induced arthritis. *Current protocols in immunology* Chapter 15: Unit 15.15.11-25.
  25. Valentine, K. M., D. Davini, T. J. Lawrence, G. N. Mullins, M. Manansala, M. Al-Kuhlani, J. M. Pinney, J. K. Davis, A. E. Beaudin, S. S. Sindi, D. M. Gravano, and K. K. Hoyer. 2018. CD8 Follicular T Cells Promote B Cell Antibody Class Switch in Autoimmune Disease. *The Journal of Immunology*.
  26. Bolger, A. M., M. Lohse, and B. Usadel. 2014. Trimmomatic: a flexible trimmer for Illumina sequence data. *Bioinformatics* 30: 2114-2120.
  27. Liao, Y., G. K. Smyth, and W. Shi. 2019. The R package Rsubread is easier, faster, cheaper and better for alignment and quantification of RNA sequencing reads. *Nucleic Acids Res* 47: e47.
  28. Liao, Y., G. K. Smyth, and W. Shi. 2014. featureCounts: an efficient general purpose program for assigning sequence reads to genomic features. *Bioinformatics* 30: 923-930.
  29. Robinson, M. D., D. J. McCarthy, and G. K. Smyth. 2010. edgeR: a Bioconductor package for differential expression analysis of digital gene expression data. *Bioinformatics* 26: 139-140.

30. Ritchie, M. E., B. Phipson, D. Wu, Y. Hu, C. W. Law, W. Shi, and G. K. Smyth. 2015. limma powers differential expression analyses for RNA-sequencing and microarray studies. *Nucleic Acids Res* 43: e47.
31. Liu, R., A. Z. Holik, S. Su, N. Jansz, K. Chen, H. S. Leong, M. E. Blewitt, M. L. Asselin-Labat, G. K. Smyth, and M. E. Ritchie. 2015. Why weight? Modelling sample and observational level variability improves power in RNA-seq analyses. *Nucleic Acids Res* 43: e97.
32. Law, C. W., Y. Chen, W. Shi, and G. K. Smyth. 2014. voom: Precision weights unlock linear model analysis tools for RNA-seq read counts. *Genome Biol* 15: R29.
33. Benjamini, Y., and Y. Hochberg. 1995. Controlling the False Discovery Rate: A Practical and Powerful Approach to Multiple Testing. *Journal of the Royal Statistical Society. Series B (Methodological)* 57: 289-300.
34. Kolde, R. 2019. pheatmap: Pretty Heatmaps. 1.0.12 ed.
35. Yu, G., L. G. Wang, Y. Han, and Q. Y. He. 2012. clusterProfiler: an R package for comparing biological themes among gene clusters. *OMICS* 16: 284-287.
36. Carlson, M. 2019. org.Mm.eg.db: Genome wide annotation for Mouse.
37. Team, R. C. 2019. R: A Language and Environment for Statistical Computing. R Foundation for Statistical Computing, Vienna, Austria.
38. Wickham, H., M. Averick, J. Bryan, W. Chang, L. D. A. McGowan, R. François, G. Grolemond, A. Hayes, L. Henry, J. Hester, M. Kuhn, T. L. Pedersen, E. Miller, S. M. Bache, K. Müller, J. Ooms, D. Robinson, D. P. Seidel, V. Spinu, K. Takahashi, D. Vaughan, C. Wilke, K. Woo, and H. Yutani. 2019. Welcome to the tidyverse. *Journal of Open Source Software* 4: 1686.
39. Ding, Y., J. D. Mountz, and H. C. Hsu. 2015. Identification of follicular T helper cells in tissue sections. *Methods Mol Biol* 1291: 13-25.
40. Elsner, R. A., D. N. Ernst, and N. Baumgarth. 2012. Single and coexpression of CXCR4 and CXCR5 identifies CD4 T helper cells in distinct lymph node niches during influenza virus infection. *J Virol* 86: 7146-7157.
41. Whiteland, J. L., C. Shimeld, S. M. Nicholls, D. L. Easty, N. A. Williams, and T. J. Hill. 1997. Immunohistochemical detection of cytokines in paraffin-embedded mouse tissues. *J Immunol Methods* 210: 103-108.
42. Yang, X., J. Yang, Y. Chu, J. Wang, M. Guan, X. Zhu, Y. Xue, and H. Zou. 2013. T follicular helper cells mediate expansion of regulatory B cells via IL-21 in Lupus-prone MRL/lpr mice. *PLoS One* 8: e62855.
43. Odegard, J. M., B. R. Marks, L. D. DiPlacido, A. C. Poholek, D. H. Kono, C. Dong, R. A. Flavell, and J. Craft. 2008. ICOS-dependent extrafollicular helper T cells elicit IgG production via IL-21 in systemic autoimmunity. *J Exp Med* 205: 2873-2886.
44. Mesin, L., J. Ersching, and G. D. Victora. 2016. Germinal Center B Cell Dynamics. *Immunity* 45: 471-482.
45. Rankin, A. L., H. Guay, D. Herber, S. A. Bertino, T. A. Duzanski, Y. Carrier, S. Keegan, M. Senices, N. Stedman, M. Ryan, L. Bloom, Q. Medley, M. Collins, C. Nickerson-Nutter, J. Craft, D. Young, and K. Dunussi-Joannopoulos. 2012. IL-21 receptor is required for the systemic accumulation of activated B and T lymphocytes in MRL/MpJ-Fas(lpr/lpr)/J mice. *J Immunol* 188: 1656-1667.
46. DiToro, D., C. J. Winstead, D. Pham, S. Witte, R. Andargachew, J. R. Singer, C. G. Wilson, C. L. Zindl, R. J. Luther, D. J. Silberger, B. T. Weaver, E. M. Kolawole, R. J. Martinez, H. Turner, R. D. Hatton, J. J. Moon, S. S. Way, B. D. Evavold, and C. T. Weaver. 2018. Differential IL-2 expression defines developmental fates of follicular versus nonfollicular helper T cells. *Science* 361.

47. Papillion, A., M. D. Powell, D. A. Chisolm, H. Bachus, M. J. Fuller, A. S. Weinmann, A. Villarino, J. J. O'Shea, B. León, K. J. Oestreich, and A. Ballesteros-Tato. 2019. Inhibition of IL-2 responsiveness by IL-6 is required for the generation of GC-T(FH) cells. *Science immunology* 4.
48. Zheng, L., R. Sharma, F. Gaskin, S. M. Fu, and S. T. Ju. 2007. A novel role of IL-2 in organ-specific autoimmune inflammation beyond regulatory T cell checkpoint: both IL-2 knockout and Fas mutation prolong lifespan of Scurfy mice but by different mechanisms. *J Immunol* 179: 8035-8041.
49. Kim, H.-J., B. Verbinnen, X. Tang, L. Lu, and H. Cantor. 2010. Inhibition of follicular T-helper cells by CD8+ regulatory T cells is essential for self tolerance. *Nature* 467: 328-332.
50. Churlaud, G., F. Pitoiset, F. Jebbawi, R. Lorenzon, B. Bellier, M. Rosenzweig, and D. Klatzmann. 2015. Human and Mouse CD8(+)CD25(+)FOXP3(+) Regulatory T Cells at Steady State and during Interleukin-2 Therapy. *Front Immunol* 6: 171.
51. Akimova, T., U. H. Beier, L. Wang, M. H. Levine, and W. W. Hancock. 2011. Helios expression is a marker of T cell activation and proliferation. *PLoS One* 6: e24226.
52. Kim, H. J., R. A. Barnitz, T. Kreslavsky, F. D. Brown, H. Moffett, M. E. Lemieux, Y. Kaygusuz, T. Meissner, T. A. Holderried, S. Chan, P. Kastner, W. N. Haining, and H. Cantor. 2015. Stable inhibitory activity of regulatory T cells requires the transcription factor Helios. *Science* 350: 334-339.
53. Rahman, M. A., K. M. McKinnon, T. S. Karpova, D. A. Ball, D. J. Venzon, W. Fan, G. Kang, Q. Li, and M. Robert-Guroff. 2018. Associations of Simian Immunodeficiency Virus (SIV)-Specific Follicular CD8(+) T Cells with Other Follicular T Cells Suggest Complex Contributions to SIV Viremia Control. *J Immunol* 200: 2714-2726.
54. Tang, J., J. Zha, X. Guo, P. Shi, and B. Xu. 2017. CXCR5(+)CD8(+) T cells present elevated capacity in mediating cytotoxicity toward autologous tumor cells through interleukin 10 in diffuse large B-cell lymphoma. *International immunopharmacology* 50: 146-151.
55. Xiao, L., L. Jia, L. Bai, L. He, B. Yang, C. Wu, and H. Li. 2016. Phenotypic and functional characteristics of IL-21-expressing CD8(+) T cells in human nasal polyps. *Scientific reports* 6: 30362.
56. Ballesteros-Tato, A., B. Leon, B. A. Graf, A. Moquin, P. S. Adams, F. E. Lund, and T. D. Randall. 2012. Interleukin-2 inhibits germinal center formation by limiting T follicular helper cell differentiation. *Immunity* 36: 847-856.
57. Johnston, R. J., Y. S. Choi, J. A. Diamond, J. A. Yang, and S. Crotty. 2012. STAT5 is a potent negative regulator of TFH cell differentiation. *J Exp Med* 209: 243-250.

## FIGURES AND FIGURE LEGENDS

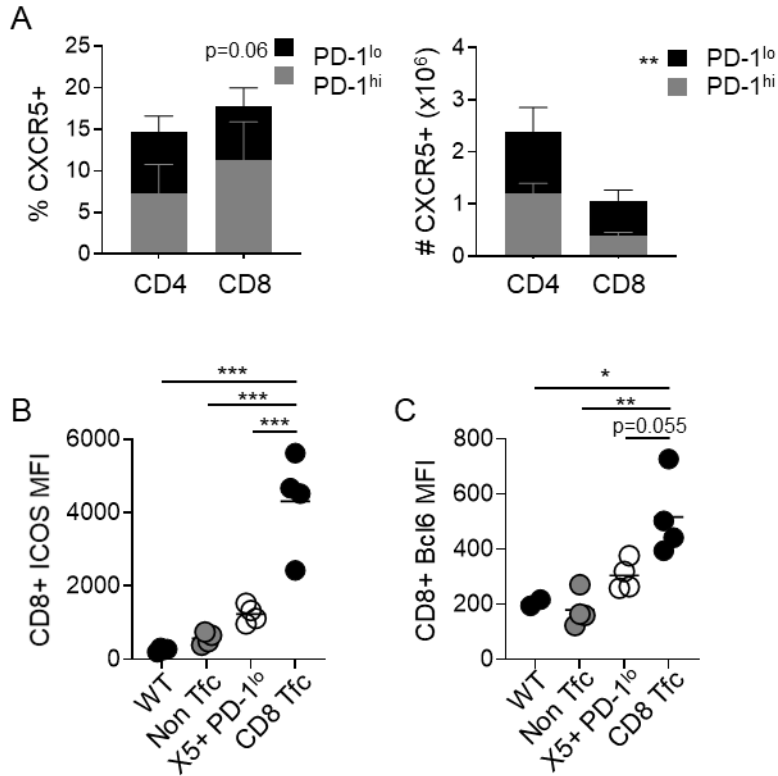


**Fig 3-1. CXCR5+ CD8 T cells constitute PD-1 high- and low-expressing populations.** Flow cytometric analysis of CXCR5 and PD-1 expression on CD4 or CD8 T cells from 17–21-day old IL-2-KO or WT LN gated on live B220<sup>-</sup>CD11c<sup>-</sup>CD11b<sup>-</sup>GR-1<sup>-</sup>. **(A)** Frequency and total number of CXCR5+ CD4 and CD8 T cells are shown as CXCR5+PD-1<sup>+</sup> and CXCR5+PD-1<sup>-</sup> subsets. **(B,C)** Mean fluorescence intensity (MFI) quantification of surface expression of ICOS **(B)** and intracellular Bcl-6 **(C)** in WT naïve CD8 T cells, IL-2-KO CD8 non-Tfh, IL-2-KO CXCR5+PD-1<sup>-</sup> (X5+PD-1<sup>-</sup>), and IL-2-KO CD8 Tfc. **(B, C)** Each symbol indicates an individual animal. Data is representative of 4 independent experiments in A and B and 2-4 independent experiments in C. Statistics: **(A)** 2-way ANOVA with multiple comparisons and Bonferroni correction, **(B)** 1-way ANOVA with multiple comparisons and Bonferroni correction.

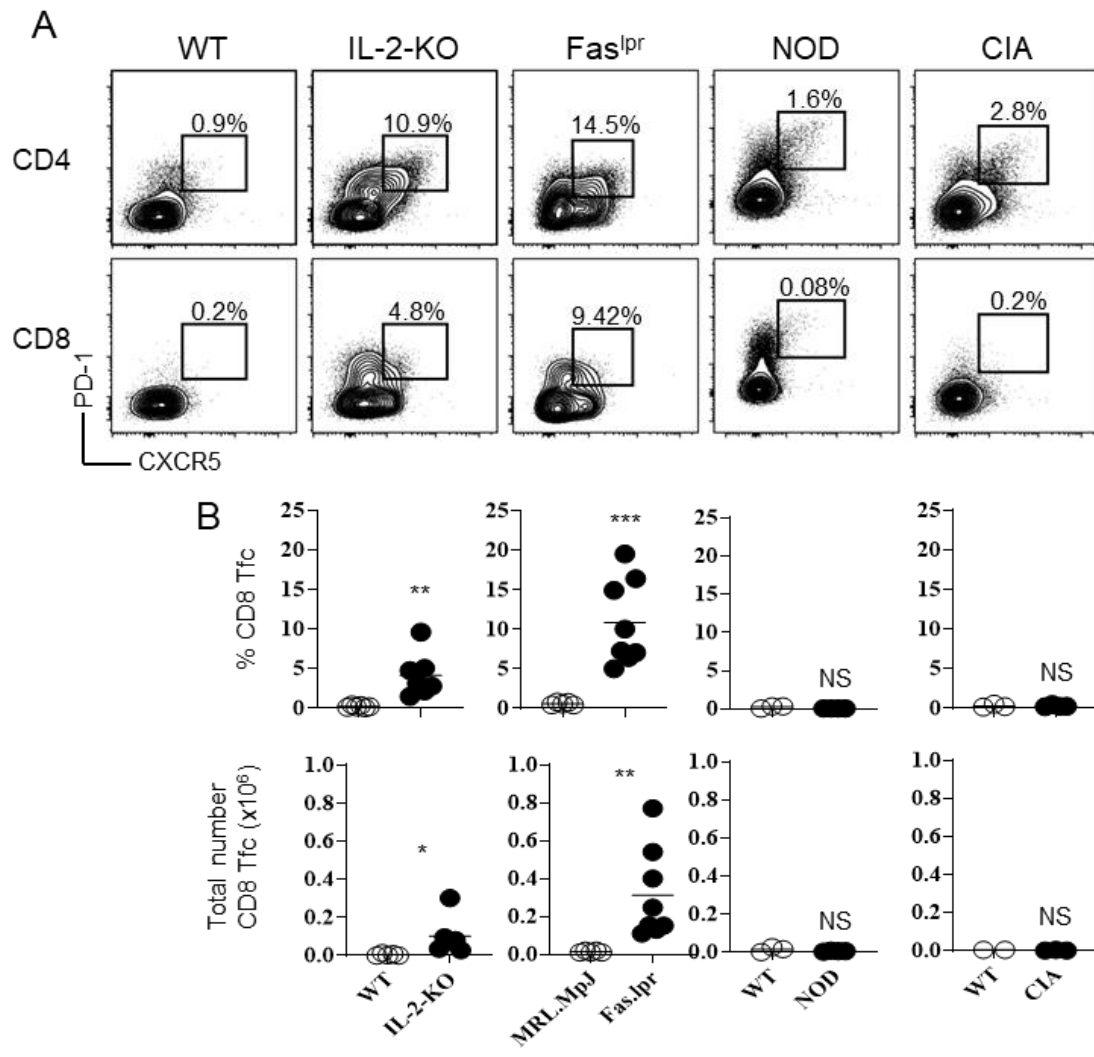


**Fig 3-2. CD8 Tfc arise in multiple models of autoimmune disease. (A)** Representative flow plots compare CXCR5 and PD-1 expression on live B220<sup>-</sup>CD11c<sup>-</sup>CD11b<sup>-</sup>GR-1<sup>-</sup> CD4 or CD8 T cells splenocytes between 17–21-day old IL-2-KO and WT littermate controls, 17-23-week old Fas<sup>lpr</sup> and MRL.MpJ controls, 11 week old diseased (urine-glucose positive) NOD and 6-14-week old WT controls, and 7-week post-induction CIA and PBS control mice. **(B)** Frequency and total number of CD8 Tfc in the indicated model is shown. Each symbol indicates an individual animal. Data representative of 1-3 independent experiments per comparison. Statistics: unpaired one-tailed Student's t-test relative to indicated controls with a Welch correction if necessary.

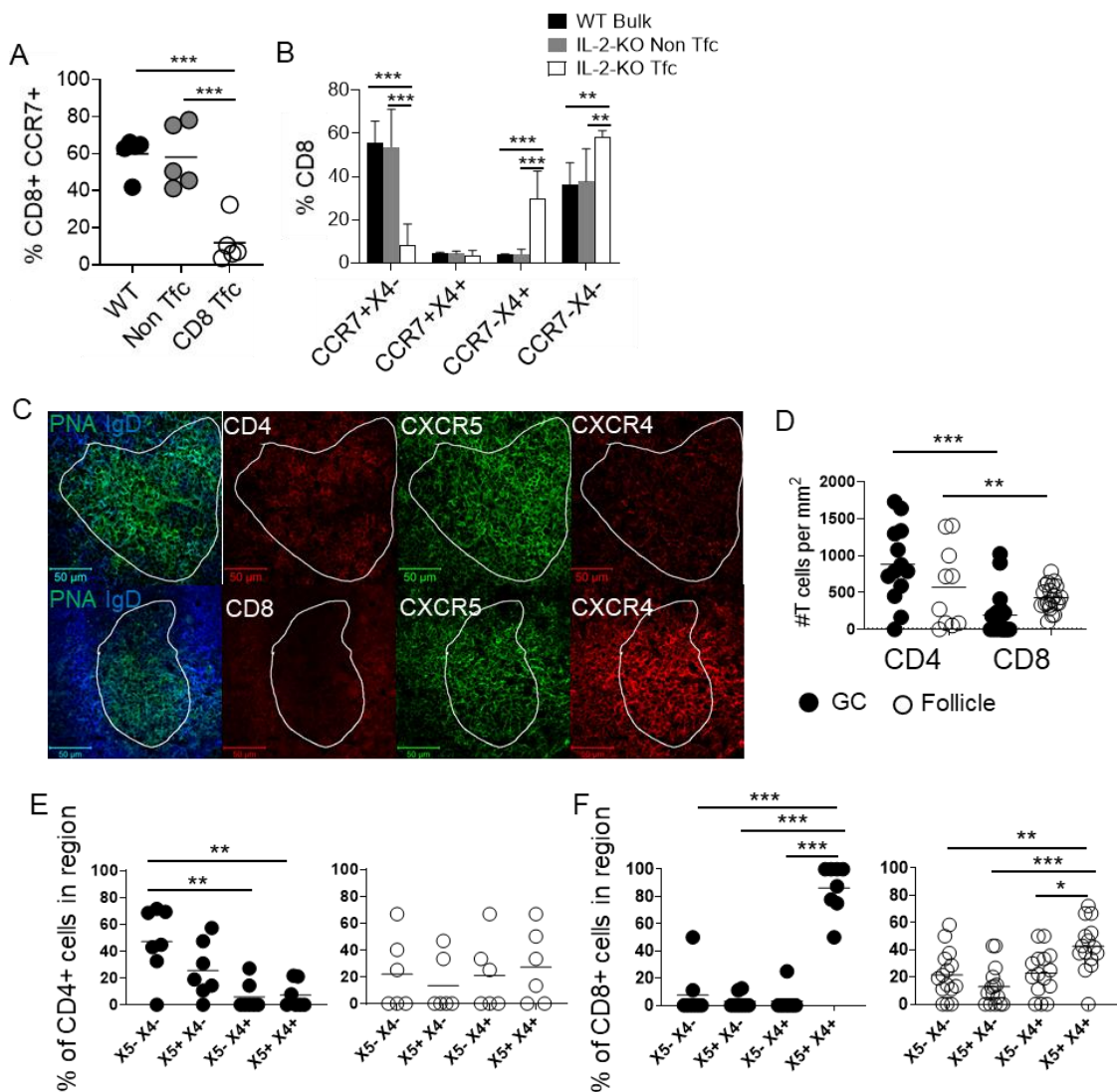


**Fig 3-3. CD8 Tfc localize to GC and follicle.** (A, B) Splenocytes from 17–21-day old IL-2-KO and WT littermate controls were stained to identify CD8 Tfc. (A) The frequency of CCR7+ or (B) the mean frequency of CCR7 and CXCR4 (X4) co-expression  $\pm$  SD was analyzed on bulk WT CD8, IL-2-KO non Tfc and IL-2-KO CD8 Tfc. (C) Representative images of 19–21-day old IL-2-KO spleen sections that were stained for CXCR5, CXCR4, PNA, IgD, and CD4 or CD8. The outlined germinal center was defined as high PNA and low IgD are shown. (D) Quantification of CD4 or CD8 T cells counted in immunofluorescence images at 40x asper  $\text{mm}^2$  of the counting area. (E) Frequency of CD4 or (F) CD8 T cells co-expressing CXCR5 and CXCR4 within the germinal center (filled circle) or follicle (open circle). Data representative of 3-4 independent experiments. (A, D-F) Each symbol indicates an individual animal. Statistics: (A, D-F) 1-way ANOVA with multiple comparisons and Bonferroni correction, (B) 2-way ANOVA with multiple comparisons and Bonferroni correction.

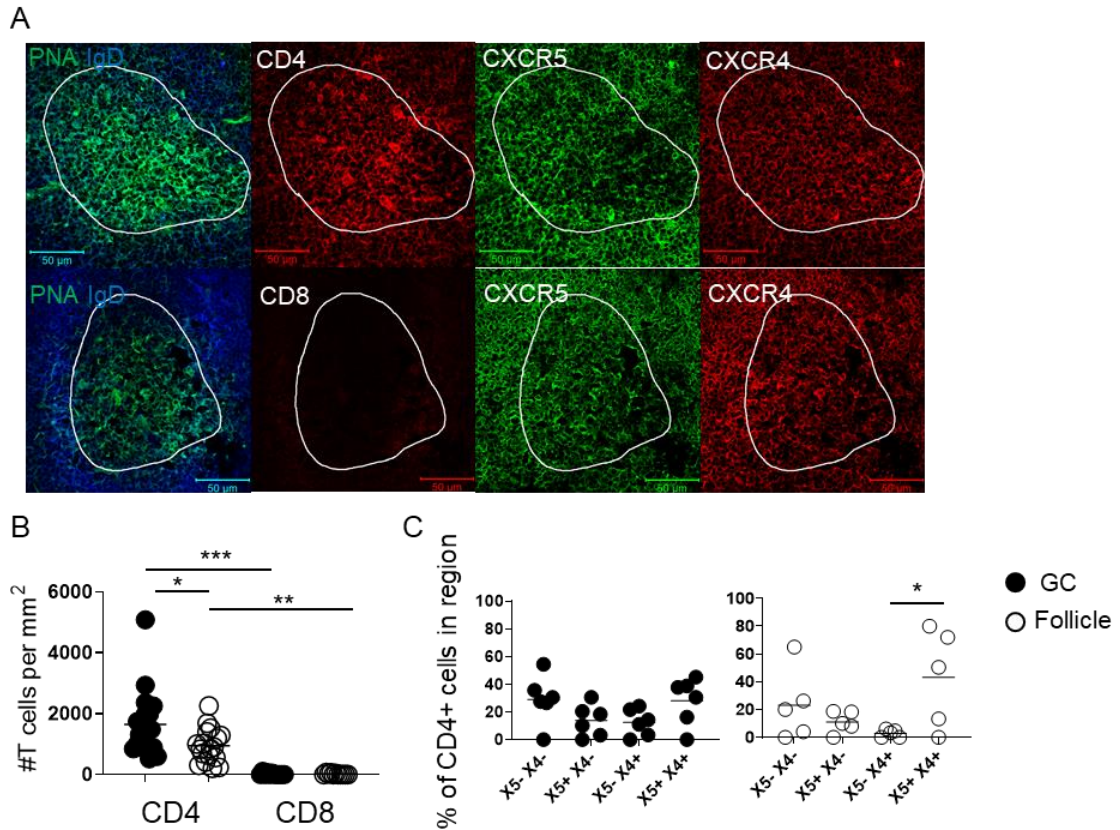


**Fig 3-4. CD8 T cells do not localize to the GC following KLH immunization.** (A) KLH-immunized WT spleen sections were stained for CXCR5, CXCR4, PNA, IgD, and CD4 or CD8. Region outlined is the germinal center, defined by high PNA and low IgD. (B) Quantification of CD4 or CD8 T cells counted in immunofluorescence images at 40x. (per mm<sup>2</sup> calculated from the area that cells were counted in) (C) Frequency of CD4 T cells expressing CXCR5 and/or CXCR4 of total CD4 T cells counted within the given region. Data representative of 4 experiments with a total n of 5-9 per group. Statistics one-way ANOVA with multiple comparisons and Bonferroni correction.

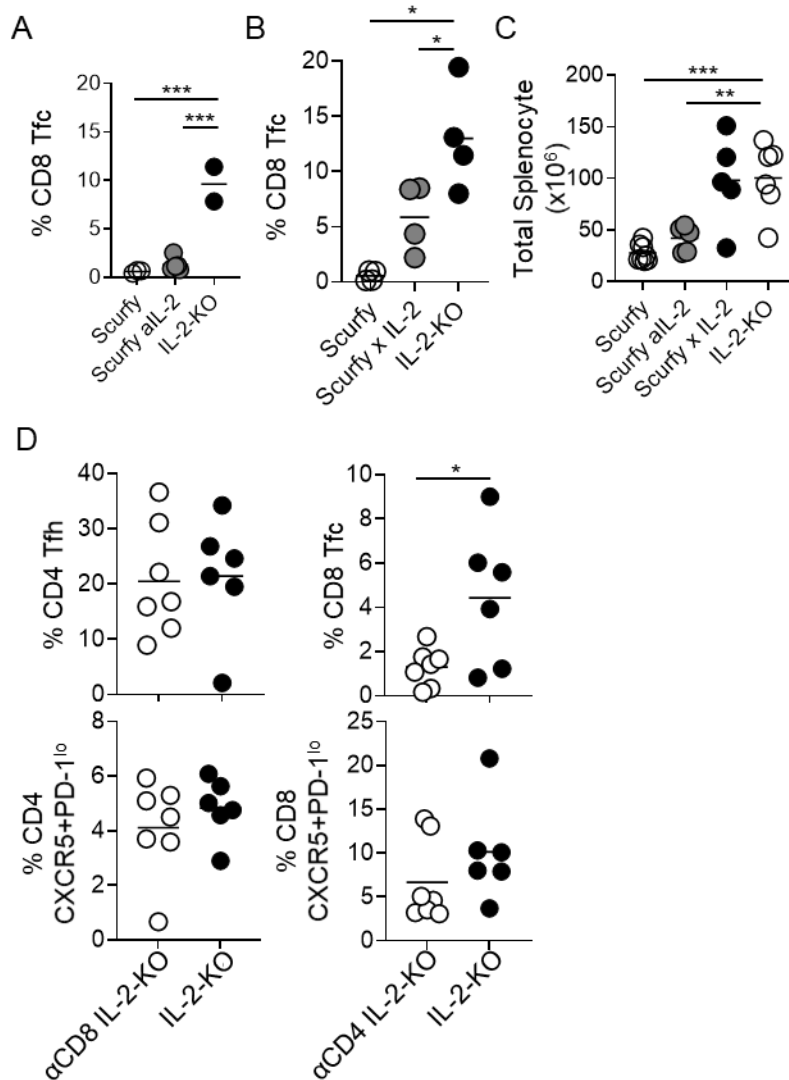


**Fig 3-5. CD4 T cells and IL-2 controls CD8 Tfc differentiation.** Splenic CD8 Tfc frequencies were compared between (A) 17-21-day old IL-2-KO, 16-21-day old scurvy mice treated 5 times with PBS (scurvy) and anti-IL-2 (scurvy all-2) or (B) 18–20-day old IL-2-KO, scurvy, and scurvy x IL-2-KO (Scurvy x IL-2) mice. (C) Total splenocyte number in scurvy, scurvy all-2, Scurvy x IL-2, and IL-2-KO mice described in A and B. (D) IL-2-KO mice were treated 5 times with anti-CD4 or anti-CD8 between 8-16-days of age to deplete either CD4 or CD8 T cells. The frequency and total number of CD4 Tfh and CD4 CXCR5+PD-1<sup>lo</sup> in the absence of CD8 T cells or CD8 Tfc and CD8 CXCR5+PD-1<sup>lo</sup> in the absence of CD4 T cell was compared to PBS-treated IL-2-KO mice. Each symbol indicates an individual animal. Data representative of 2-4 independent. Statistics: (A-C) 1-way ANOVA with multiple comparisons and Bonferroni correction. (E) unpaired Student's t-test with a Welch correction.

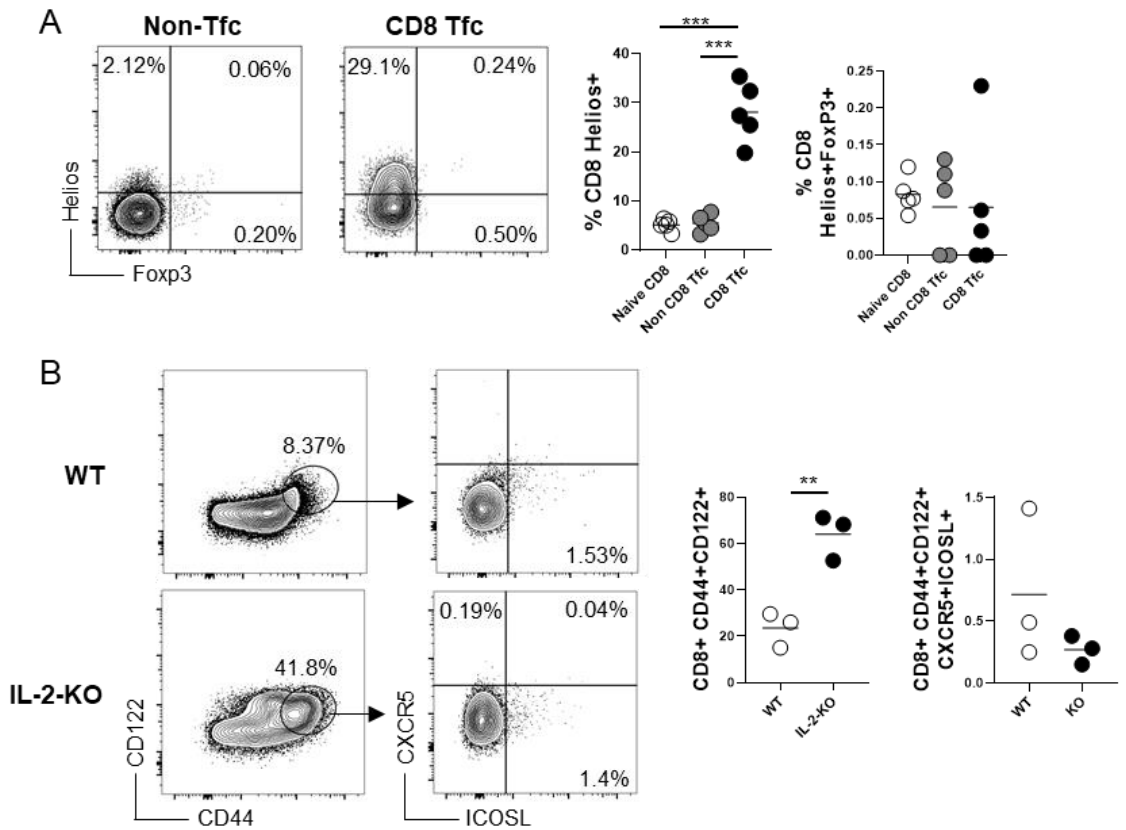


**Fig 3-6. CD8 Tfc are not CD8 Treg subsets.** Flow cytometric analysis of WT naïve CD8 T cells, IL-2-KO CD8 non-Tfh, or IL-2-KO CD8 Tfc from 17-21-day old WT or IL-2-KO LN. (A) Representative plots and frequency comparisons of total Helios expression or co-expression of Helios and Foxp3. (B) Evaluation of Qa-1 restricted CXCR5<sup>+</sup> ICOSL<sup>+</sup> CD8 Tregs first as CD122 and CD44 on CD8 T cells, then as expression of CXCR5 and ICOSL within the CD8<sup>+</sup>CD122<sup>+</sup>CD44<sup>+</sup> population. Each symbol indicates an individual animal. Data is representative of 2-4 independent experiments. Statistics: (A) 1-way ANOVA with multiple comparisons and Bonferroni correction, (B) paired Student's T test.

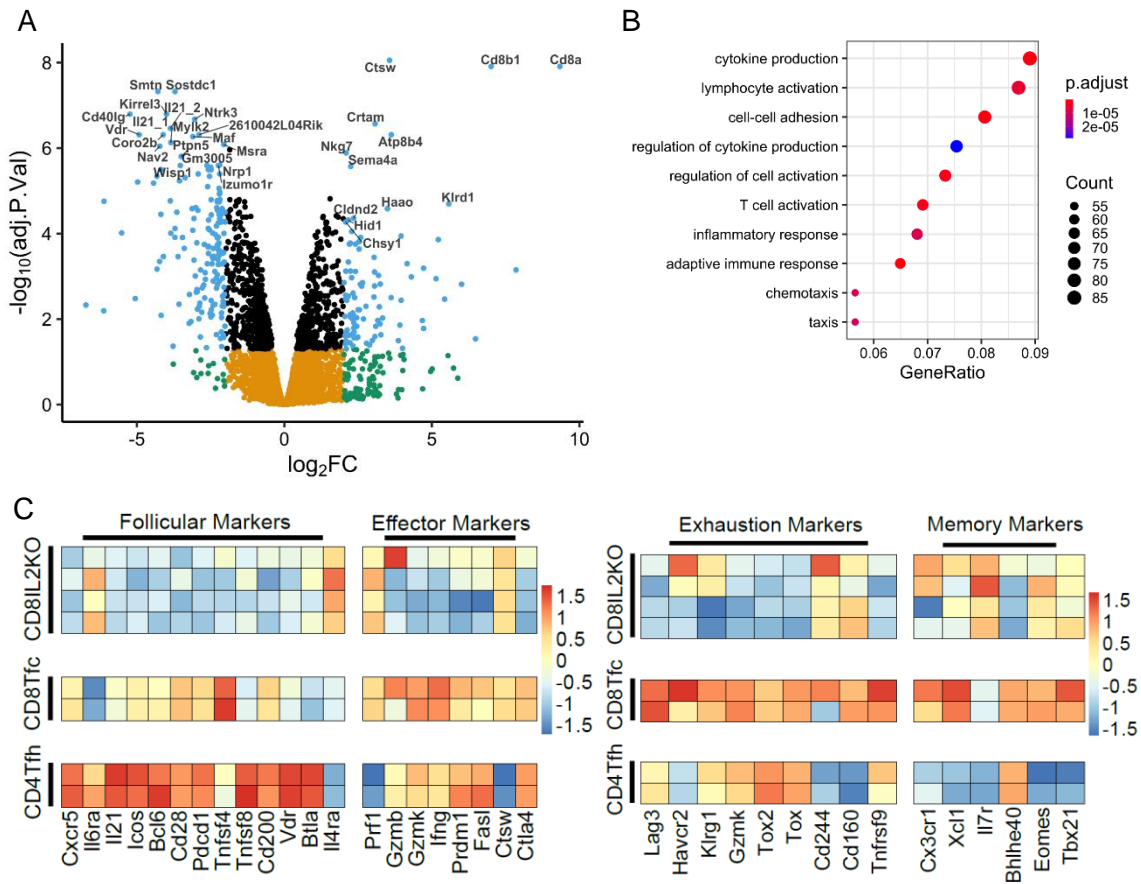


**Fig 3-7. CD8 Tfc transcriptional profiling highlights a diverse helper-like and memory phenotype.** RNAseq of 2 independent IL-2-KO CD4 Tfh and CD8 Tfc from 6-7 pooled LN and Spl. **(A)** Volcano plot of differential expression defined as log fold change (LFC) of IL-2-KO CD8 Tfc vs IL-2-KO CD4 Tfh with 479 upregulated and 639 downregulated genes. **(B)** Gene Ontology plot of top 10 categories. X-axis shows the gene ratio which indicates the quantity of genes present from each category divided by total number of differentially expressed genes. **(C)** Heatmaps containing normalized gene expression (Log-CPM) marked by different gene class. Cell type is defined as the first column labeled “CellType” of the heatmap, marker type is defined as “Gene.Class” as the first row at the top.

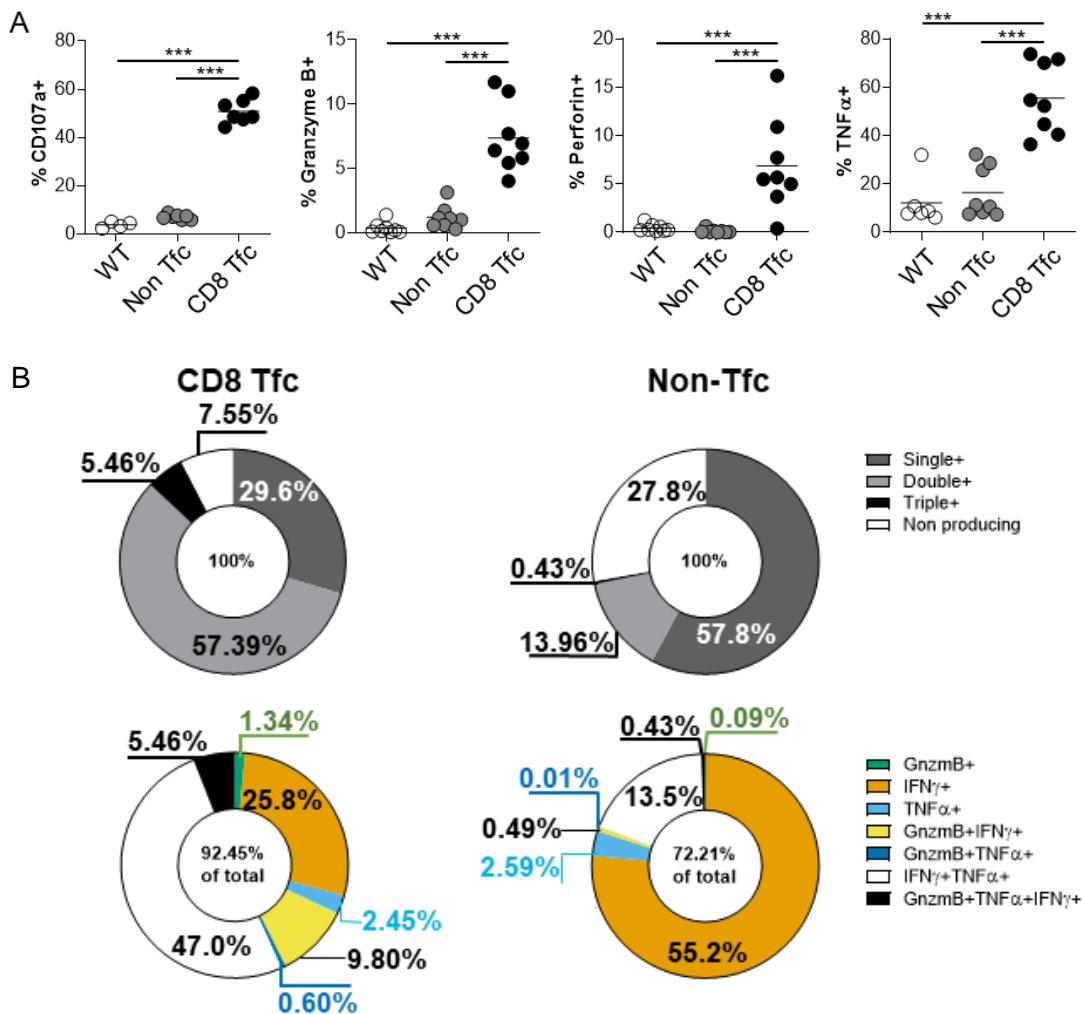


**Fig 3-8. CD8 Tfc maintain cytotoxic capacity.** IL-2-KO and WT lymphocytes were stimulated with PMA and ionomycin with BFA for 5 hours, then analyzed for cytokine expression in WT naïve CD8 T, IL-2-KO CD8 non Tfc and IL-2-KO CD8 Tfc populations. **(A)** Frequency of cytokine expressing cells and mean fluorescence intensity (MFI) of CD107a, Granzyme B, Perforin and TNF $\alpha$ . **(B)** Pie charts illustrate polyfunctional cytolytic protein expression by IL-2-KO CD8 Tfc and non-CD8 Tfc. Grey scale figures show non-producing, single, double and triple expression of the total population. Color figures show expression of Granzyme B, IFN $\gamma$  and/or TNF $\alpha$  as a percentage of the cytokine expressing population defined. Each symbol indicates an individual animal. Data representative of 3-6 independent experiments. Statistics: (A) 1-way ANOVA with multiple comparisons and Bonferroni correction.

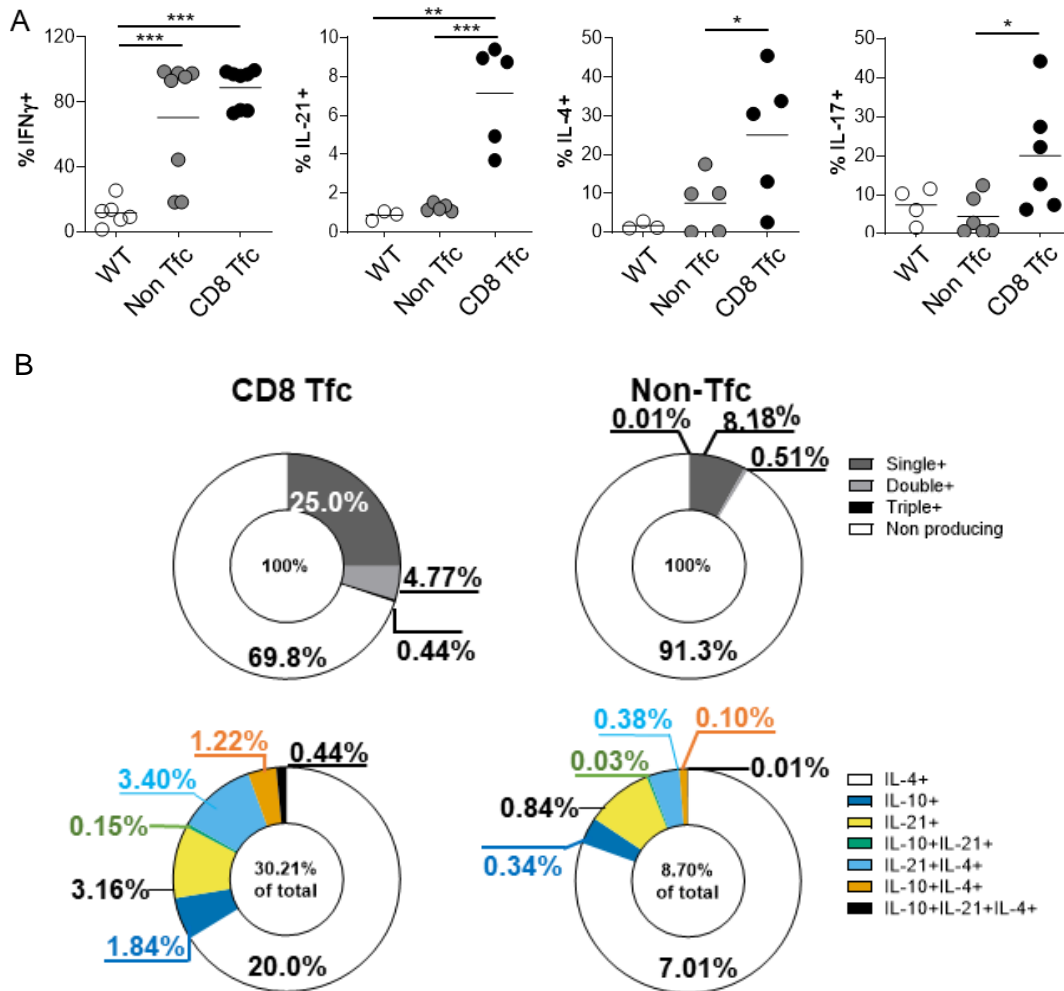


**Fig 3-9. CD8 Tfc possess helper capacity.** IL-2-KO and WT lymphocytes were stimulated with PMA and ionomycin with BFA for 5 hours, then analyzed for cytokine expression in WT naïve CD8 T, IL-2-KO CD8 non Tfc and IL-2-KO CD8 Tfc populations. **(A)** Frequency of cytokine expressing cells and MFI of IFN $\gamma$ , IL-21, IL-4, and IL-17. **(B)** Pie charts illustrate polyfunctional Tfh-associated protein expression by IL-2-KO CD8 Tfc and non-CD8 Tfc. Grey scale figures show non-producing, single, double and triple expression of the total population. Color figures show expression of IL-4, IL-10 and/or IL-21 as a percentage of the cytokine expressing population defined. Each symbol indicates an individual animal. Data representative of 3-6 independent experiments. Statistics: (A) 1-way ANOVA with multiple comparisons and Bonferroni correction.

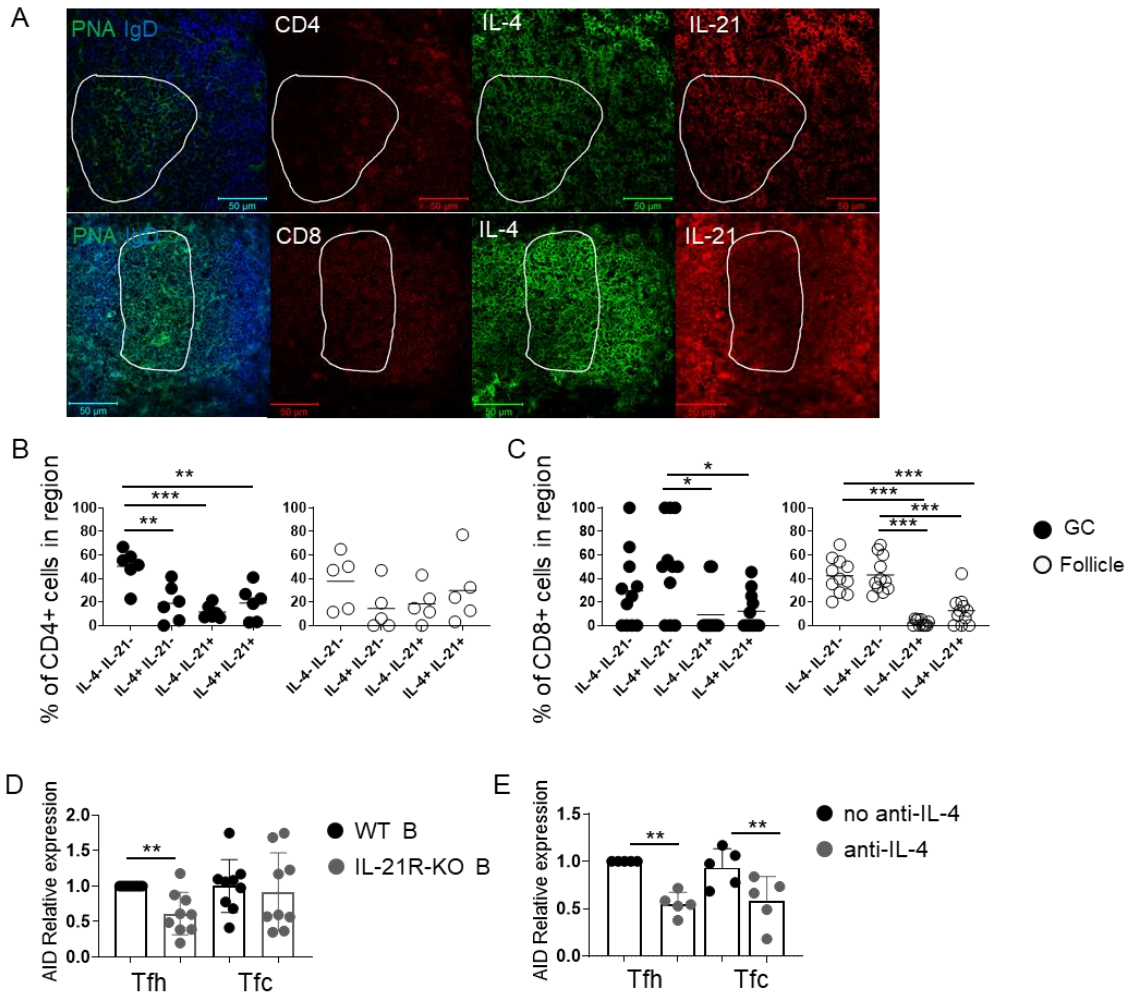


**Fig 3-10. CD8 Tfc produce IL-4 and IL-21 within GC and follicle.** (A) IL-2-KO spleen sections were stained for IL-4, IL-21, PNA, IgD, and CD4 or CD8. Region outlined is the germinal center, defined by high PNA and low IgD. (B, C) Frequency of (B) CD4 or (C) CD8 T cells expressing IL-4 and/or IL-21 of total CD4 or CD8 T cells counted within the given region. (D, E) Sorted IL-2-KO CD4 Tfh and CD8 Tfc were stimulated for 3 days with anti-CD3 and anti-CD28, with (E) or without (D) neutralizing anti-IL-4. T cell supernatant was then plated with B cells and anti-IgM and anti-CD40 for 3 days. B cells were then collected and assessed for AID expression by flow cytometry. MFI for each experiment was normalized to Tfh with WT B cells, setting that condition to 1. Data representative of 4 experiments with a total n of 4 per group for D and n of 5-8 per group for C-D. Statistics (D, E) paired Student's t-test, (B-C) one-way ANOVA with multiple comparisons and Bonferroni correction.

**CHAPTER 4**  
**Conclusion**

## CHAPTER 4: CONCLUSION AND FUTURE DIRECTIONS

### CONTRIBUTIONS TO THE FIELD

#### *Autoimmune disease*

The work presented here is the first to our knowledge to computationally assess and predict autoimmune disease kinetics in IL-2Ra-deficient mice. Peripheral blood parameters were assessed through principal component analysis to predict disease endpoint in a mouse model of autoimmune disease and use that prediction to assess parameters that drive differences in disease kinetics (Chapter 2). This work contributes to the understanding of what drives disease progression in a model of autoimmunity, including T cell activation states, signaling responsiveness, and Treg function, and suggests that multiple small changes can contribute to large differences in disease kinetics. This suggests that factors that influence human autoimmune disease progression may also be present early, but that multiple factors may need to be considered holistically in assessing disease outcomes. This approach could help with determining what early factors drive autoimmune disease progression; however, more work with autoimmune models with longer progression and kinetics may help to tease apart what factors may apply to human autoimmune disorders.

Further, our work contributes to the understanding of the role of CD8 T cells in autoimmune disease. Our work shows that the decrease of IL-10 production from CD8 T cells and CD8 Tregs, along with the decreased IL-7 responsiveness and increased apoptosis may contribute to more rapid autoimmune disease progression (Chapter 2). The work presented here adds to our understanding that CD8 T cells can contribute to both the progression and prevention, or in this case delay, of autoimmune disease (1).

#### *Germinal Center Reactions, CD8 Tfc cell regulation and function*

While the germinal center reaction has been studied extensively, and the dynamics and interactions involved are well established, there are many remaining questions. The identification of a CD8 T cell population that localizes to the B cell follicle and germinal center (Chapter 3 and (2)) raises the question of their role in the germinal center and B cell antibody responses, particularly whether CD8 Tfc cells contribute uniquely or redundantly to B cell responses. The work presented here indicates that CXCR5+ CD8 T cells localize within the B cell follicle and the germinal center and produce CD4 Tfh-associated cytokines IL-21 and IL-4, particularly IL-4. Further our work shows that CD8 T cells within the germinal center express a chemokine receptor pattern (CXCR5+ CXCR4+) suggestive of dark zone localization, but work remains to confirm that CD8 T

cells are present in this region. Work remains to determine whether CXCR5+ CD8 T cells contribute to B cell responses outside of the follicle and to what extent they rely on cell-contact dependent signals to contribute to B cell help. Further, work remains to identify whether CD8 Tfc cells contribute to germinal center reactions uniquely from CD4 Tfh cells, particularly in the context of autoimmune disease. Given the possible dark zone localization of CD8 Tfc cells there is the potential of unique contribution to B cell responses due to localizing to a region that CD4 Tfh cells do not.

Since the identification of CD8 T cells in ectopic germinal centers in rheumatoid arthritis in 2002 and subsequent work characterizing CXCR5+ CD8 T cells in a variety of settings, some of the signals that regulate this population have been identified. E2A, Tcf1, Id2, and Id3 are implicated in the differentiation of this population (3-7). Since IL-2 suppresses CD4 Tfh cell generation and the expression of Bcl6, a key transcription factor for the expression of CXCR5, IL-2 was assessed for its influence on CXCR5+ CD8 T cells (8-11). In collaboration with a prior graduate student, work presented in Chapter 3 shows that CXCR5+ CD8 T cells arise in the presence of Treg dysfunction alone, such as is present in scurfy mutant mice; however, depletion or genetic absence of IL-2 increases the frequency of this population. The increase in CXCR5+ CD8 cells is likely due to extensive lymphoproliferation rather than a direct result of IL-2 on the differentiation of CXCR5+ CD8 T cells. A study using CD8-specific deletion of STAT5 also showed CXCR5+ CD8 T cells developing, which suggests that STAT5 regulates the differentiation of this subset (12). Since several cytokines, including IL-2, IL-7, and IL-15, all utilize STAT5, more work needs to be done to assess the influence of IL-2 and other STAT5-mediated cytokines on CXCR5+ CD8 T cell development.

CXCR5+ CD8 T cells have been identified in a variety of settings – chronic viral infection, cancer, and autoimmune disease – and with a variety of proposed functionality – cytolytic, helper, and precursor to memory and exhaustion (2-4, 12-24). We have shown that CXCR5+ CD8 T cells in autoimmune disease are phenotypically and functionally similar to CD4 Tfh cells (2). We have demonstrated that CD8 T follicular (Tfc) cells produce CD4 Tfh-associated cytokines IL-21 and IL-4 (Chapter 3). We identified the possibility of CD8 T cells localizing to the dark zone of the germinal center, but the limitations of the current study did not allow for assessing whether CD8 T cells in the dark zone are also producing IL-21 or IL-4. We have further assessed the contribution of these cytokines to CD8 Tfc cell function in providing B cell help. Our work suggests that IL-21 produced by CD8 Tfc cell does not influence B cell antibody class-switching or expression of activation-induced cytidine deaminase, while IL-4 from CD8 Tfc cells induces AID (Chapter 3). The mechanisms underlying the differences between B cell responses to CD4 and CD8 derived cytokines is

unknown but may provide novel regulation cues to the tightly regulated GC reactions. Further the contribution of contact-dependent interactions from CD8 Tfc cells on B cell responses remains to be determined, as this was not assessed in the presented work.

## **FUTURE DIRECTIONS**

The work here has contributed to identifying the function of CD8 Tfc cells in autoimmune disease. CD8 Tfc cells in autoimmune disease phenotypically and functionally resemble CD4 Tfh cells, including localizing to the B cell follicle and germinal center, producing IL-4 and IL-21, and increasing B cell AID expression. Work remains assessing the role of CD8 Tfc cells in B cell responses. Previous work suggests that CD8 Tfc cells may increase plasma cell differentiation, but where CD8 Tfc cells contribute to plasma cell differentiation and whether they contribute to long-lived or short-lived plasma cells remains to be determined (Figure 4-1, (2)). It has not yet been assessed how CD8 Tfc cells may influence memory B cell differentiation, in general or in regard to specific memory B cell subsets (Figure 4-1). Further, given the potential for CD8 Tfc cells to localize to the dark zone of the germinal center, the function of these cells within this zone needs to be investigated. Since CD8 Tfc cells retain cytolytic molecule expression, CD8 Tfc cells may contribute to B cell apoptosis in the dark zone.

CXCR5+ CD8 T cells have been studied across settings and phenotypes and have the potential for cytolytic and helper function. These cells are responsive to PD-1 blockade, making them a therapeutic target for chronic viral infection and cancer. This work further suggests that CXCR5+ CD8 T cells are a progenitor effector memory population that seeds the anti-tumor and anti-virus CD8 T cells (5, 16); however, the potential of CXCR5+ CD8 T cells to promote B cell antibody production in autoimmune disease has implications for their contribution to immune adverse events that occur during checkpoint inhibitor blockade treatment ((2), Chapter 3). Thus CXCR5+ CD8 T cells should be studied further in the context of immune checkpoint blockade, particularly whether their re-activation in this scenario leads to auto-antibody production and development of immune adverse events. Given the ability of CXCR5+ CD8 T cells to promote B cell responses in autoimmune disease, these cells likely contribute to the development of autoimmune-like immune adverse events following PD-1 checkpoint blockade.

The differentiation cues for CXCR5+ CD8 T cells, particularly as this subset manifests with different phenotype and function in a variety of contexts, needs to be studied more. A few genes have been identified that regulate the development of these cells, including E2A, TCF-1, Id2, and Id3, but the cues that drive the

differentiation of these cells has yet to be determined. Further, since CXCR5+ CD8 T cells have been identified in multiple settings with a variety of functions the question remains to what extent is the regulation of these cells similar or different across settings and function. In particular an assessment of transcriptomics across settings may be necessary to fully dissect how the regulation of this subset differs across settings and how CXCR5+ CD8 T cells in these different settings relate to each other.

My work suggests that CXCR5+ CD8 T cells in autoimmune disease are phenotypically and functionally similar to CD4 Tfh cells ((2), Chapter 3). It remains to be determined whether these cells are regulated by the same signals and mechanisms that regulate the development of CD4 Tfh cells, including strong antigen and IL-6 stimulation (9, 10, 25-28). More recent work suggests that CD4 Tfh cells develop from IL-2 producing activated CD4 T cells and that these cells utilize different metabolic pathways from other effector cells (29, 30). Future work should assess whether these aspects of CD4 Tfh cell differentiation apply to the differentiation of CXCR5+ CD8 T cells, including whether CXCR5+ CD8 T cells arise from IL-2-producing activated CD8 T cells and/or CD8 T cells with the strongest TCR stimulation. Preliminary data suggests that CD8 Tfc cells and CD4 Tfh cells have similar TCR responsiveness (Figure 4-2), indicating that CD8 Tfc cells may also differentiate from CD8 T cells with strong TCR stimulation. Our work here suggests that CD8 Tfc cell differentiation is dependent on CD4 T cells, as the depletion of CD4 T cells significantly reduced CD8 Tfc cells (Chapter 3). In agreement with this, other work suggests that CD4 Tfc cells are required to help the differentiation of CXCR5+ CD8 T cells (31). Further, previous data suggests that CD8 Tfc cells alone cannot mediate B cell responses when transferred, but require CD4 Tfh cells, which suggests that CD8 Tfc cells may need established germinal centers to mediate their function or differentiation (2). Time-specific depletion of CD4 Tfh cells during the development of CD8 Tfc cells will help to confirm this theory.

## **SUMMARY**

Despite the increasing field of work assessing CXCR5+ CD8 T cells, many questions remain, particularly in regard to the regulation of these cells. To what extent the differentiation of these cells matches that of CD4 Tfh cells or are similar across settings that CXCR5+ CD8 T cells have been identified in remain to be determined. Further, the role these cells may play in immune checkpoint blockade and its associated immune adverse events remains to be assessed. Finally, CXCR5+ CD8 T cells are present in the B cell follicle and germinal center and are involved in B cell responses. This adds to our understanding of the

germinal center reaction and that these cells may contribute with overlapping and distinct contributions to the germinal center reaction.

## References

1. Gravano, D. M., and K. K. Hoyer. 2013. Promotion and prevention of autoimmune disease by CD8+ T cells. *J Autoimmun* 45: 68-79.
2. Valentine, K. M., D. Davini, T. J. Lawrence, G. N. Mullins, M. Manansala, M. Al-Kuhlani, J. M. Pinney, J. K. Davis, A. E. Beaudin, S. S. Sindi, D. M. Gravano, and K. K. Hoyer. 2018. CD8 Follicular T Cells Promote B Cell Antibody Class Switch in Autoimmune Disease. *The Journal of Immunology*.
3. He, R., S. Hou, C. Liu, A. Zhang, Q. Bai, M. Han, Y. Yang, G. Wei, T. Shen, X. Yang, L. Xu, X. Chen, Y. Hao, P. Wang, C. Zhu, J. Ou, H. Liang, T. Ni, X. Zhang, X. Zhou, K. Deng, Y. Chen, Y. Luo, J. Xu, H. Qi, Y. Wu, and L. Ye. 2016. Follicular CXCR5- expressing CD8(+) T cells curtail chronic viral infection. *Nature* 537: 412-428.
4. Leong, Y. A., Y. Chen, H. S. Ong, D. Wu, K. Man, C. Deleage, M. Minnich, B. J. Meckiff, Y. Wei, Z. Hou, D. Zotos, K. A. Fenix, A. Atnerkar, S. Preston, J. G. Chipman, G. J. Beilman, C. C. Allison, L. Sun, P. Wang, J. Xu, J. G. Toe, H. K. Lu, Y. Tao, U. Palendira, A. L. Dent, A. L. Landay, M. Pellegrini, I. Comerford, S. R. McColl, T. W. Schacker, H. M. Long, J. D. Estes, M. Busslinger, G. T. Belz, S. R. Lewin, A. Kallies, and D. Yu. 2016. CXCR5(+) follicular cytotoxic T cells control viral infection in B cell follicles. *Nat Immunol* 17: 1187-1196.
5. Im, S. J., M. Hashimoto, M. Y. Gerner, J. Lee, H. T. Kissick, M. C. Burger, Q. Shan, J. S. Hale, T. H. Nasti, A. H. Sharpe, G. J. Freeman, R. N. Germain, H. I. Nakaya, H. H. Xue, and R. Ahmed. 2016. Defining CD8+ T cells that provide the proliferative burst after PD-1 therapy. *Nature* 537: 417-421.
6. Valentine, K. M., and K. K. Hoyer. 2019. CXCR5+ CD8 T Cells: Protective or Pathogenic? *Front Immunol* 10: 1322.
7. Yu, D., and L. Ye. 2018. A Portrait of CXCR5 Follicular Cytotoxic CD8 T cells. *Trends Immunol* 39: 965-979.
8. Johnston, R. J., A. C. Poholek, D. DiToro, I. Yusuf, D. Eto, B. Barnett, A. L. Dent, J. Craft, and S. Crotty. 2009. Bcl6 and Blimp-1 are reciprocal and antagonistic regulators of T follicular helper cell differentiation. *Science* 325: 1006-1010.
9. Papillion, A., M. D. Powell, D. A. Chisolm, H. Bachus, M. J. Fuller, A. S. Weinmann, A. Villarino, J. J. O'Shea, B. León, K. J. Oestreich, and A. Ballesteros-Tato. 2019. Inhibition of IL-2 responsiveness by IL-6 is required for the generation of GC-T. *Sci Immunol* 4.
10. Jogdand, G. M., S. Mohanty, and S. Devadas. 2016. Regulators of Tfh Cell Differentiation. *Front Immunol* 7: 520.
11. Liao, W., J. X. Lin, L. Wang, P. Li, and W. J. Leonard. 2011. Modulation of cytokine receptors by IL-2 broadly regulates differentiation into helper T cell lineages. *Nat Immunol* 12: 551-559.
12. Chen, Y., M. Yu, Y. Zheng, G. Fu, G. Xin, W. Zhu, L. Luo, R. Burns, Q. Z. Li, A. L. Dent, N. Zhu, W. Cui, L. Malherbe, R. Wen, and D. Wang. 2019. CXCR5+ PD-1+ follicular helper CD8 T cells control B cell tolerance. *Nat Commun* 10: 4415.
13. Bai, M., Y. Zheng, H. Liu, B. Su, Y. Zhan, and H. He. 2017. CXCR5+ CD8+ T cells potently infiltrate pancreatic tumors and present high functionality. *Exp Cell Res* 361: 39-45.
14. E, J., F. Yan, Z. Kang, L. Zhu, J. Xing, and E. Yu. 2018. CD8 CXCR5 T cells in tumor-draining lymph nodes are highly activated and predict better prognosis in colorectal cancer. *Hum Immunol* 79: 446-452.
15. Hofland, T., A. W. J. Martens, J. A. C. van Bruggen, R. de Boer, S. Schetters, E. B. M. Remmerswaal, F. J. Bemelman, M. D. Levin, A. D. Bins, E. Eldering, A. P. Kater, and S. H.

- Tonino. 2021. Human CXCR5+ PD-1+ CD8 T cells in healthy individuals and patients with hematologic malignancies. *Eur J Immunol* 51: 703-713.
16. Im, S. J., B. T. Konieczny, W. H. Hudson, D. Masopust, and R. Ahmed. 2020. PD-1+ stemlike CD8 T cells are resident in lymphoid tissues during persistent LCMV infection. *Proc Natl Acad Sci U S A* 117: 4292-4299.
  17. Jiang, H., L. Li, J. Han, Z. Sun, Y. Rong, and Y. Jin. 2017. CXCR5+ CD8+ T cells indirectly offer B cell help and are inversely correlated with viral load in chronic hepatitis B infection. *DNA Cell Biol* 36: 321-327.
  18. Jiang, H., L. Li, J. Han, Z. Sun, Y. Rong, and Y. Jin. 2017. CXCR5+CD8+ T cells infiltrate the colorectal tumors and nearby lymph nodes, and are associated with enhanced IgG response in B cells. *DNA Cell Biol* 36: 321-327.
  19. Jin, Y., C. Lang, J. Tang, J. Geng, H. K. Song, Z. Sun, and J. Wang. 2017. CXCR5+CD8+ T cells could induce the death of tumor cells in HBV-related hepatocellular carcinoma. *Int Immunopharmacol* 53: 42-48.
  20. Le, K. S., P. Amé-Thomas, K. Tarte, F. Gondois-Rey, S. Granjeaud, F. Orlanducci, E. D. Foucher, F. Broussais, R. Bouabdallah, T. Fest, D. Leroux, S. Yadavilli, P. A. Mayes, L. Xerri, and D. Olive. 2018. CXCR5 and ICOS expression identifies a CD8 T-cell subset with Tfh features in Hodgkin lymphomas. *Blood Adv* 2: 1889-1900.
  21. Quigley, M. F., V. D. Gonzalez, A. Granath, J. Andersson, and J. K. Sandberg. 2007. CXCR5+ CCR7- CD8 T cells are early effector memory cells that infiltrate tonsil B cell follicles. *Eur J Immunol* 37: 3352-3362.
  22. Tang, J., J. Zha, X. Guo, P. Shi, and B. Xu. 2017. CXCR5+CD8+ T cells present elevated capacity in mediating cytotoxicity toward autologous tumor cells through interleukin 10 in diffuse large B-cell lymphoma. *Int Immunopharmacol* 50: 146-151.
  23. Xing, J., C. Zhang, X. Yang, S. Wang, Z. Wang, X. Li, and E. Yu. 2017. CXCR5+ CD8+ T cells infiltrate the colorectal tumors and nearby lymph nodes, and are associated with enhanced IgG response in B cells. *Exp Cell Res* 356: 57-63.
  24. Ye, L., Y. Li, H. Tang, W. Liu, Y. Chen, T. Dai, R. Liang, M. Shi, S. Yi, G. Chen, and Y. Yang. 2019. CD8+CXCR5+T cells infiltrating hepatocellular carcinomas are activated and predictive of a better prognosis. *Aging (Albany NY)* 11: 8879-8891.
  25. Crotty, S. 2011. Follicular helper CD4 T cells (TFH). *Annu Rev Immunol* 29: 621-663.
  26. Tubo, N. J., A. J. Pagán, J. J. Taylor, R. W. Nelson, J. L. Linehan, J. M. Ertelt, E. S. Huseby, S. S. Way, and M. K. Jenkins. 2013. Single naive CD4+ T cells from a diverse repertoire produce different effector cell types during infection. *Cell* 153: 785-796.
  27. Baumjohann, D., S. Preite, A. Reboldi, F. Ronchi, K. M. Ansel, A. Lanzavecchia, and F. Sallusto. 2013. Persistent antigen and germinal center B cells sustain T follicular helper cell responses and phenotype. *Immunity* 38: 596-605.
  28. Deenick, E. K., A. Chan, C. S. Ma, D. Gatto, P. L. Schwartzberg, R. Brink, and S. G. Tangye. 2010. Follicular helper T cell differentiation requires continuous antigen presentation that is independent of unique B cell signaling. *Immunity* 33: 241-253.
  29. Ray, J. P., M. M. Staron, J. A. Shyer, P. C. Ho, H. D. Marshall, S. M. Gray, B. J. Laidlaw, K. Araki, R. Ahmed, S. M. Kaech, and J. Craft. 2015. The Interleukin-2-mTORc1 Kinase Axis Defines the Signaling, Differentiation, and Metabolism of T Helper 1 and Follicular B Helper T Cells. *Immunity* 43: 690-702.
  30. DiToro, D., C. J. Winstead, D. Pham, S. Witte, R. Andargachew, J. R. Singer, C. G. Wilson, C. L. Zindl, R. J. Luther, D. J. Silberger, B. T. Weaver, E. M. Kolawole, R. J. Martinez, H.

- Turner, R. D. Hatton, J. J. Moon, S. S. Way, B. D. Evavold, and C. T. Weaver. 2018. Differential IL-2 expression defines developmental fates of follicular versus nonfollicular helper T cells. *Science* 361.
31. de Goër de Herve, M. G., M. Abdoh, S. Jaafoura, D. Durali, and Y. Taoufik. 2019. Follicular CD4 T Cells Tutor CD8 Early Memory Precursors: An Initiatory Journey to the Frontier of B Cell Territory. *iScience* 20: 100-109.

## FIGURES AND FIGURE LEGENDS

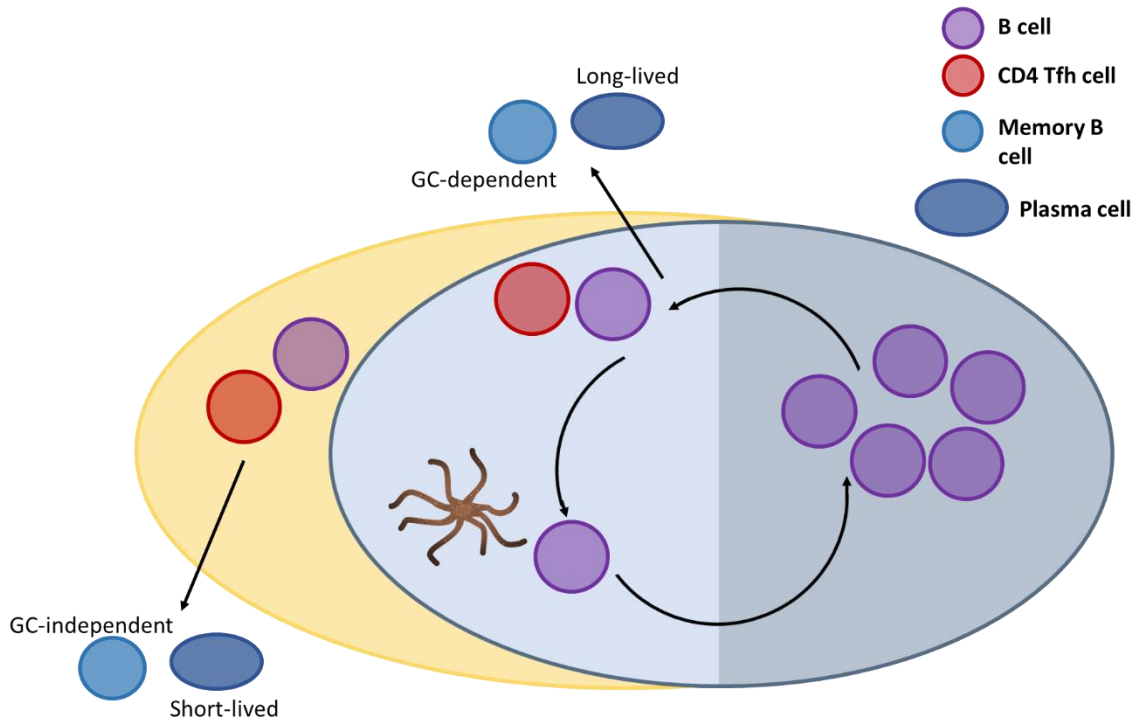


**Figure 4-1. Memory B cell and plasma cell differentiation.** B cells following T cell interactions may differentiate into plasma cells or memory B cells, but these states differ depending on where T:B cell interactions occurred. B cells differentiating into plasma cells from the germinal center (blue region) are more long-lived than plasma cells differentiating out of the follicular zone (yellow region). Memory B cells can also be categorized into GC-dependent and GC-independent based on whether they differentiate from the germinal center.

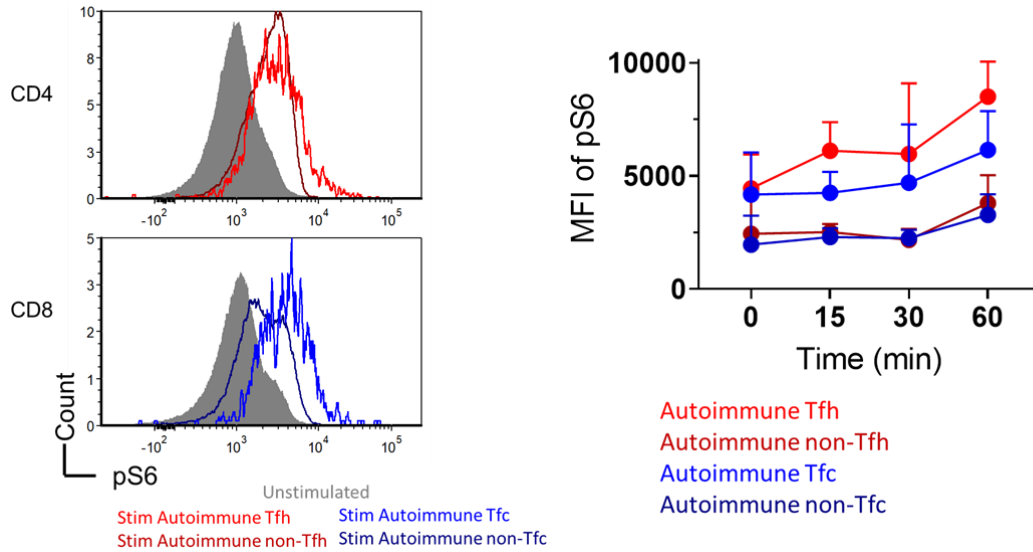


**Figure 4-2. CD8 Tfc cells and CD4 Tfh cells respond similarly to TCR stimulation.** Phosphorylation of ribosomal protein S6 was measured by flow cytometry in CD4 Tfh and CD8 Tfc cells following stimulation with 20  $\mu\text{g}/\text{mL}$   $\alpha\text{-CD3}\epsilon$  and 50  $\mu\text{g}/\text{mL}$   $\alpha\text{-Armenian hamster IgG}$  stimulation. Representative flow plot shows data from 30min post-stimulation.